SYNTHESIS AND APPLICATION OF DERIVATIZED NATURAL GUM BASED HYDROGELS

A Thesis Submitted in Partial Fulfilment of the Requirement for the Degree of

DOCTOR OF PHILOSOPHY

By

Meenakshi Tanwar

(2K19/PHDAC/503)

Under Supervision of

Prof. Archna Rani

&

Prof. Rajinder K. Gupta

DEPARTMENT OF APPLIED CHEMISTRY

DELHI TECHNOLOGICAL UNIVERSITY

DELHI-110042 (INDIA)

JUNE 2024

Dedicated
To My
Husband
&
Family

DELHI TECHNOLOGICAL UNIVERSITY
(Formerly Delhi College of Engineering)
Department of Applied Chemistry Shahbad Daulatpur
Bawana Road Delhi- 110042, India

DECLARATION

I hereby declare that the thesis entitled "**Synthesis and Application of Derivatized Natural Gum based Hydrogels**" is an original work carried out by me under the supervision of **Prof. Archna Rani** and **Prof. Rajinder K. Gupta**, Department of Applied Chemistry, Delhi Technological University, Delhi. This thesis has been prepared in conformity with the rules and regulations of the Delhi Technological University, Delhi. The research work reported and results presented in the thesis have neither partially nor fully submitted to any other university nor institute for the award of any other degree or diploma.

Place: Delhi
Date:

Meenakshi Tanwar
(2K19/PHDAC/503)
Research Scholar
Department of Applied Chemistry
Delhi Technological University,
Delhi-110042

DELHI TECHNOLOGICAL UNIVERSITY
(Formerly Delhi College of Engineering)
Department of Applied Chemistry Shahbad Daulatpur
Bawana Road Delhi- 110042, India

CERTIFICATE

This is to certify that the work embodied in the thesis entitled "**Synthesis and Application of Derivatized Natural Gum based Hydrogels**" by **Ms. Meenakshi Tanwar** (Roll No 2K19/PHDAC/503), in the partial fulfilment of the requirements for the award of the degree of **Doctor of Philosophy**, is an authentic record of student's own work carried out by her under the supervision of **Prof. Archna Rani** and **Prof. Rajinder K. Gupta**, Department of Applied Chemistry, Delhi Technological University, Delhi. This is also certified that this work has neither partially nor fully submitted to any other Institute or University for the award of any other diploma or degree.

PROF. ARCHNA RANI
Department of Applied Chemistry
Delhi Technological University
Delhi-110042

PROF. RAJINDER K. GUPTA
Department of Applied Chemistry
Delhi Technological University
Delhi-110042

PROF. ANIL KUMAR
Head, Department of Applied Chemistry
Delhi Technological University
Delhi-110042

ACKNOWLEDGEMENTS

It is my pleasure to express my deep gratitude and heartfelt thanks to my supervisors Prof. Archna Rani and Prof. Rajinder K. Gupta, Department of Applied Chemistry, Delhi Technological University, Delhi for assisting me in identifying and formulating the research problem. Despite their busy schedule, **Prof. Archna Rani and Prof. Rajinder K. Gupta** were always available for the advice and discussions. Their valuable comments and advice gave me the confidence to overcome the challenges in formulation of this Ph.D. thesis work. Without their advice, enthusiasm and insightful guidance, my Ph.D. work would never have been completed. I am extremely fortunate to have been trained and introduced into the world of research under their guidance.

I owe my heartfelt gratitude to Prof. Jai Prakash Saini, former Honourable Vice-Chancellor and Prof. Parteek Sharma, Honourable Vice Chancellor Delhi Technological University for the kind permission and Prof. Anil Kumar, Head, Department of Applied Chemistry, DTU for providing me the necessary facilities to carry out this research work. Also, my gratitude extends to Prof. Sudhir G. Warkar former Head, Department of Applied Chemistry, DTU for providing the necessary research facilities and an excellent working environment in the department. I wish to express my sincere thanks to the whole faculty members of Department of Applied Chemistry, DTU for their help and support during this research work.

I am thankful to the members of my Ph.D. SRC Committee, Prof. Sunil Kumar Sharma (University of Delhi), Prof. Arinjay Jain, GGSIPU, Delhi (SRC & DRC member) Dr. Richa Srivastava (DTU) and Dr. Asmita Das (DTU) for approving my research proposal and evaluating the progress of my research work. I am also thankful to the members of my Ph.D. DRC Committee, DRC Chairman Prof. Ram Singh and former DRC Chairman Prof. D. Kumar, DRC members (Applied Chemistry), Mahendra Nath (University of Delhi), (DRC member) for their valuable suggestions and assessment of my research work.

I am thankful to Prof. Ram Singh, Prof. Rajinder K. Gupta Faculties of Department of Applied Chemistry and Dr. Navneeta Bhardwaj, Department of Biotechnology, DTU for

teaching Ph.D. course work. I would also like to thank Dr. Richa Srivastava, Dr. Deenan Santhya, Dr. Raminder Kaur, Dr. Poonam, Prof. Roli Purwar and Dr. Manish Jain, faculty members, Department of Applied Chemistry, DTU for their valuable support.

I would like to thank all technical and non-technical staff and my friends, seniors and fellow researchers (Ms. Megha (sister-in law), Ms. Manu, Mr. Saurav, Ms. Ritu, Dr. Deepali, Dr. Ritika, Dr. Manjot and Dr. Namit Dey) who have supported me through their encouragement, support and friendship during this period of thesis research work. I would like to thank to all those who directly and indirectly supported me in carrying out this thesis work successfully.

I wish to pay my sincere thanks to Delhi Technological University for providing me financial support to carry out this research work. I am also thankful to Aakaar Biotechnologies Pvt, Ltd., Lucknow, India for providing facilities for MTT Assay. Special Thanks to Dr. Sushama Talegaonkar (Delhi Pharmaceutical Sciences and Research University, New Delhi, India) for *in-vivo* studies. I would like to thank my husband (**Mr. Sunil Tanwar**), my daughter (**Gunnika Tanwar**) and family, who have been pillars of inspiration for my academic expedition and for their blessings and unconditional love, without which I would have failed to complete this work. Above all, I owe to Almighty God (**GURUJI**) for granting me wisdom, health and strength to accept the challenges of the life.

(Meenakshi Tanwar)

TABLE OF CONTENT

LIST OF FIGURES

LIST OF TABLES

ABSTRACT

Regulating the release of drugs with safety, effectiveness, and consistency is one major problem in healthcare systems. The use of natural gum-based hydrogels for drug delivery and wound healing may be the best solution to this problem. These hydrogels, derived from natural sources such as gum tragacanth, locust bean gum offer several advantages over synthetic hydrogels, including better biocompatibility and a homogeneous polymer network. With their biocompatible, biodegradable, and non-cytotoxic properties, natural gum-based hydrogels are ideal candidates for drug delivery and wound healing applications. They can efficiently encapsulate and release therapeutic agents, such as antibiotics or growth factors, in a controlled manner, promoting wound healing and preventing infection. Furthermore, the three-dimensional structure of hydrogels allows for the diffusion of nutrients and oxygen to the wound site, facilitating tissue regeneration and reducing healing time. In conclusion, natural gum-based hydrogels have shown great potential in drug delivery and wound healing applications.

In this thesis, some novel hydrogels were synthesized as the carriers for drug delivery and wound healing. The first approach was the fabrication of the Carboxymethylated Gum Tragacanth (CMGT) based hydrogel and its application as a drug delivery carrier. For the fabrication of CMGT cross-linked Sodium Acrylate Hydrogel (CMGT-co-SAH), firstly carboxymethylation of the Gum Tragacanth (GT) was done followed by synthesis of the CMGT-co-SAH by free radical co-polymerisation technique and confirmed by the characterization- FTIR, XRD, TGA, SEM and C^{13}-NMR. Flow properties of the hydrogel were analyzed by rheological analysis by viscosity, amplitude and frequency sweep test. By using Flory-Rehner equation, network parameter

of the hydrogel was analyzed that support the results of swelling index. Application of CMGT-co-SAH as the drug delivery carrier was analyzed by using the Aceclofenac Sodium (AFS) as a model drug. AFS loading and release profile were analyzed in pH 7.4 at 37 °C. Kinetic models were applied over the release profile of the AFS and follows the fickian diffusion mechanism and fitted in the Korsmeyer-Peppas model. Moreover, synthesized CMGT-co-SAH shows less than 1% hemolysis at every concentration that confirms the cyto-compatability of the CMGT-co-SAH.

Second approach includes Synthesis and Characterization of Carboxymethylated Locust Bean Gum (CMLB) based pH Responsive Hydrogel, (CMLB-*co*-poly(SA)-*cl*-poly(MBA) for Controlled Drug Delivery of Metformin Hydrochloride (MFH). The confirmation of successful carboxymethylation and hydrogel synthesis is achieved through a comprehensive characterization process employing FTIR, XRD, TGA, SEM, and C13-NMR techniques. Rheological analysis, including viscosity, amplitude, and frequency sweep tests, provides insights into the flow properties of the hydrogel in three different solutions, i.e., Distilled water, pH 7.4, and pH 2.2 buffer solutions. The Flory-Rehner equation is employed to analyze the network parameters of the hydrogel. Furthermore, we explore the application of the hydrogel as a drug delivery carrier which shows a sustainable release of MFH in Distilled water, pH 7.4, and pH 2.2 buffer solutions. The drug loaded CMLB-*co*-poly(SA)-*cl*-poly(MBA) hydrogel followed the non-fickian diffusion mechanism. The biocompatibility of the above two synthesized hydrogels was assessed through hemolysis studies.

Last approach includes the synthesis of a novel hydrogel film based on carboxymethylated gum cross-linked with Citric Acid (CA) loaded with *Cassia fistula* essential oils (EO) that

are Rosemary essential oil (REO) (*Rosmarinus officinalis*), Turmeric essential oil (TEO) (*Curcuma longa*) and Thuja essential oil (THEO) (*Thuja occidentalis L.*) for wound healing application as these essential oils have anti-microbial, anti-inflammatory, antioxidant, and analgesic properties. Moreover, thermal analysis (TGA), structural characteristics (FTIR and XRD), morphology (SEM), mechanical strength, anti-oxidant activity, bio-degradability test, permeability test and cytotoxicity assay (*in vitro* and *in vivo*) were analyzed for the films. From the performed tests and assay, we concluded that the film can be an effective, biocompatible and biodegradable source of wound healing films. Overall, the utilization of natural gum-based hydrogels for drug delivery and wound healing represents a promising approach that has the potential to revolutionize current treatment protocols and enhance patient care.

CHAPTER – 1

INTRODUCTION

1.1 Natural Gums

Natural gums have attracted interest recently due to their possible applications in a variety of fields [1]. These can be derived from numerous sources such as animals, plants, algae and micro-organisms having metabolic and structural functions [2]. They are also known as hydrocolloids [3] and are proficient in elevating the viscosity of liquids by a minuscule quantity [4]. Natural gums have recently been considered as under-explored source of remarkable natural products, resulting in a diverse range of products. These products are an important part of worldwide aliments for nourishment, remedial [1], cosmetics, paints, textiles and pharmaceutical applications [5].

Natural gums are polysaccharides that can be classified on the basis of sources into four categories; microbial gums, plant seeds gums, plant exudate gums and sea weed gums [1]. These polysaccharides are made up of a lot of monosaccharide residues linked together by O-glycosidic bonds. The standard formula for polysaccharides is $C_x(H_2O)_y$, where, x can vary from 200 to 2500. The repeating units in the polymer backbone are usually six-carbon monosaccharides, therefore, general formula can be written as $(C_6H_{10}O_5)_n$, where, n is the number of repeating units in the polymer backbone range from 40-3000 [6].

1.2 Derivatized Natural Gums

Polysaccharides may be modified in a number of ways to develop unique drug delivery materials, making them a potential alternative to synthetic polymer. The

modified natural gums are preferred over natural gums as latter one is more polar owing to enormous -OH groups that shows H-bonding with aqueous phase thus limiting the applications of natural gums. These -OH groups will also affect controlled release functionality, excessive rate of hydration, stiffness, decrease in viscosity after prolong storage, pH dependent solubility and chances of microbial contamination. Furthermore, derivatization was necessary because -OH groups have less interaction with counter ions. Natural polysaccharides can be modified by linking them to a variety of functional moieties to drive them towards controlled drug release. Derivatization can commonly be introduced by adding various type of functional groups [7,8] all of which have been extensively investigated in previous reported literatures. Natural gums and their possible derivatives have been shown in table 1.1 and structure of gums in table 1.2.

Table 1.1: Natural gums with their molecular weight, CAS No., botanical source, chemical compositions and derivatives

Sr. No.	Natural Gums	Mol.wt and CAS No.	Sources	Chemical composition	Derivatives	Ref. (Natural Gums)
1.	Gum Tragacanth (GT)	≈ 840 kDa & CAS No. -9000-65-1	Exudate from the stem of *Astragalus gummifer*, Leguminosae	Xylose, arabinose, galactose, fucose and galacturonic acid	Carboxymethylated [9]	[1]
2.	Gum Ghatti(GG)	≈ 12000 kDa [10] & CAS No. -9000-28-6	Bark Exudate of *Anogeissus latifolia*, family Combretaceae	L-arabionose, D-glucuronic acid, D-galactose, D-mannose, and D-xylose.	Carboxymethylated [11]	[1]
3.	Locust Bean Gum(LBG)	≈50-350 kDa CAS No. -9000-40-2	Endosperm of *Ceretonia siliqua*, Leguminosae	α-d-galactopyranosyl and β-d-mannopyranosyl	Carboxymethylated [12], Sulfated, Carboxylated and Ammoniated	[13]
4.	Guar Gum(GuG)	≈ 800-1000 kDa & CAS No.-9000-30-0	Endosperm of *Cyamopsis tetragonolobus*, Leguminosae	β-D-mannopyranose, α-D-galactopyranose	Carboxymethylated [14], hydroxyethylated [15], hydroxypropylated [16] o-carboxymethyl, o-hydroxypropylated [17] acryloyloxyl [18], methacryloyl [19] methylated, sulfated [20] and esterified [21]	[22]
5.	Tara Gum (TaG)	≈1,000,000 g/mol & CAS No.-39300-88-4	Endosperm of *Caesalpinia spinosa*, Leguminosae	β-D-mannopyranose, α-D-galactopyranose	Carboxymethylated [23] and sulfated	[24]

Sr. No.	Natural Gums	Mol.wt and CAS No.	Sources	Chemical composition	Derivatives	Ref. (Natural Gums)
6.	Tamarind Kernel Gum (TKG)	≈52350 Da & CAS No.-39386-78-2	Seed kernel of *Tamarindus indica*, Fabaceae	Galactosyl, xylosyl, Glucosyl present in the ratio of 1:2:3	Carboxymethylated [25], sulfated, oxidized, thiolated and alkylaminated [26]	[27]
7.	Xanthan Gum(XG)	1000-1500 kDa & CAS No. -11138-66-2	Polysaccharide by *Xanthomonas campestris*.	D-glucuronic acid, β-D-glucose, α-D-mannose, β-D-mannose	Carboxymethylated [28] , oxidized [29], aminated [30]	[31]
8.	Gum Karaya(GK)	≈9500 kDa [10]& CAS No. -9000-36-6	Dried exudate of *Sterculia urens*, Sterculiaceae	rhamno-pyranosyl along with Galactopyranosyl having acetyl and uronic acid groups.	Carboxymethylated [32], dodecenylsuccinic anhydride derivatives [33]	[34]
9.	Cassia Gum(CG)	≈200-300 kDa	Endosperm of *Cassia tora, Cassia obtusifolia*, Fabaceae	Glucopyranosyl, galactopyranosyl and mannopyranosyl units	Carboxymethylated [35]	[36]
10.	Terminalia catappa Gum(TCG)	-	Truck exudate of *Terminalia catappa*, Combretaceae	mannose, D-galactose, L-arabinose, uronic acids and xylose.	Carboxymethylated [37]	[38]
11.	Jhingan Gum(JG)	-	Exudate of *Lannea coromandelica*, Anacardiaceae	Arabino-3,6-galactan containing D-galactose,4-O-methyl uronic acids, L-arabinose, L-rhamnose and some Proteins.	Borax-linked	[39]
12.	Fenugreek Gum(FG)	$\approx 1.4 \times 10^3$ kDa	Endosperm of *Trigonella foenum graecum*, Fabaceae	β-D-mannan units along with α-D-galactopyranosyl groups	Carboxymethylated [40]	[41]

Sr. No.	Natural Gums	Mol.wt and CAS No.	Sources	Chemical composition	Derivatives	Ref. (Natural Gums)
13.	Konjac Gum(KJG)	≈300 kDa & CAS No.-37220-17-0	Tuber of *Amorphophallus konja*, Araceae	D-glucose & D-mannose linked by β-(1, 4) glycosidic linkages	Carboxymethylated [42], oxidized [43]	[44]
14.	Psyllium Gum(PSG)	≈20x10^3 kDa [45]	Seed husks of *Plantago ovata*, Plantaginaceae	Arabinose, xylose, and traces of sugars	Hydroxypropylated [46], succinylated [47], sulphated [48]	[49]
15.	Gellan Gum(GeG)	≈500 kDa [50] & CAS No. -71010-52-1	Fermentation by *Sphingomonas paucimobilis*	Two residues of β-D-glucose, which are β-D-glucuronic and α-L-rhamnose	Carboxymethylated [51]	[52]
16.	Flaxseed Gum/Linseed Gum(LG)	≈1,322 kDa [53]	Seed husk of *Linum usitatissimum* Linaceae	Glucose, xylose, galactose, rhamnose	Carboxymethylated [54]	[55]
17.	Cashew Gum(CWG)	≈28 kDa [56]	Stem exudate of *Anacardium occidentale*, Anacardiaceae	Mannose, glucuronic acid, galactose, rhamnose, arabinose, glucose	Oxidized [57] , carboxymethylated [58], sulfated and acetylated [59]	[60]
18.	Quince seed Gum(QSG)	≈1.4x 10^3 kDa	*Cydonia oblonga*, Rosaceae	Galactose, arabinose, xylose		[61]
19.	Boswellia serrata(BSG) Gum		Injury to bark of *Boswellia serrata*, Burseraceae	β-sitosterin, phlobaphenes, uronic acid, Boswellic acids, terpenoids and oils		[62]
20.	Bael Gum(BaG)		Fruit extract of *Aegle marmelos*, Rutaceae	β-D-galactopyranosyl residues	Carboxymethylated[63]	[64]

Sr. No.	Natural Gums	Mol.wt and CAS No.	Sources	Chemical composition	Derivatives	Ref. (Natural Gums)
21.	Kondagogu Gum(KG)	≈7.23-9.83x 10^3 kDa [65]	Bark exudate of *Cochlospermum gossypium,* Bixaceae	Fructose, arabinose, rhamnose, mannose, galactose, galacturonic acid, glucuronic acid β and α -D-glucose and β-D-galactopyranose	Carboxymethylated [66]	[67]
22.	Sesbania Gum(SG)	≈2.3-3.4x10^5 [68]	Seed extract of *Sesbania aculanta,* Fabaceae	D-mannopyranose group along with D-galacto pyranose units	Carboxymethylated [69], hydroxypropylated [70] thiolated [71]	[72]
23.	Delonix regia gum/flamboyant Gum(DRG)		Endosperm of *Delonix regia,* Fabaceae	(1,4,6)- β -D- mannose, α -D-galactose and (1→ 4)- β -D-mannose.	Carboxymethylated [73]	[74]
24.	Moringa Gum(MoG)	≈190 kDa	Stem exudate of *Moringa oleifera,* Moringaceae	, D- glucuronic acid, D-xylose, L-rhamnose, L-arabinose, D-galactose, D-mannose.	Carboxymethylated [75]	[76]
25.	Okra Gum(OG)		Pods of *Albemoschus esculentu,* Malvaceae	(1→2)-rhamnose, α (1→4)-galacturonic acid & residues constitute side chains of disaccharide	Carboxymethylated [77]	[78]
26.	Neem Gum(NG)	≈6.4 x 10^5-12.0 x 10^5 g/mol	Stem injury of *Aazadirachta indica,* Meliaceae	galactose, glucuronic acid, xylose, arabinose, proteins, Amino Acids and some salts of Ca, Mg, Na, and K.	Carboxymethylated [79]	[80, 81]

Sr. No.	Natural Gums	Mol.wt and CAS No.	Sources	Chemical composition	Derivatives	Ref. (Natural Gums)
27.	Agar Gum(AG)	CAS No. -9002-18-0	Species of Red algae *Gelidium sp. and Gracilaria sp*	D -galactose, L -galactose, linked by repeated units of α -(1→ 3) and β -(1→4) glycosidic bonds	Octenyl succinic anhydride-Agar [82]	[83]
28.	Gum acacia(GA)	≈250-600 kDa [10] CAS No.-9000-01-5	*Acacia senegal, Acacia mearnsii,* Leguminosae	D-glucuronic acid, L-arabinosefuranose, L-rhamnose and D-galactose		[2]
29.	Copal Gum(CoG)	CAS No.-9000-14-0	Sap of *Bursera bipinnata*, Burseraceae	agathic acid, monomethyl ester of agathalic acid. along with cis and trans -communic acid & poly-communic acid, sandaracopimaric acid, acetoxy agatholic acid and agathalic acid		[84]
30.	Dammar Gum(DG)	CAS No. -9000-16-2	Tapping of *Dipterocarpus kerri*, Dipterocarpaceae	Series of tetracyclic dammarane skeleton, along with, ursane, pentacyclic oleanane and hopane derivatives		[85, 86]
31.	Brea Gum(BG)	1,890 x 10^3g/mol [87]	Exudate of *Cercidium praecox*, Fabaceae	β-(1,4)-l- D-xylan D-xylose, D-glucuronic acid and L-arabinose.		[87,88]
32.	Pistacia Gum(PAG)		Resin from *Pistacia atlantica*, Anacardiaceae	galactose, arabinose, rhamnose, glucose and xylose		[89]

Sr. No.	Natural Gums	Mol.wt and CAS No.	Sources	Chemical composition	Derivatives	Ref. (Natural Gums)
33.	Welan Gum(WG)	CAS No. -96949-22-3	Fermentation of sugar by *Alcaligenes sp*.	1,3-D-glucopyranosyl, β-1,4-D-glucopyranosyl, β-1,4-D-glucuronopyranosyl and β-1,4-L-rhamnopyranosyl		[90]
34.	Sage seed Gum(SSG)	4×10^2-1.5×10^3kDa	Seed of *Salvia macrosiphon*, Labiatae	Mannose and galactose		[91]
35.	Balangu seed Gum(BGSG)	3650 kDa	Seed of *Lallemantia royleana*, Labiatae	Arabinose, rhamnose, glucose, xylose, galactose		[92]
36.	Qodume Shirazi seed Gum(QSSG)	$3.66x10^2$kDa	Seed of *Alyssum homolocarpum*, Brassicaceae	Arabinose, galactose,rhamnose, glucose, xylose		[93]
37.	Espina Corona Gum (ECG)	$1.39 x10^3$kDa	Seed of *Gleditsia amorphoides*, Fabaceae	Galactomannans		[94]
38.	Qodume Shahri Gum (QoSG)		Seed of *Lepidium perfoliatum*, Brassicaceae	Xylose, arabinose, galactose rhamnose glucose,		[95]

Table 1.2: Structure of different natural gums

1.	Tragacanth gum(TG) [96]	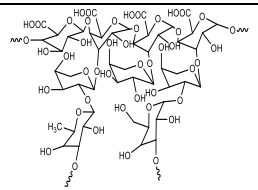	13.	Kondagogu Gum(KG) [97]	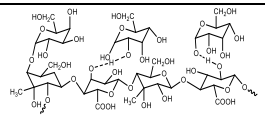
2.	Gum Ghatti(GG) [98]	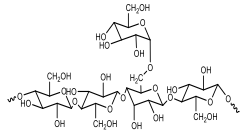	14.	Sesbania Gum(SG) [68]	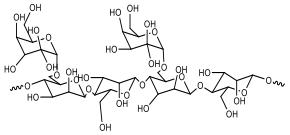
3.	Locust Bean Gum(LBG) [99]	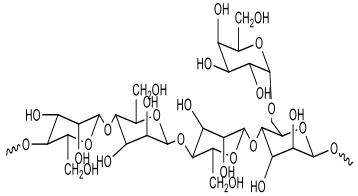	15.	Moringa Gum(MoG) [100]	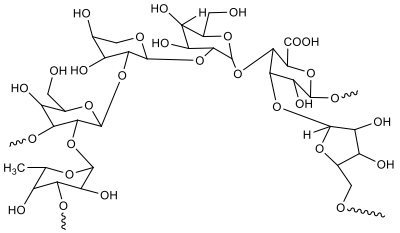
4.	Guar Gum(GuG) [101]	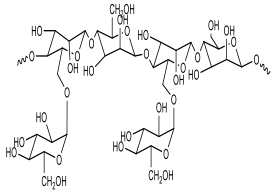	16.	Okra Gum(OG) [102]	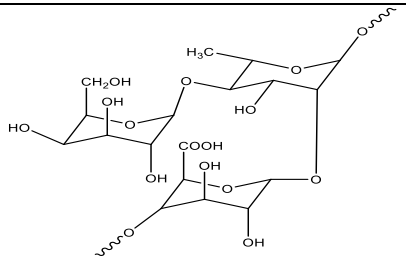

5.	Tara Gum (TaG) [103]	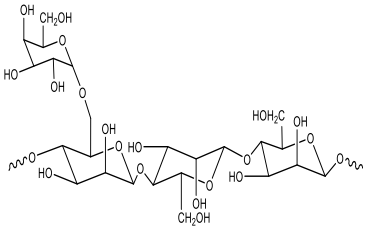	17.	Neem Gum(NG) [104]	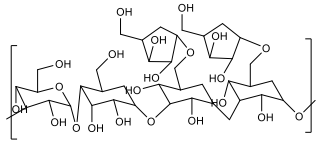
6.	Tamarind Kernel Gum (TKG) [99]	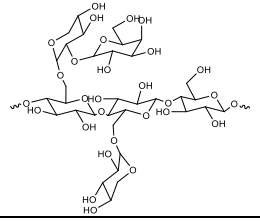	18.	Agar Gum(AG) [105]	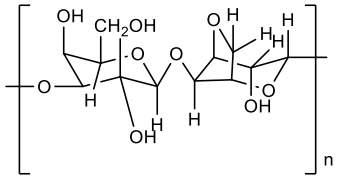
7.	Xanthan Gum(XG) [29]	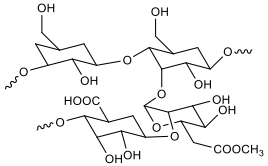	19.	Gum acacia(GA) [106]	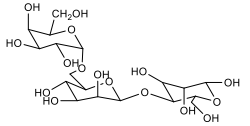
8.	Gum Karaya(GK) [107]	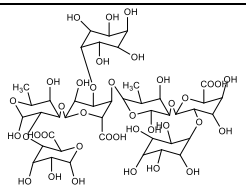	20.	Brea Gum(BG) [108]	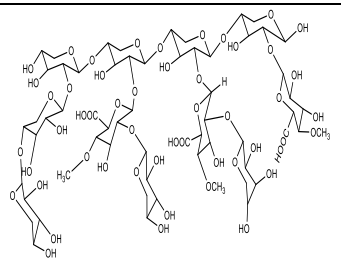
1.	Tragacanth gum(TG) [96]	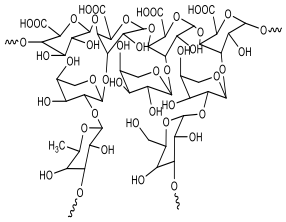	13.	Kondagogu Gum(KG) [97]	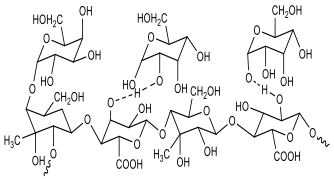

2.	Gum Ghatti(GG) [98]	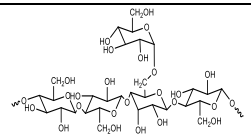	14.	Sesbania Gum(SG) [68]	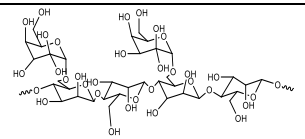
3.	Locust Bean Gum(LBG) [99]	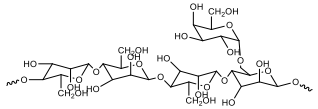	15.	Moringa Gum(MoG) [100]	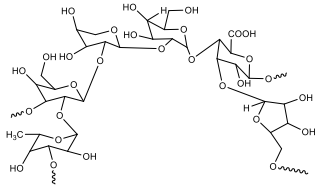
4.	Guar Gum(GuG) [101]	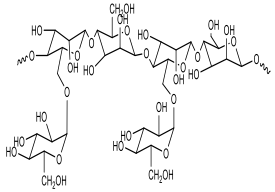	16.	Okra Gum(OG) [102]	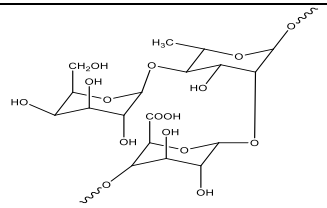
5.	Tara Gum (TaG) [103]	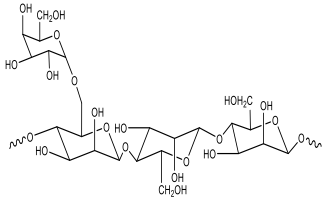	17.	Neem Gum(NG) [104]	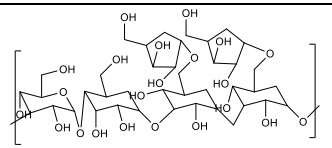
6.	Tamarind Kernel Gum (TKG) [99]	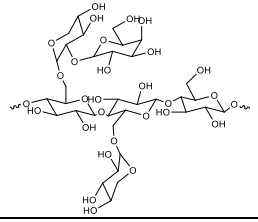	18.	Agar Gum(AG) [105]	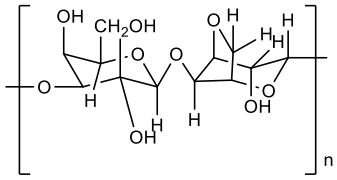

7.	Xanthan Gum(XG) [29]	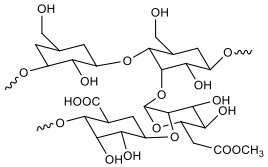	19.	Gum acacia(GA) [106]	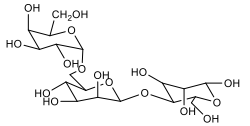
8.	Gum Karaya(GK) [107]	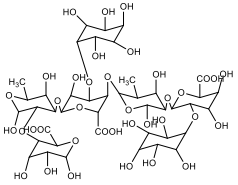	20.	Brea Gum(BG) [108]	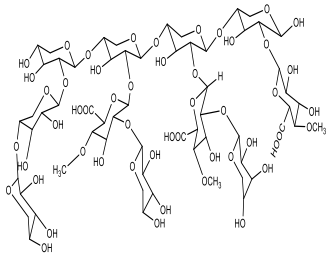
9.	Cassia Gum(CG) [109]	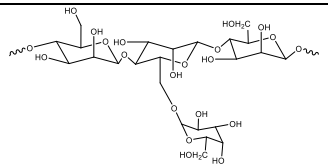	21.	Welan Gum(WG) [110]	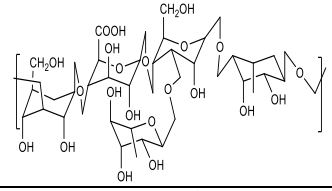
10.	Fenugreek Gum(FG) [99]	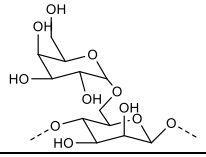	22	Gellan Gum(GeG) [111]	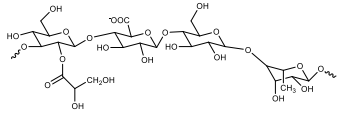

11.	Konjac Gum(KJG) [112]	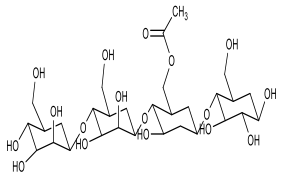	23	Cashew Gum(CWG) [113]	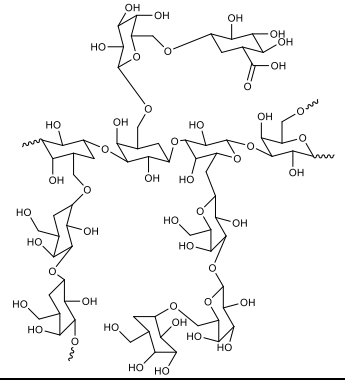
12.	Psyllium Gum(PSG) [114]	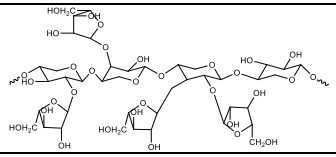	24	Quince seed Gum(QSG) [115]	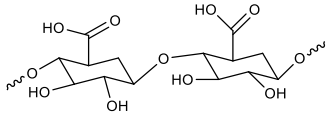

1.3 Hydrogels

Hydrogels are polymeric matrices of three-dimensional hydrophilic structures that absorb significant amounts of water or body fluids [1]. Natural gum based-hydrogels shows tunable swelling properties, due to which they become super-absorbent [116]. Hydrogels are useful material for biomedical applications, agriculture [117], separation technologies [118], biosensor [58] and tissue engineering [119]. . The limited use of these hydrogels is a result of their weak mechanical characteristics. The hydrogels' poor mechanical qualities result from the high water content in their network structure, which makes them brittle and uses energy inefficiently. Therefore, the problem has to be solved to provide hydrogels better mechanical characteristics [120]. Mechanical and thermal properties of hydrogels can be enhanced by grafting of natural polysaccharides with synthetic monomers, derivatization [121] or by adding nanoparticles [122]. Bonifacio et al. had synthesized the gellan gum based hydrogel with better mechanical property by adding manuka honey [123]. Chitin nano-crystals were used by Jung HS et al. to synthesized robust hydrogel. A wide range of hydrogels with high mechanical strength and plasticity have been developed for a variety of applications [117,118], especially in bio-medical field, for examples, commercially used wound dressings, hygiene products and contact lenses. A hydrogel's pre-gel fluidity enables it to fill irregular voids and curves without the requirement for pre-shape formation. Hydrogels are appropriate for use as scaffolds in tissue engineering because of their water-retention capacities and network structure, which are comparable to those of the extracellular matrix. Since gel solutions may be loaded with drugs and antibiotics, hydrogels are being studied for their application as drug carriers. As carrier, hydrogels protects the loaded drugs from degradation and also controlled their release [126].

Electrospun fibres of natural polymers also have enormous application. The three methods that can presently be used to create nanofibers are phase separation, self-assembly, and electrospinning. The approach that has received the greatest research attention and appears to have the most potential for use in tissue engineering is electrospinning which turns polymeric biomaterials into nanofibers and also controls the thickness and composition of synthesized nanofibers [127]. Nanofibrous biopolymers have mainly been used in the pharmaceutical and medical industries to create wound dressings and scaffolds for tissue engineering. Furthermore, wastewater treatment, environmental, biotechnology, food and energy sectors have risen significantly [128]. Azarniya et al., by combining electrospraying and electrospinning, synthesized the new composite scaffolds made of thermosensitive GT-based hydrogel particles for wound healing [129]. The electrospinning method was used to effectively create the poly lactic acid and guar gum hybrid nanofibers that were loaded with thyme essential oil for food packaging [130]. Padil T V et al. developed the membrane electrospun with GK and poly (vinyl alcohol) for the separation of nanoparticles of metal and metal oxides from aqueous phase [131]

The hydrophilic functional groups on the polymer chain, such as -NH2, -COOH, and -OH groups, enable hydrogel sponge-based superabsorbent to effectively absorb water [132]. According to previous literature, biopolymer-made sponges might be used as wound dressings for managing highly exuding wounds. Ngece et al. synthesized alginate and gum acacia sponges cross-linked by using $CaCl_2$, loaded with ampicillin and norfloxacin. The sponges showed strong water absorption and good porosity. They may be used for high-exuding wounds because they absorb water quickly [133]. Maciel S et al. using a freeze-drying technique synthesized oxidised

cashew gum and gelatin based hydrogel sponges. These mechanically durable and permeable materials can promote cell adhesion and growth, resulting in the possibility of employing them to regenerate soft tissues [57].

1.3.1 Classification and Properties Of hydrogels

Hydrogels can be classified into different categories as shown in figure 1.1 on the basis of source, cross-linking, composition, structure, physical properties, ionic charges, response and degradability.

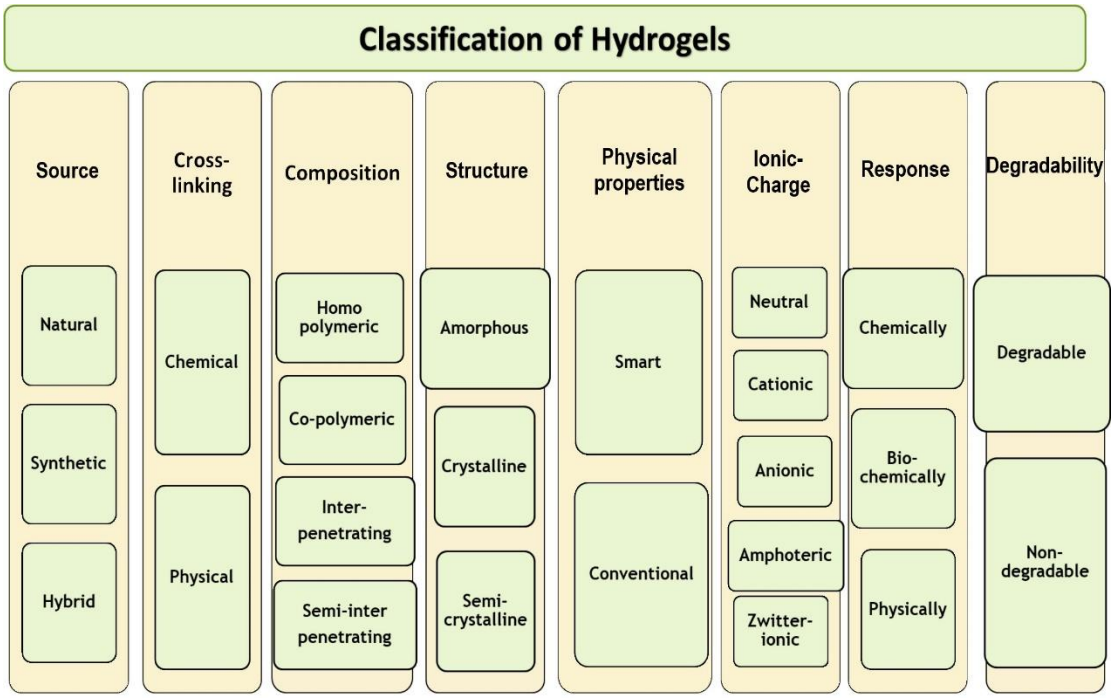

Figure 1.1: Classification of hydrogels based on various parameters

1.3.1.1 Classification on the Basis of Source

Based on its source, hydrogels are classified into three important categories, i.e., natural, synthetic and hybrid. Polysaccharides and polypeptides are two subcategories of natural hydrogels. Synthetic hydrogels, on the other hand, is generally made from polyethylene glycol and polyamides. Natural polymers have gradually been replaced

with completely synthetic or hybridized polymers during the last two decades to give improved product life, high viscosity, and moisture content [134]. In hybrid systems, a minimum of two elements, a synthetic macromolecule and a polysaccharidic domain; are combined [135].

1.3.1.2 Classification on the Basis of Linking

1.3.1.2.1 Chemical Cross-Linking

Chemical cross linking includes multiple type of cross- linking that are explained below:

1.3.1.2.1.1 Chemical Reaction

Many composed-methodologies have been endorsed to synthesize hydrogel by chemical techniques [136]. Schiff-base reaction, click reaction, epoxide coupling, addition reaction, free radical co-polymerization, genipin coupling, poly carboxylic acid-based esterification are examples of chemical cross-linking. The technique primarily involves the production of cross-linked webs by introducing new molecules between the polymeric chains [137], thus leading to the formation of a complex structure with numerous cavities. Methodology of chemical cross-linking is shown in Figure 1.2.

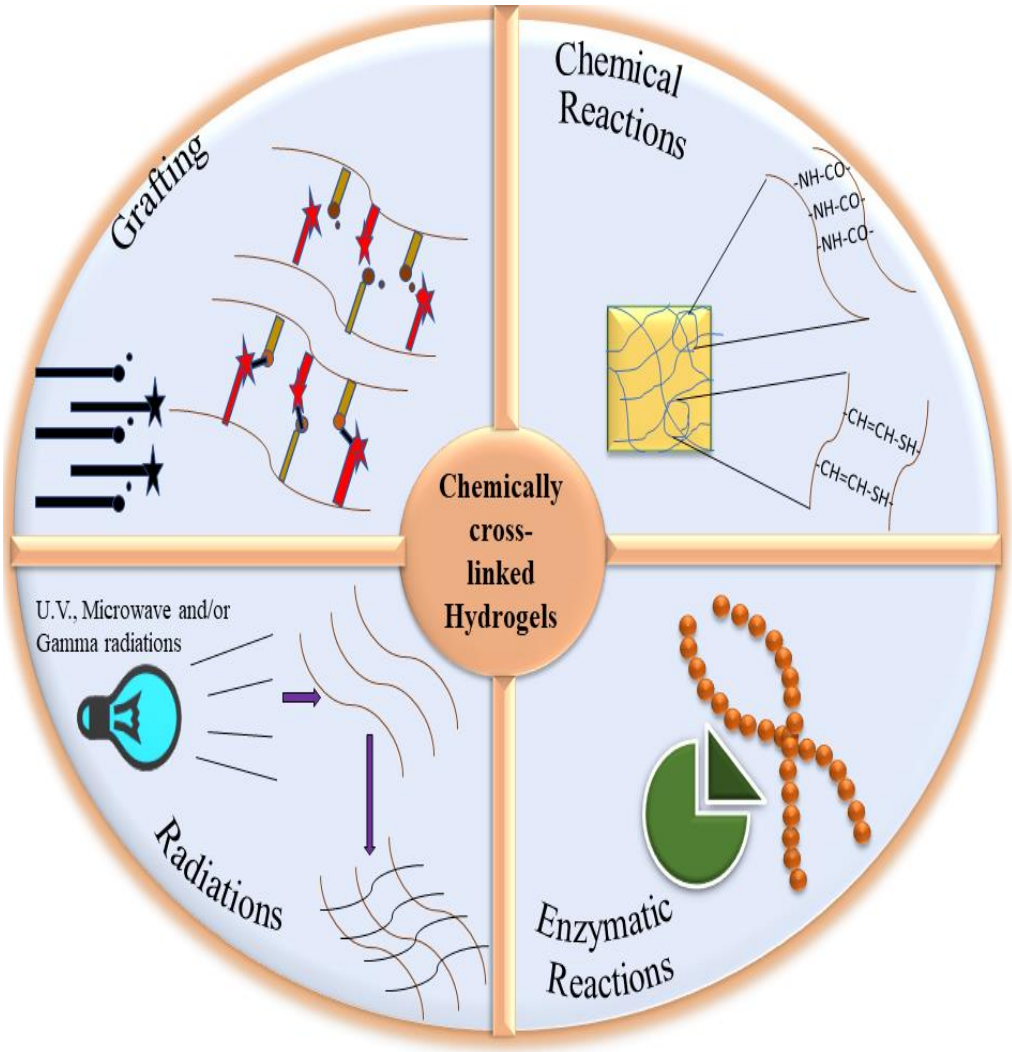

Figure 1.2: Techniques for synthesizing chemically cross-linked hydrogels

1.3.1.2.1.2 Grafting and Irradiation

Grafting is generally carried out by using chemicals or radiations, which are referred to as chemical and radiation grafting, respectively [138]. Broadly, hydrogels are made by grafting synthetic monomers onto natural polymeric chains. The main roots for the production of maximal hybrid polymer are multifunctional free-radical vinyl monomers. Every monomer has a double-bonded carbon that propagates the growth of a polymeric chain via an active radical centre. The possibility of radical formation is dependent on the type of reaction state, solvents and particular monomers that can be

initiated by photons, heat, enzymes or electron beams [139]. To initiate the polymerization process radioactive sources are also utilised which produces particle accelerators that include electrons, alpha particles, and neutrons, whereas electromagnetic radiations include X-rays and **γ**-rays. The chemical effects of different types of radiations are qualitatively similar, but differ quantitatively. Radiation dose can also controlled the swelling of the hydrogels. Singh B et al. reported Gum Tragacanth (GT) based hydrogel cross-linked by radiations and loaded with antibacterial and analgesic drugs [140]. Other hydrogels based on Sterculia gum polysaccharide with graphene oxide and carbopol have been prepared using radiation induced graft copolymerization. Swain S. et al. has developed a Guar gum & Carrageenan based micro-porous interpenetrating polymer network treated with microwave irradiation [141]. Said et al. (2004) synthesised Carboxy Methyl Cellulose based hydrogel using electron beam irradiation grafted with acrylic acid [142].

1.3.1.2.1.3 Enzymatic Reaction

The use of an enzyme-catalyzed cross-linking process between polymer chains to generate an *in-situ* hydrogel is a novel method. Peroxidases [143], tyrosinase [144] , transglutaminase [145], were also investigated as linking agents for hydrogel synthesis. Enzymes are highly specific towards a substrate. It suppresses the side reactions. Interfacial enzyme polymerization and amide bioconjugation can be utilised to control the mechanical strength of hydrogels, in general. Pan et al. demonstrated that xanthan gum and glucose oxidase enzyme with glucose or N-Hydroxy succinamide produces nitrogen radicals swiftly and efficiently to induce polymerization in absence of oxygen [146].

1.3.1.2.2 Physical Cross-Linking

Physical cross-linking comprises interaction of ions which includes polyelectrolyte complexation, hydrogen bonding & hydrophobic association [147]. The various techniques used to synthesize physically cross-linked hydrogels are shown in figure 1.3.

1.3.1.2.2.1 Heating/Cooling

Change in the temperature of a polymer solution causes the emergence of gel because of the linking of helices, helix-genesis & forming linking sectors. Cooling hot solution of carrageenan or gelatin will fabricate a gel due to the formation of the helix [148]. Jeong et al. synthesized a tri-block copolymer composed of polyethylene glycol, poly lactic acid and glycolic acid arranged as (PEG-PLGA-PEG) that included in aqueous solution which behave as a sol at ambient temperature and transforms into a gel at 37^{o}C [149].

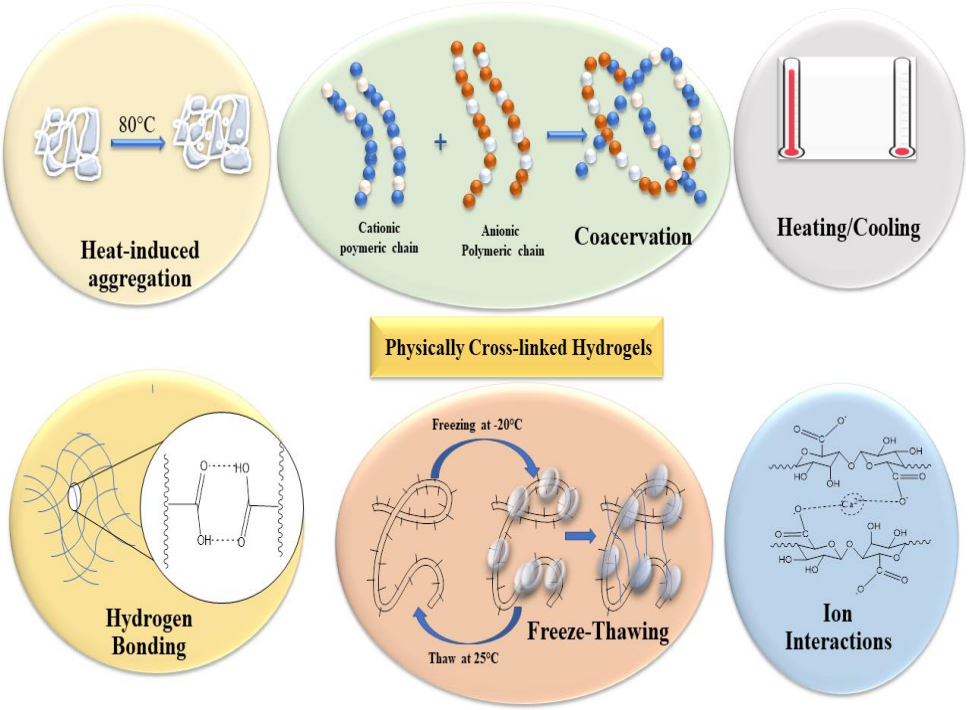

Figure 1.3: Techniques for synthesizing physically cross-linked hydrogels

1.3.1.2.2.2 Complex Coacervation

Complex coacervation demands soluble and insoluble complexes formed by the interactions of polymers with opposite charges which in addition depends on the pH and concentration of solutions [150]. Chitosan-xanthan mixture's membranes shows coacervation of polyanionic xanthan with polycationic chitosan [151].

1.3.1.2.2.3 Ionic Interaction

The fundamental principle of gelling in ionic interaction is agglomerations of polyelectrolyte solution with multivalent ions bearing opposing charges [136]. Maiti et al. fabricated a β-glycerophosphate and sodium bicarbonate crosslinked chitosan-gelatin-oxidized guar gum hydrogels [152].

1.3.1.2.2.4 Hydrogen Bonding

The H-bond is formed when an electron-deficient H-atom joins forces with electronegative functional moiety. The factors which play role in hydrogels synthesis are polymer's molar ratio, solvent type, temperature of solution and polymer's structure [153]. Tkigami et al. produced a pH-sensitive as well as H-bonded hydrogels, where casting solution was dispersed in 0.1 M HCl to produce a hydrogen-bonded carboxymethyl cellulose network [154].

1.3.1.2.2.5 Freeze Thawing

The freeze thawing process is used to synthesis gels in moderate conditions in the absence of initiators and toxic crosslinking agents [155]. This process includes freeze-thaw cycles of 18 and 6 hours respectively (time can be varied according to the type

of monomer). Microcrystals are formed in the structure as a result of this process. The process was used for the synthesis of gum cassia gum-based hydrogels [156].

1.3.1.2.2.6 Heat-Induced Aggregation

Acacia senegal was matured to enhance the agglomeration of acacia gum constituents that are linked with modest quantities of protein, resulting in the formation of more arabinogalactan protein [157] . Shengjie Lv et al. developed a hydrogel based on cross-linked polyacrylamide grafted with poly (N-isopropylacrylamide). These hydrophilic hairy thermo-responsive hydrogel particles might be used as transporters to key target areas [158].

1.3.1.3 Classification on the Basis of Compositions

Hydrogels are classified as homopolymers, copolymers, semi-interpenetrating networks(SIPN) and interpenetrating networks(IPN) based on their compositions [139]. Homo-polymerisation is done by single monomer species and act as a basic structural unit of polymeric web [159]. It includes crosslinked- structure which depends upon the type of the monomer and technique adopted for polymerisation. Chemically crosslinked PEG hydrogels are suitable biomaterials for the controlled and structured release of medicines, proteins, macromolecules, and growth factors. Co-polymerisation involves two different monomers, between two, one should be of a hydrophilic nature [160]. A co-polymerized hydrogel was developed by Hemant et al. in which hydrolysis was done on base-catalyzed and water-condensation process. These process were responsible for the dispersion of gum karaya and polyacrylic acid and help in crosslinking with acrylamide co-polymer [161]. SIPN made up of a crosslinked polymer network and a linear polymer network that are physically

entangled and interpenetrated. When compared to hydroxypropyl methyl cellulose (HPMC) alone, the SIPN of gellan gum and HPMC exhibited more tunable and improved rheological behaviours and textural qualities [162]. Ying zhao et al. developed a SIPN network hydrogel made of poly (acrylic acid) and poly (aspartic acid) that responds differently in diverse environments [163]. IPN are typically classified as the inter-connection of two polymers, and one of two gets crosslinked in the instantaneous occurrence of other [164]. IPN of chitosan and poly(acrylic acid) based hydrogels was synthesized by UV irradiation [165].

1.3.1.4 Classification on the Bases of Structure, Physical Properties, Ionic Charge, Response and Degradability

Based on the structure, hydrogels can be described as amorphous, crystalline and semi-crystalline [166]. Smart and conventional are the two categories of hydrogel on the basis of physical properties. Stimuli-responsive hydrogels are composed of favourable smart materials, respond according to the fluctuation in surrounding environment like ionic strength, pH, temperature, light and magnetic field [167]. A conventional hydrogel will not be influenced by the environmental changes [168]. When it comes to ionic charge, hydrogels can be classified as cationic, anionic, neutral, zwitter-ionic and amphoteric [169]. When exposed to varied pH buffers, hydrogels tend to alter form, making them chemically sensitive. A pH-responsive hydrogel has been synthesized by Reis et al. using arabic gum, modified chemically by using glycidyl methacrylate [170] which is DNA, Glucose and oxidation responsive as well. Tan et al. fabricated chitosan-hyaluronic acid-based glucose responsive injectable biodegradable hydrogels [171]. Hydrogels are also

biochemically responsive to antigens, enzymes and ligands. The antigenicity of hydrogels is studied by Souza et al. by developing nanostructured antigen-responsive hydrogels [172].

1.3.2 Applications of Natural Gums-Based Hydrogels in Multiple Fields

Hydrogels have vast applications in extensive fields given in figure 1.4. A numerous applications of hydrogels are explained in this review to reveal the imminent significance of the natural gums and their derivatives and the examples are enlisted in table 1.2 and 1.3 respectively.

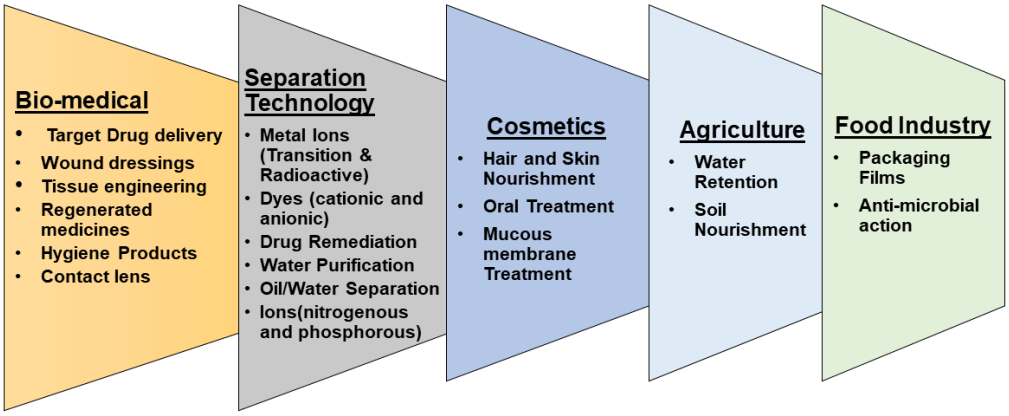

Figure 1.4: Applications of hydrogels in different fields

Table 1.3: Applications of natural gums in different fields

Sr.no.	Natural Gums	Bio-medical Applications	Agricultural Applications	Separation techniques	Cosmetics	Food Industry
1.	TG	Thermal Cross-linking of PEGDA, PVA & TG for wound dressing [173]	Lipase enzyme catalyzed TG-poly(AAm-MAA) IPN hydrogel for release of urea and calcium nitrate in soils [174]	Microwave assistedTiO2 loaded HEMA- TG hydrogel nanocomposite for malachite green dye separation [175]		Ionic cross-linked Gelatin-ZnO-NPs-TG based anti-microbial film used for packaging [122]
2.	GG	Ceric ammonium nitrate-based graft polymerisation of methyl methacrylate onto GG for metformin hydrochloride drug delivery [176]	Graft co-polymerisation of poly(MAA) onto GG for enhancing soil water retention property [177]			Ionic cross-linked GG-sorbitol/glycerol/erythritol based film for food packaging[178]
3.	GuG	Sodium alginate, PVA and GuG was blended by solution casting method for release of verapamil hydrochloride [179]	Benzoyl chloride cross-linked ethylene-glycol-di-methacrylate grafted onto GuG with boron for agricultural applications [180]	Chemically cross-linked TiO2 mediated GuG based hydrogel for methylene blue absorption [181]	GuG-Histoacryl-PVA-PVP based cosmetic- adhesive [182]	GuG-PVA-chitosan based biopolymeric film for packaging [183]
4.	TaG	TaG-co-XG hydrogel loaded with Brazilian cherry juice microparticles by freezing method [184]	Gamma radiation mediated TaG-co-AAc-based superabsorbent hydrogel [185]		TaG and Polyquaternium-7 grafted onto poly(AAc) for synthesizing antibacterial superabsorbent hydrogel [186]	TaG-co-oleic acid based edible film [187]
5.	TKG	chemically cross-linked PVA-co-TKG-co-bentonite based ciprofloxacin hydrochloride loaded composite film [188]		Free radical copolymerization of TKG and polymethyl methacrylate for removal of toxic dyes [189]	TKG-co-CNC-co-polyacrylamide based graft hydrogel for artificial skin [190]	
6.	XG	XG-g-CH-g-AMPS based hydrogel for delivery of acyclovir [191]	HEMA-g-AAc g-XG based chemically cross-linked hydrogel [192]	Physically cross-linked PVA and XG for methylene blue absorption [193]	Curcumin loaded XG and LB gum-based hydrogel [194]	XG, carrageenan and gellan gum-based citric acid mediated hydrogel for packaging application [195]

Sr.no.	Natural Gums	Bio-medical Applications	Agricultural Applications	Separation techniques	Cosmetics	Food Industry
7.	GK	Quercetin loaded GK-g-poly(AAc) based free radical polymerization of hydrogel [196]		GK-g-poly(AAc)-SiC based graft co-polymerization of malachite green and rhodamine B loaded hydrogel [197]		Cinnamaldehyde grafted GK-g-cloisite sodium-based film for packaging [198]
8.	CG			-		CG-based packaging film with glycerol and sorbitol as plasticizers [199]
9.	JG			Remazol brilliant blue R elimination using a borax cross-linked JG based hydrogel [39]		-
10.	FG	1-allyl-3-methylimidazolium chloride mediated FG and cellulose based hydrogel loaded with methylene blue for wound healing [200]	Borax cross-linked FG based hydrogel synthesized by freeze-thaw method for agricultural application [201]	Microwave and thermally synthesized hydrogel by co-polymerization of FG with AAm and CAN for water treatment [202]	TEMPO-mediated aerogel synthesized by FG and other galactomannans with laccase oxidation for cosmetics [203]	Micro-fibrillated fiber mediated Pectin and FG based film for packaging [204]
11.	KJG	Ionic cross-linked SA-g-Ha-g-KJG hydrogel loaded with l-Ascorbic Acid [205]	KJG-XG based gel loaded with urea for agricultural applications [206]	Calcium oxide based KJG and GO hydrogel used for water purification [207]	KJG, XG, pullulan and carrageenan and optically sclerotium gum-based hydrogel for cosmetics[208]	Glycerol based agar, carrageenan & KJG film for packaging [209]
12.	BG	HCl mediated BG and pectin-based hydrogel for drug delivery [88]				Using dispersion method, BG and Montmorillonite based film for packaging [210]
13.	GeG	Hydrogel synthesized by using 6-(6-aminohexyl) amino-6-deoxy-GeG-β-cyclodextrin complex loaded with dexamethasone used for cartilage regeneration [211]	Chemically cross-linked GeG and PEG hydrogel used for agricultural purpose [212]	microwave assisted GeG-g-poly(AA-g-MAA) based hydrogel used for removal of methylene blue & malachite green dyes [213]	$CaCl_2$ mediated Levan and GeG hydrogel used pharmaceutical and cosmetics [214]	EDTA mediated carrageenan-XG-GeG-citric acid-based film for packaging [195]

Sr.no.	Natural Gums	Bio-medical Applications	Agricultural Applications	Separation techniques	Cosmetics	Food Industry
14.	LG	PVP-g-Linseed based hydrogel loaded with diclofenac sodium for drug release study [215]	Epichlorohydrin cross-linked linseed and cellulose based urea loaded hydrogel for water retention property [216]			Glutaraldehyde cross-linked flaxseed gum and glycerol film used for multiple purpose [217]
15.	BSG	Gamma radiation mediated BSG-g-AAm-g-AAc silver nanocomposite-based hydrogel for antibacterial property [218]				-
16.	QSG	Chitosan-QSG based hydrogel encapsulated with curcumin loaded HNT applicable in Tissue engineering [219]		QS mucilage, $FeCl_3$, $FeCl_2$ and NH4OH based nanocomposites used for the absorption of dye [220]		QS mucilage and nano clay-based packaging film [221]
17.	DRG	CAN mediated N-isopropylacrylamide and DRG based copolymerization for the delivery of Amphotericin [222]				Different M wt. DRG with k-carrageenan based edible films [223]
18.	PAG		PAG-AAc-AAm-AN based super adsorbent hydrogel [89]			
19.	WG			WG-GO based hydrogel for multiple water-soluble dye removal from waste water [90]		
20.	CoG			Collagen-CoG-poly(AAc-AAm) based hydrogel for dye removal [224]		
21.	PSG	Glutaraldehyde and NN-MBA cross-linked PSG-g-AAc-g-AN based polymer loaded with 2-Chloro-3-(4-hydroxyphenylamino) naphthalene-1,4-dione for anticancer property [225]	KCl mediated Montmorillonite-carragennan -PSG based hydrogels for agricultural applications [226]	XG-PSG-g-poly(AAc-g-itaconic acid) based hydrogel removal of auramine-o and EBT [227]		PSG-modified starch based film for food packaging [228]

Sr.no.	Natural Gums	Bio-medical Applications	Agricultural Applications	Separation techniques	Cosmetics	Food Industry
22.	BaG	Microwave assisted Poly(AAm)-g-BaG based hydrogel loaded with diclofenac sodium [229]				GG-g-BaG-g-PVA-g-gelatin based film for food packaging [230]
23.	KG	Metronidazole loaded, UV radiation assisted PVP-KG based hydrogel [231]		SA and KG based sponge for absorption of organic solvent [232]		Glycerol based SA-g-KG packaging film for food stuff [233]
24.	SG	Microwave assisted SG-g-Poly(AAm) based hydrogel loaded with 5-FU [234]		Microwave assisted diallyldimethylammonium chloride-g-AAm-SG based copolymerization can be used for water treatment [235]		SG-deacetylated chitosan based anti-bacterial film for food packaging [236]
25.	DG	Atenolol loaded Zirconium oxychloride mediated DG-g-poly(AAm) based hydrogel [86]		DG-poly(AAm) based hydrogel incorporated with zirconium-iodo oxalate synthesized by free radical polymerization used for lead removal [85]		
26.	MoG	Levofloxacin loaded MoG-g-sterculia gum-g-poly(AAm) based hydrogel film for wound dressing [100]	Borax cross-linked PVA-g-MoG based super absorbent hydrogel applicable in agriculture [76]	MoG-Acryloyl chloride-based adsorbent for Hg^{2+} removal [237]		
27.	OG	OG-g-Gelatin-MAA based graft polymerization for cancerous drug- cytarabine delivery [238]				Ammonium acetate mediated OG-CH based films for food stuffs [239]
28.	NG	Methotrexate loaded NG-AAc based free radical polymerization for the drug delivery [240]				-
29.	CWG	Sodium metaperiodate mediated CWG-PVA-trypsin based wound healing films [241]	CWG-glycidyl methacrylate-AAm based hydrogel for agricultural application [60]			Sodium metaperiodate mediated CWG-PVA films produce by casting method for food packaging [242]

Sr.no.	Natural Gums	Bio-medical Applications	Agricultural Applications	Separation techniques	Cosmetics	Food Industry
30.	GA	Moxifloxacin loaded N-vinylpyrrolidone-GA-carbopol based free radical polymerization for wound healing [243]	GA-AAm-KA based free radical polymerization for release of drugs and agrochemicals [244]	GA-poly(acrylamide)-based free radical polymerization [245]		Fish gelatin-oxidised tannic acid-GA based gel prepared by coacervation [246]
31.	LBG	LBG-SA based IPN microspheres loaded with Ibuprofen [247]		LBG-g-poly(DMAAm) based free radical polymerization for adsorption of brilliant green dye [248]	XG-LBG based film for curcumin delivery [194]	k-carraeenan-LBG-giycerol based edible film for food stuffs [249]
32.	SSG	Laponite-SSG based physically cross linked hydrogels as bio medical carrier [250]				SSG-glycerol-PEG based films for packaging [251]

1.3.2.1 Bio-Medical Applications

Due to the similarity between the structure of hydrogels and biological soft tissues, they are frequently utilised in the field of medicines [120]. Properties of hydrogels like gel-forming capacity, bio-safety, high absorption capacity, biodegradability, non-toxicity, high stability and biocompatibility also make them more suitable for bio-medical applications [252]. Because of their high biocompatibility with live tissues, hydrogels are in high demand in tissue engineering [253]. Tissue engineering promotes tissue regeneration and repair by using thermo-responsive polymers that are also reliant on monomer qualities like degradability and biocompatibility. 3D bio-printing has become a promising technique to design and create structures that will replace damaged tissues and malfunctioning organs by using patients' own cells [254]. Natural polysaccharides and its hydrogels have drawn more attention among the various biomaterials because of their capacity to mimic the extracellular matrix and provide an environment suitable for cell viability and proliferation [166,167]. Hydrogel applications, such as new-born diapers, are gaining popularity as a result of their super absorbent properties [257]. Quantum dots (QDs) embedded in a hydrogel web have been employed as biosensors in the recent past. A glucose biosensor with extreme sensitivity has been successfully synthesized by using GT nanoparticles [258]. Figure 1.5, depict a variety of biomedical applications.

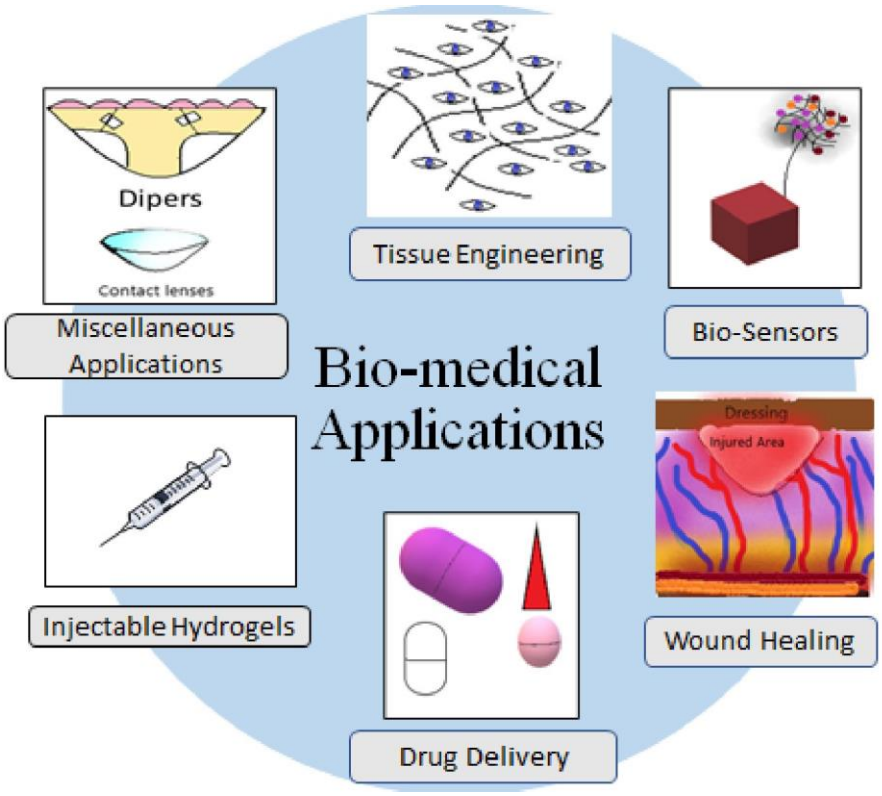

Figure 1.5: Bio-medical applications of hydrogels

When it comes to removing necrotic and injured cell structures by healing the skin epidermis and helping in tissue regeneration, hydrogels maintain their diversity and attractiveness [259]. The site of healing is prone to microbial contaminations, and is a major cause of delayed tissue repairment [260]. The ideal wound healing phenomenon must cause the reduction of tissue necrosis, enough perfusion of tissues with a moist patch for the refurbishment of the tissue anatomy and proper functioning of the damaged area [261]. Singh et al. in (2017) reported the development of a wound dressing by using natural gums [243]. The use of a renewable natural polymer mediated by a green synthetic polymerization process, which comprises drug-loaded guar gum and dimer acid films, has been described as a better wound dressing polymer due to improved wound healing properties and aesthetic features [262]. Injectable hydrogels have proven their biomedical applications by satisfying a few

conditions, like the fluidity of injectable solutions at suitable pressure, maintaining required integrity and strength, and laying quickly at the target site. The hydrogel's constituents should also be biocompatible and produce the least amount of cytotoxicity. Natural biopolymer-based hydrogels met these criteria because of their excellent biocompatibility, minimal immunogenicity, and susceptibility to hydrolysis/human enzyme degradation [263].

1.3.2.2 Agricultural Applications

Hydrogels have been employed in agricultural sector as well. Hydrogels have been utilised for micronutrient additions, controlled fertilisers release, improving the water consumption property of the soil (Figure 1.6) and achieving desired features of agricultural product without harming the environment [264], that can be only possible by the biodegradability of the polymer. The word "biodegradable" is frequently used to describe a variety of polymers and polymer composites that can disintegrate into their component parts under physiological or physiologically sound environments. These polymers have chemical linkages at the molecular level that can be broken down under favourable ecological factors. Both in vivo and environmental deterioration are examples of ecologically suitable conditions [265].

A super-absorbent hydrogel based on guar gum and loaded with Boron was developed for improved soil fertility [180]. Water retention capacity and fertilizer availability in the soil can improve agricultural production. A cashew gum based superabsorbent-hydrogels loaded with potassium hydrogen phosphate as a fertilizer was reported by Rodrigues et al. to show the improvement in soil property [266].

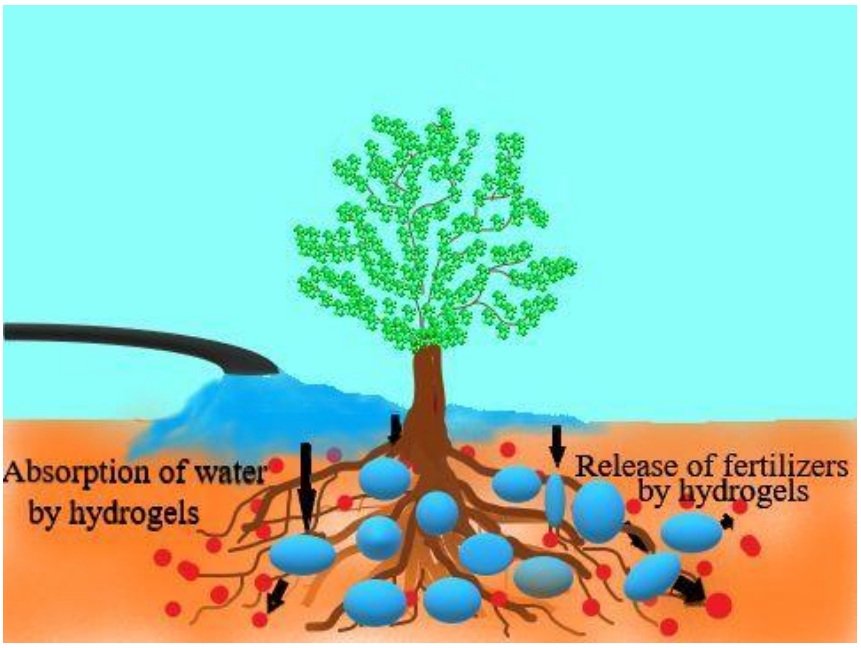

Figure 1.6: Hydrogel applications in Agriculture

1.3.2.3 Applications of Hydrogels in Separation Technology

The major pollutants of fresh water are heavy metals like cadmium, arsenic, lead, nickel, copper, mercury, chromium and zinc due to their non-biodegradability, toxicity and continual property [267]. Therefore, it is necessary to eliminate or reduce the level of these pollutants in water sources. Among the different strategies for removing pollutants, absorption is the most easy, cheap, and incredibly efficient method [268]. Ranjbar-Mohammadi et al. [269] developed a methylene blue adsorbent polymer based on GT. Another green-polymer-based adsorbent i.e., GT and carboxyl-functionalized carbon nanotube hydrogel, was developed to remove methylene blue from water [270].

1.3.2.4 Applications of Hydrogels in Cosmetics

When used in cosmetics, hydrogels are applied topically to hair, skin, and can be orally consumed. The key advantage of hydrogels in cosmetics is that they can reduce

drug medication frequency while also extending the time spent on the application site. Various hydrogel-based cosmetic formulations including active cosmetic components have been synthesized for many years. Various biopolymers, such as gelatin, collagen, alginate, chitosan, pectin, xanthan gum, cellulose, hyaluronic acid, starch, and their derivatives, have been used to create these formulations. These biopolymer-based hydrogels have been used to create face masks. These masks claim to restore skin elasticity, enhance skin hydration and have anti-aging properties [271]. Hydrogels synthesized with incorporation of silver nanoparticles were used in cosmetics as anti-bacterial agents [272]. Fan Z et al. synthesized the gellan gum based hydrogel that is having the potential benefits in cosmetics and bio-medical fields [273]. Mensah A et al. successfully synthesized Icariin- β-cyclodextrin inclusion complex and it is equally competent for possible use as biomedical materials for target drug carriers, scaffolds and facemasks were accomplished [274].

1.3.2.5 Applications of Hydrogels in Food Industries

Today, polymers' food packaging performance attracts industry due to improved biodegradability, swelling characteristics, thermal and mechanical properties of hydrogels. The coatings and films are examples of biodegradable packaging materials. Films are the layers that have been prepared by casting and drying of different type of polymer into the appropriate forms and coatings are of edible polymers [275]. Hydrogels in a polymeric web can absorb water and other hydrophilic solvents to a maximum percent of their dry weight [276]. The important function of these hydrogels is to maintain a dry atmosphere inside the food packaging by controlling humidity which may be produced by the transpiration of vegetables and fruits, or

through loss of water caused by physiochemical changes in food inside packing, or by change in the environment [277]. Another application of hydrogels in food industries is 3D food printing technology, food inks that are shear-thinned hydrogels work well as printing inks. Hydrogels can improve natural food gels' flow behaviour since they are visco-plastic and their printing functions of complicated geometric patterns [278]. Guar gum, xanthan gum, κ-carrageenan, and gum arabic were reported by Azam et al. to have substantial influence on the rheological characteristics, microstructure, and 3D printing behaviour of the mixture of orange juice concentrate and wheat starch [279]. Today more than ever, the packaging material's biodegradability is crucial as the breakdown by-products are harmful. Polysaccharides are widely known for being non-toxic and having a high level of biocompatibility [280]. In order to synthesize biodegradable edible packaging coatings, lipids, proteins, and polysaccharides have been employed as the main source. They can be biodegraded by bacteria and the enzymes found in the human colon [275]. By estimating the biological oxygen demand (BOD) in accordance with ISO 14851: 1999, the biodegradability of the improved films was examined [281]. Table 1.2, offers a list of applications for natural gums-based hydrogels in different fields.

1.4 Derivatized Natural Gum-Based Hydrogels

In the form of food additives or medicine carriers, the majority of natural gums are suitable for oral ingestion as they are broken down into their component sugars by the intestinal microbiota. Non-reducing galactose residues at the end of polymer chains, may be hydrolysed by α-galactosidase to provide free α-d-galactose. But, natural gums, on the other hand, has certain drawbacks, like pH-dependent solubility, thickening, overwhelming rates of hydration, microbiological contamination and viscosity reduction during storage. These drawbacks can be overcome by derivatizing the natural gums by different functional group moieties which may be used in specialized drug applications. Water soluble properties and gelling behaviour have been improved via carboxymethylation and also improves bio-adhesive characteristics of natural polymers [51]. Williamson' synthesis was used to synthesize carboxymethylated gums, in which the -CH_2COOH group replaced the primary and secondary -OH of polysaccharides and boost the bio-adhesion capability [282] Another chemical modification, i.e., hydroxypropylation, which is also known as etherification, is often used for the synthesis of hydroxypropylated derivatives [70]. Oxidised gum arabic was utilised to make biocompatible IPN hydrogels with better mechanical qualities, as well as adhesive and self-healing capabilities [283]. There are still many natural macromolecules that have not been investigated, and research on these sources could be very useful. In fact, natural gums and their derivatizations will continue to be of interest in the development of improved materials for drug delivery applications for years ahead [284]. Few examples of derivatized natural gum-based hydrogels are given in table 1.3.

Table 1.4: Applications of derivatized natural gums based hydrogels

Sr. no.	Derivatives of natural gums	Key features	Applications	References
1.	CMGT	$AlCl_3$ cross-linked CMGT based beads for diclofenac sodium drug delivery	Drug delivery	[9]
2.	CMGT	Free radical graft polymerisation of CMTG-AAc for superabsorbent hydrogel synthesis	Agricultural use	[116]
3.	CMGG	$AlCl_3$ cross-linked CMGG based microsphere of ropinirole hydrochloride	Sustained oral delivery	[11]
4.	CMGuG	Curcumin loaded CMGu-g-gelatin film	Antimicrobial activity	[14]
5.	CMGuG	Epichlorohydrin mediated chemically cross-linked two oppositely charged GuG-based hydrogel	Dye separation	[285]
6.	CMGuG	CMGu-co-CMTKG grafted with PEPO based polymer	Food packaging	[286]
7.	HPGuG	N,N-Dimethyl AAm-co-HP GuG based graft polymerization for excellent healing of hydrogel	Biomedical devices	[16]
8.	HPGuG	Borax-mediated HPGuG and glycerol-based gel	For the removal of black patina from stucco ornamentation	[287]
9.	Aminated GuG	Aminated GuG-co-Fe_3O_4-co-ZnS NP based injectable hydrogel loaded with doxorubicin hydrochloride	Drug delivery	[288]
10.	Acryloyl(A) GuG	AGuG-g-poly(MAA) and AGuG-g-poly(AAc) hydrogel for release of two drugs; L-Dopa and L-Tyrosine	Drug delivery	[289]
11.	CMTaG	Vitamin D_3 microencapsulated into gelatin and CMTaG microcapsule by complex coacervation	Drug delivery	[290]
12.	CMTKG	Moxifloxacin hydrochloride loaded, citric acid cross-linked CMTKG based hydrogel film	Drug delivery	[291]
13.	CMTKG	CMTKG-co-sodium acrylate-based Zn loaded hydrogel	Agricultural use	[292]

Sr. no.	Derivatives of natural gums	Key features	Applications	References
14.	CMTKG	CMTKG-co-silica/polyacrylamide-based graft polymerisation of hydrogel	Methylene blue dye absorption	[293]
15.	CMTKG	CM guar-co-CMTKG grafted with PEPO based polymer	Food packaging	[286]
16.	CMXG	Ciprofloxacin loaded CMXG-g-trimethyl chitosan-based hydrogel	Drug delivery	[294]
17.	CMFG	CMFG-g-poly(N-isopropylacrylamide-g-bentonite based nanocomposites for delivery of erlotinib	Drug delivery	[204]
18.	CMKJG	Complex coacervation of CMKJG and CH to form microsphere	Drug delivery	[42]
19.	CMKJG	$AlCl_3$ based CMKJG and GeG microsphere cross-linked with glutaraldehyde	Uranium adsorption	[295]
20.	CMGeG	$CaCl_2$ cross-linked metformin loaded CMGeG beads for faster drug release	drug delivery	[51]
21.	CMGeG	Glycerol mediated CMGeG and pullulan based edible films	Food packaging	[296]
22.	Oxidized(O)DRG	ODRG-g-Isopropylacrylamide using Schiff-base, 2-aminoethanethiol hydrochloride	Drug delivery	[297]
23.	CMKG	$CaCl_2$ mediated CMKG beads loaded with metformin	Drug delivery	[282]
24.	CMSG	Metformin hydrochloride loaded CMSG and $CaCl_2$ beads	Drug delivery	[69]
25.	CMMoG	CMMoG-CH based nanocarrier loaded with ofloxacin	Drug delivery	[75]
26.	CMOG	CAN cross-linked CMOG-g-polymethacrylamide polymerization by microwave irradiation for delivery of diclofenac	Drug delivery	[77]
27.	CMLBG	$AlCl_3$ cross-linked CMLBG-SA hydrogel for the delivery of glipizide	Drug delivery	[298]
28.	Sulfated(S)LBG	$AlCl_3$ cross-linked SLBG based hydrogel beads loaded with tramadol HCl	Drug delivery	[299]

1.5 Research Gap

The literature survey encompasses various types of natural gums and their derivatives, thoroughly exploring advancements in hydrogels and their applications. Nonetheless, there's a notable gap in research regarding the potential applications of Gum Tragacanth, Locust bean gum, and *Cassia fistula* gums, particularly in fields like biomedical and agriculture. This research aims to address this gap by focusing on these three gums and exploring their potential biomedical applications, specifically as carriers for drug delivery and wound healing.

1.6 Aim and Objectives

The aim of this thesis research work is to synthesize a wide range of hydrogels with high mechanical strength and plasticity along with applications, especially in the bio-medical field and explore their utility in pharmaceutical industries as commercial used carriers for wound dressings and drug delivery. To achieve this aim the given below research objectives were optimized.

1.7 Research Objectives

- Synthesis and characterization of carboxymethylated natural gums and their hydrogels.
- Characterization through various techniques like XRD, SEM, TGA, FTIR, C^{13}-NMR.
- Swelling studies of synthesized hydrogels in different pH medium.
- Rheological analysis of synthesized hydrogels.
- Application of synthesized hydrogels.

1.8 References

[1] S. Ahmad, M. Ahmad, K. Manzoor, R. Purwar, and S. Ikram, "A review on latest innovations in natural gums based hydrogels: Preparations & applications," *Int. J. Biol. Macromol.*, vol. 136, pp. 870–890, Sep. 2019, doi: 10.1016/j.ijbiomac.2019.06.113.

[2] S. Barak, D. Mudgil, and S. Taneja, "Exudate gums: chemistry, properties and food applications – a review," *J. Sci. Food Agric.*, vol. 100, no. 7, pp. 2828–2835, May 2020, doi: 10.1002/jsfa.10302.

[3] W. Samutsri and M. Suphantharika, "Effect of salts on pasting, thermal, and rheological properties of rice starch in the presence of non-ionic and ionic hydrocolloids," *Carbohydr. Polym.*, vol. 87, no. 2, pp. 1559–1568, Jan. 2012, doi: 10.1016/j.carbpol.2011.09.055.

[4] N. K. Andrikopoulos, A. C. Kaliora, A. N. Assimopoulou, and V. P. Papapeorgiou, "Biological activity of some naturally occurring resins, gums and pigments againstin vitro LDL oxidation," *Phyther. Res.*, vol. 17, no. 5, pp. 501–507, May 2003, doi: 10.1002/ptr.1185.

[5] P. D. Choudhary and H. A. Pawar, "Recently Investigated Natural Gums and Mucilages as Pharmaceutical Excipients: An Overview," *J. Pharm.*, vol. 2014, no. 1, pp. 1–9, 2014, doi: 10.1155/2014/204849.

[6] R. Bhosale, "Natural Gums and Mucilages: A Review on Multifaceted Excipients in Lung delivery of nanoliposomal salbutamol sulphate dry powder for inhalation View project," *Pharm. Sci. Res. Artic. Int. J. Pharmacogn. Phytochem. Res.*, vol. 6, no. 4, pp. 901–912, 2014, [Online]. Available:

https://www.researchgate.net/publication/269109103

[7] G. A. Towle and R. L. Whistler, "Chemical Modification of Gums," in *Industrial Gums: Polysaccharides and Their Derivatives: Third Edition*, Elsevier Inc., 2012, pp. 53–67. doi: 10.1016/B978-0-08-092654-4.50007-3.

[8] V. Rana, P. Rai, A. K. Tiwary, R. S. Singh, J. F. Kennedy, and C. J. Knill, "Modified gums: Approaches and applications in drug delivery," *Carbohydr. Polym.*, vol. 83, no. 3, pp. 1031–1047, 2011, doi: 10.1016/j.carbpol.2010.09.010.

[9] A. K. Veeramachineni, T. Sathasivam, R. Paramasivam, S. Muniyandy, and J. Pushpamalar, "Synthesis and Characterization of a Novel pH-Sensitive Aluminum Crosslinked Carboxymethyl Tragacanth Beads for Extended and Enteric Drug Delivery," *J. Polym. Environ.*, vol. 27, no. 7, pp. 1516–1528, Jul. 2019, doi: 10.1007/s10924-019-01448-5.

[10] H. N. Murthy, "Chemical Constituents and Applications of Gums, Resins, and Latexes of Plant Origin," in *Gums, Resins and Latexes of Plant Origin: Chemistry, Biological Activities and Uses*, 2022, pp. 3–23. doi: 10.1007/978-3-030-91378-6_1.

[11] S. Ray, G. Roy, S. Maiti, U. K. Bhattacharyya, A. Sil, and R. Mitra, "Development of smart hydrogels of etherified gum ghatti for sustained oral delivery of ropinirole hydrochloride," *Int. J. Biol. Macromol.*, vol. 103, pp. 347–354, Oct. 2017, doi: 10.1016/j.ijbiomac.2017.04.059.

[12] S. Kaity and A. Ghosh, "Carboxymethylation of locust bean gum: Application in interpenetrating polymer network microspheres for controlled drug

delivery," *Ind. Eng. Chem. Res.*, vol. 52, no. 30, pp. 10033–10045, Jul. 2013, doi: 10.1021/ie400445h.

[13] L. Braz et al., "Synthesis and characterization of Locust Bean Gum derivatives and their application in the production of nanoparticles," *Carbohydr. Polym.*, vol. 181, pp. 974–985, Feb. 2018, doi: 10.1016/j.carbpol.2017.11.052.

[14] P. J. Manna, T. Mitra, N. Pramanik, V. Kavitha, A. Gnanamani, and P. P. Kundu, "Potential use of curcumin loaded carboxymethylated guar gum grafted gelatin film for biomedical applications," *Int. J. Biol. Macromol.*, vol. 75, pp. 437–446, Apr. 2015, doi: 10.1016/j.ijbiomac.2015.01.047.

[15] R. Lapasin, S. Pricl, and P. Tracanelli, "Rheology of Hydroxyethyl Guar Gum Derivatives," *Carbohydr. Polym.*, vol. 14, pp. 411–427, 1991.

[16] J. Zhu, P. Guo, D. Chen, K. Xu, P. Wang, and S. Guan, "Fast and excellent healing of hydroxypropyl guar gum/poly(N,N-dimethyl acrylamide) hydrogels," *J. Polym. Sci. Part B Polym. Phys.*, vol. 56, no. 3, pp. 239–247, Feb. 2018, doi: 10.1002/polb.24514.

[17] H. Y. Shi and L. M. Zhang, "New grafted polysaccharides based on O-carboxymethyl-O-hydroxypropyl guar gum and N-isopropylacrylamide: Synthesis and phase transition behavior in aqueous media," *Carbohydr. Polym.*, vol. 67, no. 3, pp. 337–342, Feb. 2007, doi: 10.1016/j.carbpol.2006.06.005.

[18] M. A. Shenoy and D. J. D'Melo, "Synthesis and characterization of acryloyloxy guar gum," *J. Appl. Polym. Sci.*, vol. 117, no. 1, pp. 148–154, Jul. 2010, doi: 10.1002/app.31872.

[19] W. Xiao and L. Dong, "Novel excellent property film prepared from methacryloyl chloride-graft-Guar gum matrixes," in *International Conference on Consumer Electronics, Communications and Networks, CECNet 2011 - Proceedings*, 2011, pp. 1442–1445. doi: 10.1109/CECNET.2011.5768424.

[20] A. S. Kazachenko et al., "Theoretical and experimental study of Guar gum sulfation," *J. Moecular Mpdeling*, vol. 27, no. 1, p. 5, 2021, doi: 10.1007/s00894-020-04645-5/Published.

[21] C. Dong and B. Tian, "Studies on Preparation and Emulsifying Properties of Guar Galactomannan Ester of Palmitic Acid," *J Appl Polym Sci*, vol. 72, pp. 639–645, 1999.

[22] S. Jana, S. Maiti, S. Jana, K. K. Sen, and A. K. Nayak, "Guar gum in drug delivery applications," *Nat. Polysaccharides Drug Deliv. Biomed. Appl.*, pp. 187–201, 2019, doi: 10.1016/B978-0-12-817055-7.00007-8.

[23] M. B. Santos, C. H. C. dos Santos, M. G. de Carvalho, C. W. P. de Carvalho, and E. E. Garcia-Rojas, "Physicochemical, thermal and rheological properties of synthesized carboxymethyl Tara gum (*Caesalpinia spinosa*)," *Int. J. Biol. Macromol.*, vol. 134, pp. 595–603, Aug. 2019, doi: 10.1016/j.ijbiomac.2019.05.025.

[24] Y. Wu, W. Ding, L. Jia, and Q. He, "The rheological properties of tara gum (*Caesalpinia spinosa*)," *Food Chem.*, vol. 168, pp. 366–371, Feb. 2015, doi: 10.1016/j.foodchem.2014.07.083.

[25] P. Goyal, V. Kumar, and P. Sharma, "Carboxymethylation of Tamarind kernel powder," *Carbohydr. Polym.*, vol. 69, no. 2, pp. 251–255, Jun. 2007, doi:

10.1016/j.carbpol.2006.10.001.

[26] A. K. Shukla, R. S. Bishnoi, M. Kumar, V. Fenin, and C. P. Jain, "Applications of Tamarind seeds Polysaccharide-based copolymers in Controlled Drug Delivery: An overview," *Asian J. Pharm. Pharmacol.*, vol. 4, no. 1, pp. 23–30, Feb. 2018, doi: 10.31024/ajpp.2018.4.1.5.

[27] N. A. Ibrahim, M. H. Abo-Shosha, E. A. Allam, and E. M. El-Zairy, "New thickening agents based on Tamarind seed gum and karaya gum polysaccharides," *Carbohydr. Polym.*, vol. 81, no. 2, pp. 402–408, Jun. 2010, doi: 10.1016/j.carbpol.2010.02.040.

[28] H. R. Badwaik, K. Sakure, A. Alexander, Ajazuddin, H. Dhongade, and D. K. Tripathi, "Synthesis and characterisation of poly(acryalamide) grafted carboxymethyl Xanthan gum copolymer," *Int. J. Biol. Macromol.*, vol. 85, pp. 361–369, Apr. 2016, doi: 10.1016/j.ijbiomac.2016.01.014.

[29] F. A. Ngwabebhoh, O. Zandraa, R. Patwa, N. Saha, Z. Capáková, and P. Saha, "Self-crosslinked chitosan/dialdehyde xanthan gum blended hypromellose hydrogel for the controlled delivery of ampicillin, minocycline and rifampicin," *Int. J. Biol. Macromol.*, vol. 167, pp. 1468–1478, Jan. 2021, doi: 10.1016/j.ijbiomac.2020.11.100.

[30] S. B. Kalbhare, V. Kumar Redasani, M. J. Bhandwalkar, R. K. Pawar, and A. M. Bhagwat, "Role of Aminated derivatives of Natural Gum in Release Modulating Matrix Systems of Losartan Potassium: Optimization of Formulation using Box-Behnken Design," *Asian J. Pharm. Res.*, vol. 11, no. 2, pp. 73–84, May 2021, doi: 10.52711/2231-5691.2021.00015.

[31] J. Patel, B. Maji, N. S. H. N. Moorthy, and S. Maiti, "Xanthan gum derivatives: Review of synthesis, properties and diverse applications," *RSC Adv.*, vol. 10, no. 45, pp. 27103–27136, 2020, doi: 10.1039/d0ra04366d.

[32] B. R. Gangapuram, R. Bandi, R. Dadigala, G. M. Kotu, and V. Guttena, "Facile Green Synthesis of Gold Nanoparticles with Carboxymethyl Gum Karaya, Selective and Sensitive Colorimetric Detection of Copper (II) Ions," *J. Clust. Sci.*, vol. 28, no. 5, pp. 2873–2890, 2017, doi: 10.1007/s10876-017-1264-3.

[33] V. V. T. Padil, C. Senan, and M. Černík, "Dodecenylsuccinic Anhydride Derivatives of Gum Karaya (*Sterculia urens*): Preparation, Characterization, and Their Antibacterial Properties," *J. Agric. Food Chem.*, vol. 63, no. 14, pp. 3757–3765, Apr. 2015, doi: 10.1021/jf505783e.

[34] E. Fosso-Kankeu, H. Mittal, F. Waanders, I. O. Ntwampe, and S. S. Ray, "Preparation and characterization of Gum Karaya hydrogel nanocomposite flocculant for metal ions removal from mine effluents," *Int. J. Environ. Sci. Technol.*, vol. 13, no. 2, pp. 711–724, 2016, doi: 10.1007/s13762-015-0915-x.

[35] B. Raj Sharma, V. Kumar, P. L. Soni, and P. Sharma, "Carboxymethylation of *Cassia tora* Gum," *J. Appl. Polym. Sci.*, vol. 89, pp. 3216–3219, 2003.

[36] K. P. Y. Shak and T. Y. Wu, "Coagulation-flocculation treatment of high-strength agro-industrial wastewater using natural *Cassia obtusifolia* seed gum: Treatment efficiencies and flocs characterization," *Chem. Eng. J.*, vol. 256, pp. 293–305, Nov. 2014, doi: 10.1016/j.cej.2014.06.093.

[37] R. Sharma and V. Rana, "Effect of carboxymethylation on rheological and

drug release characteristics of *Terminalia catappa* gum," *Carbohydr. Polym.*, vol. 175, pp. 728–738, Nov. 2017, doi: 10.1016/j.carbpol.2017.08.047.

[38] A. V. Samrot, B. Suvedhaa, C. S. Sahithya, and A. Madankumar, "Purification and Utilization of Gum from Terminalia Catappa L. for Synthesis of Curcumin Loaded Nanoparticle and Its In Vitro Bioactivity Studies," *J. Clust. Sci.*, vol. 29, no. 6, pp. 989–1002, Nov. 2018, doi: 10.1007/s10876-018-1412-4.

[39] C. J. Mate and S. Mishra, "Synthesis of borax cross-linked Jhingan gum hydrogel for remediation of Remazol Brilliant Blue R (RBBR) dye from water: Adsorption isotherm, kinetic, thermodynamic and biodegradation studies," *Int. J. Biol. Macromol.*, vol. 151, pp. 677–690, May 2020, doi: 10.1016/j.ijbiomac.2020.02.192.

[40] L. Qiu, Y. Shen, H. Fan, X. Yang, and C. Wang, "Carboxymethyl fenugreek gum: Rheological characterization and as a novel binder for silicon anode of lithium-ion batteries," *Int. J. Biol. Macromol.*, vol. 115, pp. 672–679, Aug. 2018, doi: 10.1016/j.ijbiomac.2018.04.062.

[41] H. Bera, S. Mothe, S. Maiti, and S. Vanga, "Carboxymethyl fenugreek galactomannan-Gellan gum-calcium silicate composite beads for glimepiride delivery," *Int. J. Biol. Macromol.*, vol. 107, pp. 604–614, Feb. 2018, doi: 10.1016/j.ijbiomac.2017.09.027.

[42] J.-X. Xiao, L.-H. Wang, T.-C. Xu, and G.-Q. Huang, "Complex coacervation of carboxymethyl Konjac glucomannan and chitosan and coacervate characterization," *Int. J. Biol. Macromol.*, vol. 123, pp. 436–445, Feb. 2019, doi: 10.1016/j.ijbiomac.2018.11.086.

[43] Y. Wang et al., "A self-adapting hydrogel based on chitosan/oxidized konjac glucomannan/AgNPs for repairing irregular wounds," *Biomater. Sci.*, vol. 8, no. 7, pp. 1910–1922, 2020, doi: 10.1039/c9bm01635j.

[44] S. E. Case and D. D. Hamann, "Fracture properties of konjac mannan gel: effect of gel temperature," *Food Hydrocoll.*, vol. 8, no. 2, pp. 147–154, May 1994, doi: 10.1016/S0268-005X(09)80040-4.

[45] J. Kang, Q. Guo, and S. W. Cui, "Other emerging gums: Flaxseed gum, yellow mustard gum, and psyllium gums," in *Handbook of Hydrocolloids*, Elsevier, 2021, pp. 597–624. doi: 10.1016/B978-0-12-820104-6.00030-9.

[46] W. Liu et al., "Effects of hydroxypropylation on the functional properties of Psyllium," *J. Agric. Food Chem.*, vol. 58, no. 3, pp. 1615–1621, Feb. 2010, doi: 10.1021/jf903691z.

[47] Y. Niu, Z. Xie, J. Hao, W. Yao, J. Yue, and L. (Lucy) Yu, "Preparation of succinylated derivatives of psyllium and their physicochemical and bile acid-binding properties," *Food Chem.*, vol. 132, no. 2, pp. 1025–1032, May 2012, doi: 10.1016/j.foodchem.2011.11.090.

[48] Y. Niu, Z. Xie, H. Zhang, Y. Sheng, and L. Yu, "Effects of structural modifications on physicochemical and bile acid-binding properties of psyllium," *J. Agric. Food Chem.*, vol. 61, no. 3, pp. 596–601, Jan. 2013, doi: 10.1021/jf3043117.

[49] M. H. Fischer, N. Yu, G. R. Gray, J. Ralph, L. Anderson, and J. A. Marlett, "The gel-forming polysaccharide of psyllium husk (*Plantago ovata Forsk*)," *Carbohydr. Res.*, vol. 339, no. 11, pp. 2009–2017, Aug. 2004, doi:

10.1016/j.carres.2004.05.023.

[50] K. V. Sajna, L. D. Gottumukkala, R. K. Sukumaran, and A. Pandey, "White Biotechnology in Cosmetics," in *Industrial Biorefineries & White Biotechnology*, Elsevier, 2015, pp. 607–652. doi: 10.1016/B978-0-444-63453-5.00020-3.

[51] M. Ahuja, S. Singh, and A. Kumar, "Evaluation of carboxymethyl gellan gum as a mucoadhesive polymer," *Int. J. Biol. Macromol.*, vol. 53, pp. 114–121, Feb. 2013, doi: 10.1016/j.ijbiomac.2012.10.033.

[52] J. Zhang, Y. Dong, L. Fan, Z. Jiao, and Q. Chen, "Optimization of culture medium compositions for gellan gum production by a halobacterium *Sphingomonas paucimobilis*," *Carbohydr. Polym.*, vol. 115, pp. 694–700, Jan. 2015, doi: 10.1016/j.carbpol.2014.09.029.

[53] B. Safdar et al., "Flaxseed gum: Extraction, bioactive composition, structural characterization, and its potential antioxidant activity," *J. Food Biochem.*, vol. 44, no. 2, Feb. 2020, doi: 10.1111/jfbc.13134.

[54] J. Niu, D. Li, L. Wang, B. Adhikari, and X. D. Chen, "Synthesis of Carboxymethyl Flaxseed Gum and Study of Nonlinear Rheological Properties of Its Solutions," *Int. J. Food Eng.*, vol. 14, no. 1, p. 20170185, Jan. 2018, doi: 10.1515/ijfe-2017-0185.

[55] J. Liu, Y. Y. Shim, T. J. Tse, Y. Wang, and M. J. T. Reaney, "Flaxseed gum a versatile natural hydrocolloid for food and non-food applications," *Trends Food Sci. Technol.*, vol. 75, pp. 146–157, 2018, doi: 10.1016/j.tifs.2018.01.011.

[56] S. Kim, A. Biswas, V. Boddu, H.-S. Hwang, and J. Adkins, "Solubilization of cashew gum from *Anacardium occidentale* in aqueous medium," *Carbohydr. Polym.*, vol. 199, pp. 205–209, Nov. 2018, doi: 10.1016/j.carbpol.2018.07.022.

[57] J. S. Maciel et al., "Oxidized Cashew Gum Scaffolds for Tissue Engineering," *Macromol. Mater. Eng.*, vol. 304, no. 3, pp. 1–11, 2019, doi: 10.1002/mame.201800574.

[58] A. M. A. Melo et al., "Preparation and characterization of carboxymethyl cashew gum grafted with immobilized antibody for potential biosensor application," *Carbohydr. Polym.*, vol. 228, p. 115408, Jan. 2020, doi: 10.1016/j.carbpol.2019.115408.

[59] A. J. Ribeiro et al., "Gums' based delivery systems: Review on cashew gum and its derivatives," *Carbohydr. Polym.*, vol. 147, pp. 188–200, Aug. 2016, doi: 10.1016/j.carbpol.2016.02.042.

[60] M. R. Guilherme, A. V. Reis, S. H. Takahashi, A. F. Rubira, J. P. A. Feitosa, and E. C. Muniz, "Synthesis of a novel superabsorbent hydrogel by copolymerization of acrylamide and cashew gum modified with glycidyl methacrylate," *Carbohydr. Polym.*, vol. 61, no. 4, pp. 464–471, Sep. 2005, doi: 10.1016/j.carbpol.2005.06.017.

[61] L. Wang, H. M. Liu, C. Y. Zhu, A. J. Xie, B. J. Ma, and P. Z. Zhang, "Chinese quince seed gum: Flow behaviour, thixotropy and viscoelasticity," *Carbohydr. Polym.*, vol. 209, no. 2019, pp. 230–238, 2019, doi: 10.1016/j.carbpol.2018.12.101.

[62] M. Malandkar, "II. Chemical Constitution of the Gum from *Boswellia serrata*," *J. Indian Inst. Sci.*, vol. 8, no. Part A, pp. 221–244, 1925.

[63] A. Srivastava, D. V. Gowda, U. Hani, C. G. Shinde, and R. A. M. Osmani, "Fabrication and characterization of carboxymethylated bael fruit gum with potential mucoadhesive applications," *RSC Adv.*, vol. 5, no. 55, pp. 44652–44659, 2015, doi: 10.1039/c5ra05760d.

[64] N. Mahammed, D. V. Gowda, R. D. Deshpande, and S. Thirumaleshwar, "Design of phosphated cross-linked microspheres of bael fruit gum as a biodegradable carrier," *Arch. Pharm. Res.*, vol. 38, no. 1, pp. 42–51, 2015, doi: 10.1007/s12272-014-0355-z.

[65] V. T. P. Vinod and R. B. Sashidhar, "Solution and conformational properties of gum kondagogu (*Cochlospermum gossypium*) – A natural product with immense potential as a food additive," *Food Chem.*, vol. 116, no. 3, pp. 686–692, Oct. 2009, doi: 10.1016/j.foodchem.2009.03.009.

[66] K. Seku et al., "Eco-friendly synthesis of gold nanoparticles using carboxymethylated gum *Cochlospermum gossypium* (CMGK) and their catalytic and antibacterial applications," *Chem. Pap.*, vol. 73, no. 7, pp. 1695–1704, Jul. 2019, doi: 10.1007/s11696-019-00722-z.

[67] H. S. Rathore et al., "Fabrication of biomimetic porous novel sponge from gum kondagogu for wound dressing," *Mater. Lett.*, vol. 177, pp. 108–111, Aug. 2016, doi: 10.1016/j.matlet.2016.04.185.

[68] Q. Zhang, Y. Gao, Y. A. Zhai, F. Q. Liu, and G. Gao, "Synthesis of Sesbania gum supported dithiocarbamate chelating resin and studies on its adsorption

performance for metal ions," *Carbohydr. Polym.*, vol. 73, no. 2, pp. 359–363, Jul. 2008, doi: 10.1016/j.carbpol.2007.11.028.

[69] S. Verma and M. Ahuja, "Carboxymethyl Sesbania gum: Synthesis, characterization and evaluation for drug delivery," *Int. J. Biol. Macromol.*, vol. 98, pp. 75–83, May 2017, doi: 10.1016/j.ijbiomac.2017.01.070.

[70] H. Tang, Y. Liu, Y. Li, Q. Li, and X. Liu, "Hydroxypropylation of cross-linked Sesbania gum, characterization and properties," *Int. J. Biol. Macromol.*, vol. 152, pp. 1010–1019, Jun. 2020, doi: 10.1016/j.ijbiomac.2019.10.188.

[71] S. Verma and M. Ahuja, "Thiol functionalization of Sesbania gum and its evaluation for mucoadhesive sustained drug delivery," *Acta Pharm. Sci.*, vol. 59, no. 1, pp. 581–602, 2021, doi: 10.23893/1307-2080.APS.05903.

[72] R. Li, X. Jia, Y. Wang, Y. Li, and Y. Cheng, "The effects of extrusion processing on rheological and physicochemical properties of Sesbania gum," *Food Hydrocoll.*, vol. 90, pp. 35–40, May 2019, doi: 10.1016/j.foodhyd.2018.11.048.

[73] L. Jorge Corzo-Rios, S. R. Drago, S. Gallegos-Tintor David Betancur-Ancona, and L. Chel-Guerrero, "Study of the Interaction of *Phaseolus lunatus* Hydrolysed Proteins and *Delonix regia* Carboxymethylated Gum Using Capillary Electrophoresis," *Chiang Mai J. Sci*, vol. 45, no. 1, pp. 308–317, 2018, [Online]. Available: http://epg.science.cmu.ac.th/ejournal/

[74] E. I. Okoye, C. Edochie, and J. O. Adegbemi, "Preliminary Evaluation of *Delonix regia* Seed Gum as a Suspending Agent in a Liquid Oral Dosage Form," *Int. J. Pharm. Sci. Drug Res.*, vol. 6, no. 2, pp. 114–119, 2014,

[Online]. Available: www.ijpsdr.com

[75] Rimpy, Abhishek, and M. Ahuja, "Evaluation of carboxymethyl moringa gum as nanometric carrier," *Carbohydr. Polym.*, vol. 174, pp. 896–903, Oct. 2017, doi: 10.1016/j.carbpol.2017.07.022.

[76] S. Ahmad, K. Manzoor, R. Purwar, and S. Ikram, "Morphological and Swelling Potential Evaluation of *Moringa oleifera* Gum/Poly(vinyl alcohol) Hydrogels as a Superabsorbent," *ACS Omega*, vol. 5, no. 29, pp. 17955–17961, Jul. 2020, doi: 10.1021/acsomega.0c01023.

[77] S. Patra, N. N. Bala, and G. Nandi, "Synthesis, characterization and fabrication of sodium carboxymethyl-okra-gum-grafted-polymethacrylamide into sustained release tablet matrix," *Int. J. Biol. Macromol.*, vol. 164, pp. 3885–3900, Dec. 2020, doi: 10.1016/j.ijbiomac.2020.09.025.

[78] A. Roy, S. L. Shrivastava, and S. M. Mandal, "Functional properties of Okra *Abelmoschus esculentus L.* (Moench): traditional claims and scientific evidences," *Plant Sci. Today*, vol. 1, no. 3, pp. 121–130, Jul. 2014, doi: 10.14719/pst.2014.1.3.63.

[79] R. Malviya, P. K. Sharma, and S. K. Dubey, "Stability facilitation of nanoparticles prepared by ultrasound assisted solvent-antisolvent method: Effect of neem gum, acrylamide grafted neem gum and carboxymethylated neem gum over size, morphology and drug release," *Mater. Sci. Eng. C*, vol. 91, pp. 772–784, Oct. 2018, doi: 10.1016/j.msec.2018.06.013.

[80] P. Mankotia et al., "Neem gum based pH responsive hydrogel matrix: A new pharmaceutical excipient for the sustained release of anticancer drug," *Int. J.*

Biol. Macromol., vol. 142, no. 2, pp. 742–755, Jan. 2020, doi: 10.1016/j.ijbiomac.2019.10.015.

[81] D. A. Bhagwat, V. R. Kolekar, S. J. Nadaf, P. B. Choudhari, H. N. More, and S. G. Killedar, "Acrylamide grafted neem (*Azadirachta indica*) gum polymer: Screening and exploration as a drug release retardant for tablet formulation," *Carbohydr. Polym.*, vol. 229, p. 115357, Feb. 2020, doi: 10.1016/j.carbpol.2019.115357.

[82] H. Chen et al., "Structure and physicochemical properties of amphiphilic agar modified with octenyl succinic anhydride," *Carbohydr. Polym.*, vol. 251, p. 117031, Jan. 2021, doi: 10.1016/j.carbpol.2020.117031.

[83] V. Kulkarni, K. Butte, and S. Rathod, "Natural Polymers – A Comprehensive Review," *Int. J. Res. Pharm. Biomed. Sci.*, vol. 3, no. 4, pp. 1597–1613, 2012.

[84] S. Kaur, R. Jindal, and J. Kaur Bhatia, "Synthesis and RSM-CCD optimization of microwave-induced green interpenetrating network hydrogel adsorbent based on gum copal for selective removal of malachite green from waste water," *Polym. Eng. Sci.*, vol. 58, no. 12, pp. 2293–2303, Dec. 2018, doi: 10.1002/pen.24851.

[85] P. Sharma, R. Jindal, M. Maiti, and A. K. Jana, "Novel organic–inorganic composite material as a cation exchanger from a triterpenoidal system of Dammar gum: synthesis, characterization and application," *Iran. Polym. J. (English Ed.*, vol. 25, no. 8, pp. 671–685, Aug. 2016, doi: 10.1007/s13726-016-0456-2.

[86] P. Sharma, H. Mittal, R. Jindal, D. Jindal, and S. M. Alhassan, "Sustained

delivery of atenolol drug using Gum Dammar crosslinked polyacrylamide and zirconium based biodegradable hydrogel composites," *Colloids Surfaces A Physicochem. Eng. Asp.*, vol. 562, pp. 136–145, Feb. 2019, doi: 10.1016/j.colsurfa.2018.11.039.

[87] M. Masuelli, A. Slatvustky, A. Ochoa, and M. Bertuzzi, "Physicochemical Parameters for Brea Gum Exudate from *Cercidium praecox* Tree," *Colloids and Interfaces*, vol. 2, no. 4, p. 72, Dec. 2018, doi: 10.3390/colloids2040072.

[88] A. M. Slavutsky and M. A. Bertuzzi, "Formulation and characterization of hydrogel based on pectin and brea gum," *Int. J. Biol. Macromol.*, vol. 123, pp. 784–791, Feb. 2019, doi: 10.1016/j.ijbiomac.2018.11.038.

[89] Hasan Fathinejad Jirandehi, "Synthesis and Comparison of hydrogels based on *Pistacia atlantica* Gum," *Int. J. Biosci.*, vol. 5, no. 1, pp. 185–189, Jul. 2014, doi: 10.12692/ijb/5.1.185-189.

[90] M. Yu et al., "3D welan gum–graphene oxide composite hydrogels with efficient dye adsorption capacity," *RSC Adv.*, vol. 5, no. 92, pp. 75589–75599, 2015, doi: 10.1039/C5RA12806D.

[91] S. M. A. Razavi, A. Alghooneh, and F. Behrouzian, "Sage (*Salvia macrosiphon*) seed gum," *Emerg. Nat. Hydrocoll. Rheol. Funct.*, pp. 159–181, 2019, doi: 10.1002/9781119418511.ch6.

[92] S. M. A. Razavi, S. W. Cui, and H. Ding, "Structural and physicochemical characteristics of a novel water-soluble gum from *Lallemantia royleana* seed," *Int. J. Biol. Macromol.*, vol. 83, pp. 142–151, 2016, doi: 10.1016/j.ijbiomac.2015.11.076.

[93] L. M. Marvdashti, M. Yavarmanesh, and A. Koocheki, "Controlled release of nisin from polyvinyl alcohol - *Alyssum homolocarpum* seed gum composite films: Nisin kinetics," *Food Biosci.*, vol. 28, pp. 133–139, 2019, doi: 10.1016/j.fbio.2019.01.010.

[94] M. J. Perduca, M. J. Spotti, L. G. Santiago, M. A. Judis, A. C. Rubiolo, and C. R. Carrara, "Rheological characterization of the hydrocolloid from *Gleditsia amorphoides* seeds," *LWT - Food Sci. Technol.*, vol. 51, no. 1, pp. 143–147, 2013, doi: 10.1016/j.lwt.2012.09.007.

[95] A. Koocheki and M. A. Hesarinejad, "Qodume Shahri (*Lepidium perfoliatum*) Seed Gum," in *Emerging Natural Hydrocolloids*, Chichester, UK: John Wiley & Sons, Ltd, 2019, pp. 251–272. doi: 10.1002/9781119418511.ch10.

[96] B. Singh and V. Sharma, "Influence of polymer network parameters of tragacanth gum-based pH responsive hydrogels on drug delivery," *Carbohydr. Polym.*, vol. 101, no. 1, pp. 928–940, 2014, doi: 10.1016/j.carbpol.2013.10.022.

[97] L. Rastogi, R. B. Sashidhar, D. Karunasagar, and J. Arunachalam, "Gum kondagogu reduced/stabilized silver nanoparticles as direct colorimetric sensor for the sensitive detection of Hg^{2+} in aqueous system," *Talanta*, vol. 118, pp. 111–117, 2014, doi: 10.1016/j.talanta.2013.10.012.

[98] A. S. Deshmukh, C. M. Setty, A. M. Badiger, and K. S. Muralikrishna, "Gum ghatti: A promising polysaccharide for pharmaceutical applications," *Carbohydr. Polym.*, vol. 87, no. 2, pp. 980–986, Jan. 2012, doi: 10.1016/j.carbpol.2011.08.099.

[99] H. Mirhosseini and B. T. Amid, "A review study on chemical composition and molecular structure of newly plant gum exudates and seed gums," *Food Res. Int.*, vol. 46, no. 1, pp. 387–398, 2012, doi: 10.1016/j.foodres.2011.11.017.

[100] B. Singh, V. Sharma, and R. and A. Kumar, "Designing moringa gum-sterculia gum-polyacrylamide hydrogel wound dressings for drug delivery applications," *Carbohydr. Polym. Technol. Appl.*, vol. 2, p. 100062, Dec. 2021, doi: 10.1016/j.carpta.2021.100062.

[101] D. Mudgil, S. Barak, and B. S. Khatkar, "Guar gum: Processing, properties and food applications - A Review," *Journal of Food Science and Technology*, vol. 51, no. 3. pp. 409–418, 2014. doi: 10.1007/s13197-011-0522-x.

[102] N. D. Zaharuddin, M. I. Noordin, and A. Kadivar, "The Use of *Hibiscus esculentus* (Okra) Gum in Sustaining the Release of Propranolol Hydrochloride in a Solid Oral Dosage Form The Use of Hibiscus esculentus (Okra) Gum in Sustaining the Release of Propranolol Hydrochloride in," no. February, 2014, doi: 10.1155/2014/735891.

[103] A. Mortensen et al., "Re-evaluation of Tara gum (E 417) as a food additive," *EFSA J.*, vol. 15, no. 6, Jun. 2017, doi: 10.2903/j.efsa.2017.4863.

[104] B. Singh, M. Mohan, and B. Singh, "Synthesis and characterization of the *azadirachta indica* gum – polyacrylamide interpenetrating network for biomedical applications," *Carbohydr. Polym. Technol. Appl.*, vol. 1, no. November, p. 100017, 2020, doi: 10.1016/j.carpta.2020.100017.

[105] M. Lahaye, "Developments on gelling algal galactans , their structure and physico- chemistry Developments on gelling algal galactans , their structure

and," no. May, 2015, doi: 10.1023/A.

[106] N. Aliabbasi, M. Fathi, and Z. Emam-Djomeh, "Gum arabic-based nanocarriers for drug and bioactive compounds delivery," *Micro- Nanoeng. Gum-Based Biomater. Drug Deliv. Biomed. Appl.*, pp. 333–345, Jan. 2022, doi: 10.1016/B978-0-323-90986-0.00017-0.

[107] Mishra Manoj Kumar, Singh Abhishek, Patel Amit Kumar, Srivastava Rajat, and Kushwaha Krishna, "Recently investigated polymeric natural gums and mucilages for various drug delivery system," *World J. Adv. Res. Rev.*, vol. 6, no. 1, pp. 050–072, Apr. 2020, doi: 10.30574/wjarr.2020.6.1.0084.

[108] A. S. Cerezo, M. Stacey, and J. M. Webber, "Some structural studies of Brea gum (an exudate from *Cercidium australe jonhst.*)," *Carbohydr. Res.*, vol. 9, no. 4, pp. 505–517, Apr. 1969, doi: 10.1016/S0008-6215(00)80035-X.

[109] K. Huanbutta and W. Sittikijyothin, "Development and characterization of seed gums from *Tamarindus indica* and *Cassia fistula* as disintegrating agent for fast disintegrating Thai cordial tablet," *Asian J. Pharm. Sci.*, vol. 12, no. 4, pp. 370–377, Jul. 2017, doi: 10.1016/j.ajps.2017.02.004.

[110] J. Plank, S. Ng, and S. Foraita, "Intercalation of the microbial biopolymers Welan gum and EPS I into layered double hydroxides," *Zeitschrift fur Naturforsch. - Sect. B J. Chem. Sci.*, vol. 67, no. 5, pp. 479–487, 2012, doi: 10.5560/ZNB.2012-0081.

[111] Z. Kohajdová and J. Karovičová, "Application of hydrocolloids as baking improvers," vol. 63, no. 1, pp. 26–38, 2009, doi: 10.2478/s11696-008-0085-0.

[112] A. Mortensen et al., "Re-evaluation of konjac gum (E 425 i) and konjac

glucomannan (E 425 ii) as food additives," *EFSA J.*, vol. 15, no. 6, 2017, doi: 10.2903/j.efsa.2017.4864.

[113] A. B. Barros et al., "Evaluation of antitumor potential of cashew gum extracted from *Anacardium occidentale Linn*," *Int. J. Biol. Macromol.*, vol. 154, no. 2020, pp. 319–328, 2020, doi: 10.1016/j.ijbiomac.2020.03.096.

[114] D. Kumar, "Psyllium Mucilage and Its Use in Pharmaceutical Field : An Overview Current Synthetic and Systems Biology Psyllium Mucilage and Its Use in Pharmaceutical Field : An Overview," no. February 2020, 2017, doi: 10.4172/2332-0737.1000134.

[115] L. Y. Maroufi, N. Shahabi, M. dokht Ghanbarzadeh, and M. Ghorbani, "Development of Antimicrobial Active Food Packaging Film Based on Gelatin/Dialdehyde Quince Seed Gum Incorporated with Apple Peel Polyphenols," *Food Bioprocess Technol.*, vol. 15, no. 3, pp. 693–705, 2022, doi: 10.1007/s11947-022-02774-8.

[116] M. Behrouzi and P. N. Moghadam, "Synthesis of a new superabsorbent copolymer based on acrylic acid grafted onto carboxymethyl tragacanth," *Carbohydr. Polym.*, vol. 202, pp. 227–235, Dec. 2018, doi: 10.1016/j.carbpol.2018.08.094.

[117] F. E. O. L. O. Ekebafe, D. E. Ogbeifun, "Polymer Applications in Agriculture," *Biokemistri*, vol. 23, no. 3, pp. 81–89, 2011.

[118] L. Dai et al., "A self-assembling guar gum hydrogel for efficient oil/water separation in harsh environments," *Sep. Purif. Technol.*, vol. 225, pp. 129–135, Oct. 2019, doi: 10.1016/j.seppur.2019.05.070.

[119] H. J. Chung and T. G. Park, "Self-assembled and nanostructured hydrogels for drug delivery and tissue engineering," *Nano Today*, vol. 4, no. 5, pp. 429–437, Oct. 2009, doi: 10.1016/j.nantod.2009.08.008.

[120] M. Khan et al., "Synthesis of physically cross-linked gum Arabic-based polymer hydrogels with enhanced mechanical, load bearing and shape memory behavior," *Iran. Polym. J. (English Ed.*, vol. 29, no. 4, pp. 351–360, 2020, doi: 10.1007/s13726-020-00801-z.

[121] W. Chen et al., "Development of high-strength, tough, and self-healing carboxymethyl guar gum-based hydrogels for human motion detection," *J. Mater. Chem. C*, vol. 8, no. 3, pp. 900–908, 2020, doi: 10.1039/C9TC05797H.

[122] R. Shahvalizadeh et al., "Antimicrobial bio-nanocomposite films based on gelatin, Tragacanth, and zinc oxide nanoparticles – Microstructural, mechanical, thermo-physical, and barrier properties," *Food Chem.*, vol. 354, p. 129492, Aug. 2021, doi: 10.1016/j.foodchem.2021.129492.

[123] M. A. Bonifacio et al., "Data in Brief Data on Manuka Honey / Gellan Gum composite hydrogels for cartilage repair," *Data Br.*, vol. 20, pp. 831–839, 2018, doi: 10.1016/j.dib.2018.08.155.

[124] S. Ma, B. Yu, X. Pei, and F. Zhou, "Structural hydrogels," *Polymer (Guildf).*, vol. 98, pp. 516–535, 2016, doi: 10.1016/j.polymer.2016.06.053.

[125] E. M. Ahmed, F. S. Aggor, A. M. Awad, and A. T. El-Aref, "An innovative method for preparation of nanometal hydroxide superabsorbent hydrogel," *Carbohydr. Polym.*, vol. 91, no. 2, pp. 693–698, Jan. 2013, doi: 10.1016/j.carbpol.2012.08.056.

[126] D. L. Taylor and M. in het Panhuis, "Self-Healing Hydrogels," *Adv. Mater.*, vol. 28, no. 41, pp. 9060–9093, 2016.

[127] R. Vasita and D. S. Katti, "Nanofibers and their applications in tissue engineering," *Int. J. Nanomedicine*, vol. 1, no. 1, pp. 15–30, 2006, doi: 10.2147/nano.2006.1.1.15.

[128] V. V. T. Padil, S. Wacławek, M. Černík, and R. S. Varma, "Tree gum-based renewable materials: Sustainable applications in nanotechnology, biomedical and environmental fields," *Biotechnol. Adv.*, vol. 36, no. 7, pp. 1984–2016, 2018, doi: 10.1016/j.biotechadv.2018.08.008.

[129] A. Azarniya, E. Tamjid, N. Eslahi, and A. Simchi, "Modification of bacterial cellulose/keratin nanofibrous mats by a Tragacanth gum-conjugated hydrogel for wound healing," *Int. J. Biol. Macromol.*, vol. 134, pp. 280–289, Aug. 2019, doi: 10.1016/j.ijbiomac.2019.05.023.

[130] L. Yavari, M. Ghorbani, M. Mohammadi, and A. Pezeshki, "Colloids and Surfaces A : Physicochemical and Engineering Aspects Improvement of the physico-mechanical properties of antibacterial electrospun poly lactic acid nanofibers by incorporation of guar gum and thyme essential oil," *Colloids Surfaces A Physicochem. Eng. Asp.*, vol. 622, no. April, p. 126659, 2021, doi: 10.1016/j.colsurfa.2021.126659.

[131] V. V. T. Padil and M. Černík, "Poly (vinyl alcohol)/gum karaya electrospun plasma treated membrane for the removal of nanoparticles (Au, Ag, Pt, CuO and Fe_3O_4) from aqueous solutions," *J. Hazard. Mater.*, vol. 287, pp. 102–110, Apr. 2015, doi: 10.1016/j.jhazmat.2014.12.042.

[132] T. S. Vo, T. T. B. C. Vo, T. T. Tran, and N. D. Pham, "Enhancement of water absorption capacity and compressibility of hydrogel sponges prepared from gelatin/chitosan matrix with different polyols," *Prog. Nat. Sci. Mater. Int.*, vol. 32, no. 1, pp. 54–62, 2022, doi: 10.1016/j.pnsc.2021.10.001.

[133] K. Ngece, B. A. Aderibigbe, D. T. Ndinteh, Y. T. Fonkui, and P. Kumar, "Alginate-gum acacia based sponges as potential wound dressings for exuding and bleeding wounds," *Int. J. Biol. Macromol.*, vol. 172, pp. 350–359, 2021, doi: 10.1016/j.ijbiomac.2021.01.055.

[134] I. M. Garnica-Palafox and F. M. Sánchez-Arévalo, "Influence of natural and synthetic crosslinking reagents on the structural and mechanical properties of chitosan-based hybrid hydrogels," *Carbohydr. Polym.*, vol. 151, pp. 1073–1081, Oct. 2016, doi: 10.1016/j.carbpol.2016.06.036.

[135] J. Kopeček and J. Yang, "Smart Self-Assembled Hybrid Hydrogel Biomaterials," *Angew. Chemie Int. Ed.*, vol. 51, no. 30, pp. 7396–7417, Jul. 2012, doi: 10.1002/anie.201201040.

[136] K. Varaprasad, G. M. Raghavendra, T. Jayaramudu, M. M. Yallapu, and R. Sadiku, "A mini review on hydrogels classification and recent developments in miscellaneous applications," *Mater. Sci. Eng. C*, vol. 79, pp. 958–971, Oct. 2017, doi: 10.1016/j.msec.2017.05.096.

[137] W. E. Hennink and C. F. van Nostrum, "Novel crosslinking methods to design hydrogels," *Adv. Drug Deliv. Rev.*, vol. 64, pp. 13–36, Dec. 2012, doi: 10.1016/j.addr.2012.09.009.

[138] R. R. Palem, K. Madhusudana Rao, and T. J. Kang, "Self-healable and dual-

functional guar gum-grafted-polyacrylamidoglycolic acid-based hydrogels with nano-silver for wound dressings," *Carbohydr. Polym.*, vol. 223, p. 115074, Nov. 2019, doi: 10.1016/j.carbpol.2019.115074.

[139] F. Ullah, M. B. H. Othman, F. Javed, Z. Ahmad, and H. M. Akil, "Classification, processing and application of hydrogels: A review," *Mater. Sci. Eng. C*, vol. 57, pp. 414–433, Dec. 2015, doi: 10.1016/j.msec.2015.07.053.

[140] B. Singh, L. Varshney, S. Francis, and Rajneesh, "Synthesis and characterization of tragacanth gum based hydrogels by radiation method for use in wound dressing application," *Radiat. Phys. Chem.*, vol. 135, pp. 94–105, Jun. 2017, doi: 10.1016/j.radphyschem.2017.01.044.

[141] S. Swain and T. Bal, "Carrageenan-guar gum microwave irradiated micro-porous interpenetrating polymer network: A system for drug delivery," *Int. J. Polym. Mater. Polym. Biomater.*, vol. 68, no. 5, pp. 256–265, Mar. 2019, doi: 10.1080/00914037.2018.1443931.

[142] H. M. Said, S. G. Abd Alla, and A. W. M. El-Naggar, "Synthesis and characterization of novel gels based on carboxymethyl cellulose/acrylic acid prepared by electron beam irradiation," *React. Funct. Polym.*, vol. 61, no. 3, pp. 397–404, Nov. 2004, doi: 10.1016/j.reactfunctpolym.2004.07.002.

[143] R. Jin et al., "Injectable chitosan-based hydrogels for cartilage tissue engineering," *Biomaterials*, vol. 30, no. 13, pp. 2544–2551, May 2009, doi: 10.1016/j.biomaterials.2009.01.020.

[144] T. Chen, H. D. Embree, L.-Q. Wu, and G. F. Payne, "In vitro protein-

polysaccharide conjugation: Tyrosinase-catalyzed conjugation of gelatin and chitosan," *Biopolymers*, vol. 64, no. 6, pp. 292–302, Sep. 2002, doi: 10.1002/bip.10196.

[145] C. W. Yung, L. Q. Wu, J. A. Tullman, G. F. Payne, W. E. Bentley, and T. A. Barbari, "Transglutaminase crosslinked gelatin as a tissue engineering scaffold," *J. Biomed. Mater. Res. - Part A*, vol. 83, no. 4, pp. 1039–1046, Dec. 2007, doi: 10.1002/jbm.a.31431.

[146] H. Pan et al., "Strength-tunable printing of xanthan gum hydrogel via enzymatic polymerization and amide bioconjugation," *Chem. Commun.*, vol. 56, no. 23, pp. 3457–3460, 2020, doi: 10.1039/D0CC00326C.

[147] Nandini Sahu, Diksha Gupta, and Ujjwal Nautiyal, "Hydrogel: Preparation, Characterization and Applications," *Asian Pacific J. Nurs. Heal. Sci.*, vol. 3, no. 1, pp. 1–11, 2020, doi: 10.46811/apjnh/3.1.2.

[148] T. Funami, M. Hiroe, S. Noda, I. Asai, S. Ikeda, and K. Nishinari, "Influence of molecular structure imaged with atomic force microscopy on the rheological behavior of carrageenan aqueous systems in the presence or absence of cations," *Food Hydrocoll.*, vol. 21, no. 4, pp. 617–629, Jun. 2007, doi: 10.1016/j.foodhyd.2006.07.013.

[149] B. Jeong, Y. H. Bae, and S. W. Kim, "Thermoreversible gelation of PEG-PLGA-PEG triblock copolymer aqueous solutions," *Macromolecules*, vol. 32, no. 21, pp. 7064–7069, Oct. 1999, doi: 10.1021/ma9908999.

[150] D. Magnin, "Physicochemical and structural characterization of a polyionic matrix of interest in biotechnology, in the pharmaceutical and biomedical

fields," *Carbohydr. Polym.*, vol. 55, no. 4, pp. 437–453, Mar. 2004, doi: 10.1016/j.carbpol.2003.11.013.

[151] I. G. Veiga and Â. M. Moraes, "Study of the swelling and stability properties of Chitosan-Xanthan membranes," *J. Appl. Polym. Sci.*, vol. 124, no. S1, pp. E154–E160, Jun. 2012, doi: 10.1002/app.35526.

[152] S. Maiti, P. S. Khillar, D. Mishra, N. A. Nambiraj, and A. K. Jaiswal, "Physical and self–crosslinking mechanism and characterization of chitosan-gelatin-oxidized guar gum hydrogel," *Polym. Test.*, vol. 97, p. 107155, May 2021, doi: 10.1016/j.polymertesting.2021.107155.

[153] E. M. Ahmed, "Hydrogel: Preparation, characterization, and applications: A review," *J. Adv. Res.*, vol. 6, no. 2, pp. 105–121, 2015, doi: 10.1016/j.jare.2013.07.006.

[154] M. Takigami et al., "Preparation and Properties of CMC Gel," *Trans. Mater. Res. Soc. Japan*, vol. 32, no. 3, pp. 713–716, 2007, doi: 10.14723/tmrsj.32.713.

[155] H. Zhang, F. Zhang, and J. Wu, "Physically crosslinked hydrogels from polysaccharides prepared by freeze-thaw technique," *React. Funct. Polym.*, vol. 73, no. 7, pp. 923–928, 2013, doi: 10.1016/j.reactfunctpolym.2012.12.014.

[156] M. Iijima, T. Hatakeyama, and H. Hatakeyama, "Gelation of cassia gum by freezing and thawing," *J. Therm. Anal. Calorim.*, vol. 113, no. 3, pp. 1073–1078, Sep. 2013, doi: 10.1007/s10973-013-3023-5.

[157] S. Al-Assaf, G. O. Phillips, H. Aoki, and Y. Sasaki, "Characterization and

properties of *Acacia senegal (L.)* Willd. var. senegal with enhanced properties (Acacia (Sen) Super Gum[tm]): Part 1—Controlled maturation of *Acacia senegal* var. senegal to increase viscoelasticity, produce a hydrogel form and convert a p," *Food Hydrocoll.*, vol. 21, no. 3, pp. 319–328, May 2007, doi: 10.1016/j.foodhyd.2006.04.011.

[158] Shengjie Lv, Lianying Liu, and Wantai yang*, "Preparation of Soft Hydrogel Nanoparticles with PNIPAm Hair and Characterization of their Temperature-Induced Aggregation," *Langmuir* , vol. 26, pp. 2076–2082, Sep. 2010.

[159] T. Iizawa, H. Taketa, M. Maruta, T. Ishido, T. Gotoh, and S. Sakohara, "Synthesis of porous poly(N-isopropylacrylamide) gel beads by sedimentation polymerization and their morphology," *J. Appl. Polym. Sci.*, vol. 104, no. 2, pp. 842–850, Apr. 2007, doi: 10.1002/app.25605.

[160] C. Y. Gong et al., "Synthesis and characterization of PEG-PCL-PEG thermosensitive hydrogel," *Int. J. Pharm.*, vol. 365, no. 1–2, pp. 89–99, Jan. 2009, doi: 10.1016/j.ijpharm.2008.08.027.

[161] H. Mittal, A. Maity, and S. S. Ray, "Synthesis of co-polymer-grafted gum karaya and silica hybrid organic-inorganic hydrogel nanocomposite for the highly effective removal of methylene blue," *Chem. Eng. J.*, vol. 279, pp. 166–179, Nov. 2015, doi: 10.1016/j.cej.2015.05.002.

[162] N. Yang et al., "Rheological behaviors and texture properties of semi-interpenetrating networks of hydroxypropyl methylcellulose and gellan," *Food Hydrocoll.*, vol. 122, p. 107097, Jan. 2022, doi: 10.1016/j.foodhyd.2021.107097.

[163] Y. Zhao, J. Kang, and T. Tan, "Salt-, pH- and temperature-responsive semi-interpenetrating polymer network hydrogel based on poly(aspartic acid) and poly(acrylic acid)," *Polymer (Guildf).*, vol. 47, no. 22, pp. 7702–7710, Oct. 2006, doi: 10.1016/j.polymer.2006.08.056.

[164] Y. S. Lipatov, "Polymer blends and interpenetrating polymer networks at the interface with solids," *Prog. Polym. Sci.*, vol. 27, no. 9, pp. 1721–1801, 2002, doi: 10.1016/S0079-6700(02)00021-7.

[165] M. S. Shin, S. J. Kim, S. J. Park, Y. H. Lee, and S. I. Kim, "Synthesis and characteristics of the interpenetrating polymer network hydrogel composed of chitosan and polyallylamine," *J. Appl. Polym. Sci.*, vol. 86, no. 2, pp. 498–503, 2002, doi: 10.1002/app.11008.

[166] U. S. K. Madduma-Bandarage and S. V. Madihally, "Synthetic hydrogels: Synthesis, novel trends, and applications," *J. Appl. Polym. Sci.*, vol. 138, no. 19, p. 50376, May 2021, doi: 10.1002/app.50376.

[167] J. Qu, X. Zhao, Y. Liang, T. Zhang, P. X. Ma, and B. Guo, "Antibacterial adhesive injectable hydrogels with rapid self-healing, extensibility and compressibility as wound dressing for joints skin wound healing," *Biomaterials*, vol. 183, pp. 185–199, Nov. 2018, doi: 10.1016/j.biomaterials.2018.08.044.

[168] A. S. Hoffman, "Conventional and Environmentally-Sensitive Hydrogels for Medical and Industrial Uses: A Review Paper," in *Polymer Gels*, Boston, MA: Springer US, 1991, pp. 289–297. doi: 10.1007/978-1-4684-5892-3_21.

[169] W. Zhang et al., "Factors affecting the properties of superabsorbent polymer

hydrogels and methods to improve their performance: a review," *J. Mater. Sci.*, vol. 56, no. 29, pp. 16223–16242, Oct. 2021, doi: 10.1007/s10853-021-06306-1.

[170] A. V. Reis, M. R. Guilherme, O. A. Cavalcanti, A. F. Rubira, and E. C. Muniz, "Synthesis and characterization of pH-responsive hydrogels based on chemically modified Arabic gum polysaccharide," *Polymer (Guildf).*, vol. 47, no. 6, pp. 2023–2029, Mar. 2006, doi: 10.1016/j.polymer.2006.01.058.

[171] H. Tan, J. P. Rubin, and K. G. Marra, "Injectable in situ forming biodegradable chitosan-hyaluronic acid based hydrogels for adipose tissue regeneration," *Organogenesis*, vol. 6, no. 3, pp. 173–180, Jul. 2010, doi: 10.4161/org.6.3.12037.

[172] S. Souza, S. Kogikoski Jr., E. Silva, and W. Alves, "Nanostructured Antigen-Responsive Hydrogels Based on Peptides for Leishmaniasis Detection," *J. Braz. Chem. Soc.*, vol. 28, no. 9, pp. 1619–1629, 2016, doi: 10.21577/0103-5053.20160301.

[173] F. Hemmatgir, N. Koupaei, and E. Poorazizi, "Characterization of a novel semi-interpenetrating hydrogel network fabricated by polyethylene glycol diacrylate/polyvinyl alcohol/tragacanth gum as a wound dressing," *Burns*, vol. 48, no. 1, pp. 146–155, May 2022, doi: 10.1016/j.burns.2021.04.025.

[174] Saruchi, V. Kumar, H. Mittal, and S. M. Alhassan, "Biodegradable hydrogels of Tragacanth gum polysaccharide to improve water retention capacity of soil and environment-friendly controlled release of agrochemicals," *Int. J. Biol. Macromol.*, vol. 132, pp. 1252–1261, Jul. 2019, doi:

10.1016/j.ijbiomac.2019.04.023.

[175] B. Sharma et al., "Titania modified gum tragacanth based hydrogel nanocomposite for water remediation," *J. Environ. Chem. Eng.*, vol. 9, no. 1, p. 104608, Feb. 2021, doi: 10.1016/j.jece.2020.104608.

[176] R. R. Bhosale et al., "Ghatti gum-base graft copolymer: A plausible platform for pH-controlled delivery of antidiabetic drugs," *RSC Adv.*, vol. 11, no. 24, pp. 14871–14882, 2021, doi: 10.1039/d1ra01536b.

[177] K. Sharma et al., "A study of the biodegradation behaviour of poly(methacrylic acid/aniline)-grafted gum Ghatti by a soil burial method," *RSC Adv.*, vol. 4, no. 49, pp. 25637–25649, 2014, doi: 10.1039/c4ra03765k.

[178] P. Zhang, Y. Zhao, and Q. Shi, "Characterization of a novel edible film based on gum ghatti: Effect of plasticizer type and concentration," *Carbohydr. Polym.*, vol. 153, pp. 345–355, Nov. 2016, doi: 10.1016/j.carbpol.2016.07.082.

[179] H. Daud et al., "Preparation and characterization of guar gum based biopolymeric hydrogels for controlled release of antihypertensive drug," *Arab. J. Chem.*, vol. 14, no. 5, p. 103111, May 2021, doi: 10.1016/j.arabjc.2021.103111.

[180] N. Thombare, S. Mishra, R. Shinde, M. Z. Siddiqui, and U. Jha, "Guar gum based hydrogel as controlled micronutrient delivery system: Mechanism and kinetics of boron release for agricultural applications," *Biopolymers*, vol. 112, p. e23418, Mar. 2021, doi: 10.1002/bip.23418.

[181] S. P. Santoso et al., "TiO_2/guar gum hydrogel composite for adsorption and

photodegradation of methylene blue," *Int. J. Biol. Macromol.*, vol. 193, pp. 721–733, Oct. 2021, doi: 10.1016/j.ijbiomac.2021.10.044.

[182] J. H. Kim, H. J. Min, K. Park, and J. Kim, "Preparation and evaluation of a cosmetic adhesive containing guar gum," *Korean J. Chem. Eng.*, vol. 34, no. 8, pp. 2236–2240, Aug. 2017, doi: 10.1007/s11814-017-0133-y.

[183] S. Rahman, A. Konwar, G. Majumdar, and D. Chowdhury, "Guar gum-chitosan composite film as excellent material for packaging application," *Carbohydr. Polym. Technol. Appl.*, vol. 2, p. 100158, Dec. 2021, doi: 10.1016/j.carpta.2021.100158.

[184] J. K. Rutz et al., "Microencapsulation of purple Brazilian cherry juice in xanthan, tara gums and xanthan-tara hydrogel matrixes," *Carbohydr. Polym.*, vol. 98, no. 2, pp. 1256–1265, Nov. 2013, doi: 10.1016/j.carbpol.2013.07.058.

[185] S. G. Abd Alla, M. Sen, and A. W. M. El-Naggar, "Swelling and mechanical properties of superabsorbent hydrogels based on Tara gum/acrylic acid synthesized by gamma radiation," *Carbohydr. Polym.*, vol. 89, no. 2, pp. 478–485, Jun. 2012, doi: 10.1016/j.carbpol.2012.03.031.

[186] J. Shen, B. Li, X. Zhan, and L. Wang, "A One Pot Method for Preparing an Antibacterial Superabsorbent Hydrogel with a Semi-IPN Structure Based on Tara Gum and Polyquaternium-7," *Polymers (Basel).*, vol. 10, no. 7, p. 696, Jun. 2018, doi: 10.3390/polym10070696.

[187] Q. Ma, D. Hu, H. Wang, and L. Wang, "Tara gum edible film incorporated with oleic acid," *Food Hydrocoll.*, vol. 56, pp. 127–133, May 2016, doi: 10.1016/j.foodhyd.2015.11.033.

[188] D. Qureshi et al., "Synthesis of novel poly (vinyl alcohol)/tamarind gum/bentonite-based composite films for drug delivery applications," *Colloids Surfaces A Physicochem. Eng. Asp.*, vol. 613, p. 126043, Mar. 2021, doi: 10.1016/j.colsurfa.2020.126043.

[189] A. Pal and S. Pal, "Amphiphilic copolymer derived from tamarind gum and poly (methyl methacrylate) via ATRP towards selective removal of toxic dyes," *Carbohydr. Polym.*, vol. 160, pp. 1–8, Mar. 2017, doi: 10.1016/j.carbpol.2016.12.008.

[190] P. He et al., "Tough and super-stretchable conductive double network hydrogels with multiple sensations and moisture-electric generation," *Chem. Eng. J.*, vol. 414, p. 128726, Jun. 2021, doi: 10.1016/j.cej.2021.128726.

[191] N. S. Malik et al., "Chitosan/Xanthan Gum Based Hydrogels as Potential Carrier for an Antiviral Drug: Fabrication, Characterization, and Safety Evaluation," *Front. Chem.*, vol. 8, p. 50, Feb. 2020, doi: 10.3389/fchem.2020.00050.

[192] P. S. Gils, D. Ray, and P. K. Sahoo, "Characteristics of xanthan gum-based biodegradable superporous hydrogel," *Int. J. Biol. Macromol.*, vol. 45, no. 4, pp. 364–371, Nov. 2009, doi: 10.1016/j.ijbiomac.2009.07.007.

[193] Q. Zhang, X. M. Hu, M. Y. Wu, M. M. Wang, Y. Y. Zhao, and T. T. Li, "Synthesis and performance characterization of poly(vinyl alcohol)-xanthan gum composite hydrogel," *React. Funct. Polym.*, vol. 136, pp. 34–43, Mar. 2019, doi: 10.1016/j.reactfunctpolym.2019.01.002.

[194] E. J. Da-Lozzo, R. C. A. Moledo, C. D. Faraco, C. F. Ortolani-Machado, T.

M. B. Bresolin, and J. L. M. Silveira, "Curcumin/xanthan–galactomannan hydrogels: Rheological analysis and biocompatibility," *Carbohydr. Polym.*, vol. 93, no. 1, pp. 279–284, Mar. 2013, doi: 10.1016/j.carbpol.2012.02.036.

[195] R. Balasubramanian, S. S. Kim, and J. Lee, "Novel synergistic transparent k-Carrageenan/Xanthan gum/Gellan gum hydrogel film: Mechanical, thermal and water barrier properties," *Int. J. Biol. Macromol.*, vol. 118, pp. 561–568, Oct. 2018, doi: 10.1016/j.ijbiomac.2018.06.110.

[196] S. Bashir, Y. Y. Teo, S. Ramesh, and K. Ramesh, "Synthesis and characterization of karaya gum-g- poly (acrylic acid) hydrogels and in vitro release of hydrophobic quercetin," *Polymer (Guildf).*, vol. 147, pp. 108–120, Jul. 2018, doi: 10.1016/j.polymer.2018.05.071.

[197] H. Mittal, A. Maity, and S. S. Ray, "Gum karaya based hydrogel nanocomposites for the effective removal of cationic dyes from aqueous solutions," *Appl. Surf. Sci.*, vol. 364, pp. 917–930, Feb. 2016, doi: 10.1016/j.apsusc.2015.12.241.

[198] T. L. Cao and K. Bin Song, "Active gum karaya/Cloisite Na+ nanocomposite films containing cinnamaldehyde," *Food Hydrocoll.*, vol. 89, pp. 453–460, Apr. 2019, doi: 10.1016/j.foodhyd.2018.11.004.

[199] L. Cao, W. Liu, and L. Wang, "Developing a green and edible film from Cassia gum: The effects of glycerol and sorbitol," *J. Clean. Prod.*, vol. 175, pp. 276–282, Feb. 2018, doi: 10.1016/j.jclepro.2017.12.064.

[200] Y. Deng et al., "Novel fenugreek gum-cellulose composite hydrogel with wound healing synergism: Facile preparation, characterization and wound

healing activity evaluation," *Int. J. Biol. Macromol.*, vol. 160, pp. 1242–1251, Oct. 2020, doi: 10.1016/j.ijbiomac.2020.05.220.

[201] C. Liu, F. Lei, P. Li, J. Jiang, and K. Wang, "Borax crosslinked fenugreek galactomannan hydrogel as potential water-retaining agent in agriculture," *Carbohydr. Polym.*, vol. 236, p. 116100, May 2020, doi: 10.1016/j.carbpol.2020.116100.

[202] S. Mishra and K. Kundu, "Synthesis, characterization and applications of polyacrylamide grafted fenugreek gum (FG-g-PAM) as flocculant: Microwave vs thermal synthesis approach," *Int. J. Biol. Macromol.*, vol. 141, pp. 792–808, Dec. 2019, doi: 10.1016/j.ijbiomac.2019.09.033.

[203] B. Rossi, E. Ponzini, L. Merlini, R. Grandori, and Y. M. Galante, "Characterization of aerogels from chemo-enzymatically oxidized galactomannans as novel polymeric biomaterials," *Eur. Polym. J.*, vol. 93, pp. 347–357, Aug. 2017, doi: 10.1016/j.eurpolymj.2017.06.016.

[204] M. Jayaprada and M. J. Umapathy, "Preparation and properties of a microfibrillated cellulose reinforced pectin/fenugreek gum biocomposite," *New J. Chem.*, vol. 44, no. 43, pp. 18792–18802, 2020, doi: 10.1039/D0NJ03101A.

[205] Y. Niu, T. Yang, R. Ke, and C. Wang, "Preparation and characterization of pH-responsive sodium alginate/humic acid/konjac hydrogel for L-ascorbic acid controlled release," *Mater. Express*, vol. 9, no. 6, pp. 563–569, Sep. 2019, doi: 10.1166/mex.2019.1537.

[206] Z. Wei and G. Li, "Preparation of konjac glucomannan/xanthan gum plural gel

embedding urea and its release performance," *Huagong Xuebao/CIESC J.*, vol. 62, no. 1, pp. 255–261, 2011.

[207] L. Gan, S. Shang, E. Hu, C. W. M. Yuen, and S. Jiang, "Konjac glucomannan/graphene oxide hydrogel with enhanced dyes adsorption capability for methyl blue and methyl orange," *Appl. Surf. Sci.*, vol. 357, pp. 866–872, Dec. 2015, doi: 10.1016/j.apsusc.2015.09.106.

[208] C. Schnitzler, Iris; Hausen, Christian; Klein, "Hydrogel comprising natural polysaccharides konjac mannan, xanthan gum, pullulan and carrageenan, and optionally sclerotium gum, for skin care cosmetics," 2011

[209] J.-W. Rhim and L.-F. Wang, "Mechanical and water barrier properties of agar/κ-carrageenan/konjac glucomannan ternary blend biohydrogel films," *Carbohydr. Polym.*, vol. 96, no. 1, pp. 71–81, Jul. 2013, doi: 10.1016/j.carbpol.2013.03.083.

[210] A. M. Slavutsky, M. A. Bertuzzi, M. Armada, M. G. García, and N. A. Ochoa, "Preparation and characterization of montmorillonite/brea gum nanocomposites films," *Food Hydrocoll.*, vol. 35, pp. 270–278, Mar. 2014, doi: 10.1016/j.foodhyd.2013.06.008.

[211] J. H. Choi et al., "Preparation and characterization of an injectable dexamethasone-cyclodextrin complexes-loaded gellan gum hydrogel for cartilage tissue engineering," *J. Control. Release*, vol. 327, pp. 747–765, Nov. 2020, doi: 10.1016/j.jconrel.2020.08.049.

[212] R. C. Sabadini, M. M. Silva, A. Pawlicka, and J. Kanicki, "Gellan gum- *O,O'*-bis(2-aminopropyl)-polyethylene glycol hydrogel for controlled fertilizer

release," *J. Appl. Polym. Sci.*, vol. 135, no. 2, p. 45636, Jan. 2018, doi: 10.1002/app.45636.

[213] S. Choudhary, K. Sharma, V. Kumar, J. K. Bhatia, S. Sharma, and V. Sharma, "Microwave-assisted synthesis of gum gellan-cl-poly(acrylic-co- methacrylic acid) hydrogel for cationic dyes removal," *Polym. Bull.*, vol. 77, no. 9, pp. 4917–4935, Sep. 2020, doi: 10.1007/s00289-019-02998-3.

[214] R. Nair and A. Roy Choudhury, "Synthesis and rheological characterization of a novel shear thinning levan gellan hydrogel," *Int. J. Biol. Macromol.*, vol. 159, pp. 922–930, Sep. 2020, doi: 10.1016/j.ijbiomac.2020.05.119.

[215] M. T. Haseeb, M. A. Hussain, S. H. Yuk, S. Bashir, and M. Nauman, "Polysaccharides based superabsorbent hydrogel from Linseed: Dynamic swelling, stimuli responsive on-off switching and drug release," *Carbohydr. Polym.*, vol. 136, pp. 750–756, Jan. 2016, doi: 10.1016/j.carbpol.2015.09.092.

[216] H. Zhang et al., "A facile and efficient strategy for the fabrication of porous linseed gum/cellulose superabsorbent hydrogels for water conservation," *Carbohydr. Polym.*, vol. 157, pp. 1830–1836, Feb. 2017, doi: 10.1016/j.carbpol.2016.11.070.

[217] N. S. Prado et al., "Nanocomposite films based on flaxseed gum and cellulose nanocrystals," *Mater. Res.*, vol. 21, no. 6, p. e20180134, Oct. 2018, doi: 10.1590/1980-5373-MR-2018-0134.

[218] A. K. Sharma, B. S. Kaith, U. Shanker, and B. Gupta, "γ-radiation induced synthesis of antibacterial silver nanocomposite scaffolds derived from natural gum *Boswellia serrata*," *J. Drug Deliv. Sci. Technol.*, vol. 56, p. 101550, Apr.

2020, doi: 10.1016/j.jddst.2020.101550.

[219] L. Yavari Maroufi and M. Ghorbani, "Injectable chitosan-quince seed gum hydrogels encapsulated with curcumin loaded-halloysite nanotubes designed for tissue engineering application," *Int. J. Biol. Macromol.*, vol. 177, pp. 485–494, Apr. 2021, doi: 10.1016/j.ijbiomac.2021.02.113.

[220] H. Hosseinzadeh and S. Mohammadi, "Quince seed mucilage magnetic nanocomposites as novel bioadsorbents for efficient removal of cationic dyes from aqueous solutions," *Carbohydr. Polym.*, vol. 134, pp. 213–221, Dec. 2015, doi: 10.1016/j.carbpol.2015.08.008.

[221] A. S. Shekarabi, A. R. Oromiehie, A. Vaziri, M. Ardjmand, and A. A. Safekordi, "Investigation of the effect of nanoclay on the properties of quince seed mucilage edible films," *Food Sci. Nutr.*, vol. 2, no. 6, pp. 821–827, Nov. 2014, doi: 10.1002/fsn3.177.

[222] L. R. M. Lima et al., "Thermal responsive poly-N-isopropylacrylamide/galactomannan copolymer nanoparticles as a potential amphotericin delivery carrier," *Carbohydr. Polym. Technol. Appl.*, vol. 2, p. 100126, Dec. 2021, doi: 10.1016/j.carpta.2021.100126.

[223] W. Rodriguez-Canto, M. A. Cerqueira, L. Chel-Guerrero, L. M. Pastrana, and M. Aguilar-Vega, "*Delonix regia* galactomannan-based edible films: Effect of molecular weight and k-carrageenan on physicochemical properties," *Food Hydrocoll.*, vol. 103, p. 105632, Jun. 2020, doi: 10.1016/j.foodhyd.2019.105632.

[224] S. Kaur and R. Jindal, "Synthesis of interpenetrating network hydrogel from

(gum copal alcohols-collagen)-co-poly(acrylamide) and acrylic acid: Isotherms and kinetics study for removal of methylene blue dye from aqueous solution," *Mater. Chem. Phys.*, vol. 220, pp. 75–86, Dec. 2018, doi: 10.1016/j.matchemphys.2018.08.008.

[225] D. Kumar, J. Pandey, and P. Kumar, "Microwave assisted synthesis of binary grafted psyllium and its utility in anticancer formulation," *Carbohydr. Polym.*, vol. 179, pp. 408–414, Jan. 2018, doi: 10.1016/j.carbpol.2017.09.093.

[226] D. Aydınoğlu, N. Karaca, and Ö. Ceylan, "Natural Carrageenan/Psyllium Composite Hydrogels Embedded Montmorillonite and Investigation of Their Use in Agricultural Water Management," *J. Polym. Environ.*, vol. 29, no. 3, pp. 785–798, Mar. 2021, doi: 10.1007/s10924-020-01914-5.

[227] S. chaudhary, J. Sharma, B. S. Kaith, S. yadav, A. K. Sharma, and A. Goel, "Gum xanthan-psyllium-cl-poly(acrylic acid-co-itaconic acid) based adsorbent for effective removal of cationic and anionic dyes: Adsorption isotherms, kinetics and thermodynamic studies," *Ecotoxicol. Environ. Saf.*, vol. 149, pp. 150–158, Mar. 2018, doi: 10.1016/j.ecoenv.2017.11.030.

[228] F. Askari et al., "The physicochemical and structural properties of psyllium gum/modified starch composite edible film," *J. Food Process. Preserv.*, vol. 42, no. 10, p. e13715, Oct. 2018, doi: 10.1111/jfpp.13715.

[229] A. Setia and R. Kumar, "Microwave assisted synthesis and optimization of Aegle marmelos-g-poly(acrylamide): Release kinetics studies," *Int. J. Biol. Macromol.*, vol. 65, pp. 462–470, Apr. 2014, doi: 10.1016/j.ijbiomac.2014.02.006.

[230] B. Sharma, A. Sandilya, U. Patel, A. Shukla, and S. D. Sadhu, "A bio-inspired exploration of eco-friendly bael gum and guar gum-based bioadhesive as tackifiers for packaging applications," *Int. J. Adhes. Adhes.*, vol. 110, p. 102946, Oct. 2021, doi: 10.1016/j.ijadhadh.2021.102946.

[231] S. Malik, A. Kumar, and M. Ahuja, "Synthesis of gum kondagogu-g-poly(N-vinyl-2-pyrrolidone) and its evaluation as a mucoadhesive polymer," *Int. J. Biol. Macromol.*, vol. 51, no. 5, pp. 756–762, Dec. 2012, doi: 10.1016/j.ijbiomac.2012.07.009.

[232] R. K. Ramakrishnan, V. V. T. Padil, M. Škodová, S. Wacławek, M. Černík, and S. Agarwal, "Hierarchically Porous Bio-Based Sustainable Conjugate Sponge for Highly Selective Oil/Organic Solvent Absorption," *Adv. Funct. Mater.*, vol. 31, no. 18, p. 2100640, May 2021, doi: 10.1002/adfm.202100640.

[233] R. K. Ramakrishnan, S. Wacławek, M. Černík, and V. V. T. Padil, "Biomacromolecule assembly based on gum kondagogu-sodium alginate composites and their expediency in flexible packaging films," *Int. J. Biol. Macromol.*, vol. 177, pp. 526–534, Apr. 2021, doi: 10.1016/j.ijbiomac.2021.02.156.

[234] P. Pal, J. P. Pandey, and G. Sen, "Sesbania gum based hydrogel as platform for sustained drug delivery: An 'in vitro' study of 5-Fu release," *Int. J. Biol. Macromol.*, vol. 113, pp. 1116–1124, Jul. 2018, doi: 10.1016/j.ijbiomac.2018.02.143.

[235] P. Pal, A. Banerjee, U. Halder, J. P. Pandey, G. Sen, and R. Bandopadhyay, "Conferring Antibacterial Properties on Sesbania Gum via Microwave-

Assisted Graft Copolymerization of DADMAC," *J. Polym. Environ.*, vol. 26, no. 8, pp. 3272–3282, Aug. 2018, doi: 10.1007/s10924-018-1213-8.

[236] W. Liu, Z. Ling, C. Huang, C. Lai, and Q. Yong, "Investigation of galactomannan/deacetylated chitosan nanocomposite films and their anti-bacterial capabilities," *Mater. Today Commun.*, vol. 30, p. 103002, Mar. 2022, doi: 10.1016/j.mtcomm.2021.103002.

[237] S. Ranote, B. Ram, D. Kumar, G. S. Chauhan, and V. Joshi, "Functionalization of *Moringa oleifera* gum for use as Hg^{2+} ions adsorbent," *J. Environ. Chem. Eng.*, vol. 6, no. 2, pp. 1805–1813, Apr. 2018, doi: 10.1016/j.jece.2018.02.032.

[238] S. Maryam et al., "Polymeric blends of okra gum/gelatin prepared by aqueous polymerization technique: their characterization and toxicological evaluation," *Polym. Bull.*, 2021, doi: 10.1007/s00289-021-03561-9.

[239] M. Nagpal, G. Aggarwal, U. K. Jain, and J. Madan, "Okra fruit gum-chitosan impregnated polymer network films: Formulation and substantial depiction," *Asian J. Pharm. Clin. Res.*, vol. 10, no. 10, pp. 219–222, Oct. 2017, doi: 10.22159/ajpcr.2017.v10i10.20362.

[240] P. Mankotia et al., "Neem gum based pH responsive hydrogel matrix: A new pharmaceutical excipient for the sustained release of anticancer drug," *Int. J. Biol. Macromol.*, vol. 142, pp. 742–755, Jan. 2020, doi: 10.1016/j.ijbiomac.2019.10.015.

[241] B. R. Moreira, K. A. Batista, E. G. Castro, E. M. Lima, and K. F. Fernandes, "A bioactive film based on cashew gum polysaccharide for wound dressing

applications," *Carbohydr. Polym.*, vol. 122, pp. 69–76, May 2015, doi: 10.1016/j.carbpol.2014.12.067.

[242] B. D. S. Silva et al., "Biodegradable and bioactive CGP/PVA film for fungal growth inhibition," *Carbohydr. Polym.*, vol. 89, no. 3, pp. 964–970, Jul. 2012, doi: 10.1016/j.carbpol.2012.04.052.

[243] B. Singh, S. Sharma, and A. Dhiman, "Acacia gum polysaccharide based hydrogel wound dressings: Synthesis, characterization, drug delivery and biomedical properties," *Carbohydr. Polym.*, vol. 165, pp. 294–303, Jun. 2017, doi: 10.1016/j.carbpol.2017.02.039.

[244] M. J. Zohuriaan-Mehr, Z. Motazedi, K. Kabiri, A. Ershad-Langroudi, and I. Allahdadi, "Gum arabic–acrylic superabsorbing hydrogel hybrids: Studies on swelling rate and environmental responsiveness," *J. Appl. Polym. Sci.*, vol. 102, no. 6, pp. 5667–5674, Dec. 2006, doi: 10.1002/app.25033.

[245] B. S. Kaith, R. Sharma, K. Sharma, S. Choudhary, V. Kumar, and S. P. Lochab, "Effects of O 7+ and Ni 9+ swift heavy ions irradiation on polyacrylamide grafted Gum acacia thin film and sorption of methylene blue," *Vacuum*, vol. 111, pp. 73–82, Jan. 2015, doi: 10.1016/j.vacuum.2014.09.020.

[246] M. Anvari and D. Chung, "Dynamic rheological and structural characterization of fish gelatin – Gum arabic coacervate gels cross-linked by tannic acid," *Food Hydrocoll.*, vol. 60, pp. 516–524, Oct. 2016, doi: 10.1016/j.foodhyd.2016.04.028.

[247] E. Bulut and M. Dilek, "Development and characterization of pH-sensitive locust bean gum-alginate microspheres for controlled release of ibuprofen," *J.*

Drug Deliv. Sci. Technol., vol. 24, no. 6, pp. 613–619, 2014, doi: 10.1016/S1773-2247(14)50127-X.

[248] S. Pandey, J. Y. Do, J. Kim, and M. Kang, "Fast and highly efficient removal of dye from aqueous solution using natural locust bean gum based hydrogels as adsorbent," *Int. J. Biol. Macromol.*, vol. 143, pp. 60–75, Jan. 2020, doi: 10.1016/j.ijbiomac.2019.12.002.

[249] J. T. Martins, M. A. Cerqueira, A. I. Bourbon, A. C. Pinheiro, B. W. S. Souza, and A. A. Vicente, "Synergistic effects between κ-carrageenan and locust bean gum on physicochemical properties of edible films made thereof," *Food Hydrocoll.*, vol. 29, no. 2, pp. 280–289, Dec. 2012, doi: 10.1016/j.foodhyd.2012.03.004.

[250] S. A. Oleyaei, S. M. A. Razavi, and K. S. Mikkonen, "Novel nanobiocomposite hydrogels based on sage seed gum-laponite: Physico-chemical and rheological characterization," *Carbohydr. Polym.*, vol. 192, pp. 282–290, 2018, doi: 10.1016/j.carbpol.2018.03.081.

[251] S. M. A. Razavi, A. Mohammad Amini, and Y. Zahedi, "Characterisation of a new biodegradable edible film based on sage seed gum: Influence of plasticiser type and concentration," *Food Hydrocoll.*, vol. 43, pp. 290–298, 2015, doi: 10.1016/j.foodhyd.2014.05.028.

[252] D. Verma and S. K. Sharma, "Recent advances in guar gum based drug delivery systems and their administrative routes," *Int. J. Biol. Macromol.*, vol. 181, pp. 653–671, Jun. 2021, doi: 10.1016/j.ijbiomac.2021.03.087.

[253] B. S. Kaith, A. Singh, A. K. Sharma, and D. Sud, "Hydrogels: Synthesis,

Classification, Properties and Potential Applications—A Brief Review," *J. Polym. Environ.*, vol. 29, no. 12, pp. 3827–3841, Dec. 2021, doi: 10.1007/s10924-021-02184-5.

[254] M. Taghizadeh et al., "Chitosan-based inks for 3D printing and bioprinting," *Green Chem.*, vol. 24, no. 1, pp. 62–101, 2022, doi: 10.1039/d1gc01799c.

[255] F. Cleymand et al., "Development of novel chitosan / guar gum inks for extrusion-based 3D bioprinting: Process, printability and properties," *Bioprinting*, vol. 21, pp. 1–25, 2021, doi: 10.1016/j.bprint.2020.e00122.

[256] O. E. Adedeji et al., "Formulation and characterization of an interpenetrating network hydrogel of locust bean gum and cellulose microfibrils for 3D printing," *Innov. Food Sci. Emerg. Technol.*, vol. 80, no. April, p. 103086, 2022, doi: 10.1016/j.ifset.2022.103086.

[257] C. Lacoste, J. M. Lopez-Cuesta, and A. Bergeret, "Development of a biobased superabsorbent polymer from recycled cellulose for diapers applications," *Eur. Polym. J.*, vol. 116, pp. 38–44, 2019, doi: 10.1016/j.eurpolymj.2019.03.013.

[258] S. Qasemi and M. Ghaemy, "Highly sensitive and strongly fluorescent gum tragacanth based superabsorbent hydrogel as a new biosensor for glucose optical detection," *J. Mater. Chem. C*, vol. 8, no. 12, pp. 4148–4156, Mar. 2020, doi: 10.1039/c9tc07014a.

[259] S. Patel and A. Goyal, "Applications of Natural Polymer Gum Arabic: A Review," *Int. J. Food Prop.*, vol. 18, no. 5, pp. 986–998, May 2015, doi: 10.1080/10942912.2013.809541.

[260] A. Ali et al., "A novel herbal hydrogel formulation of *Moringa oleifera* for

wound healing," *Plants*, vol. 10, no. 1, pp. 1–13, Jan. 2021, doi: 10.3390/plants10010025.

[261] G. F. Pierce, Ph.D., M.D and T. A. Mustoe, M.D, "Pharmacologic enhancement of wound healing," *Annu. Rev. Med.*, vol. 46, no. 1, pp. 467–481, Feb. 1995, doi: 10.1146/annurev.med.46.1.467.

[262] A. Bajpai and V. Raj, "Hydrophobically modified guar gum films for wound dressing," *Polym. Bull.*, vol. 78, no. 8, pp. 4109–4128, 2021, doi: 10.1007/s00289-020-03302-4.

[263] N. Pettinelli, S. Rodríguez-Llamazares, R. Bouza, L. Barral, S. Feijoo-Bandín, and F. Lago, "Carrageenan-based physically crosslinked injectable hydrogel for wound healing and tissue repairing applications," *Int. J. Pharm.*, vol. 589, p. 119828, Nov. 2020, doi: 10.1016/j.ijpharm.2020.119828.

[264] M. R. Guilherme et al., "Superabsorbent hydrogels based on polysaccharides for application in agriculture as soil conditioner and nutrient carrier: A review," *Eur. Polym. J.*, vol. 72, pp. 365–385, Nov. 2015, doi: 10.1016/j.eurpolymj.2015.04.017.

[265] J. A. Chiong, H. Tran, Y. Lin, Y. Zheng, and Z. Bao, "Integrating Emerging Polymer Chemistries for the Advancement of Recyclable, Biodegradable, and Biocompatible Electronics," *Adv. Sci.*, vol. 8, no. 14, pp. 1–30, 2021, doi: 10.1002/advs.202101233.

[266] H. R. Sousa et al., "Superabsorbent hydrogels based to polyacrylamide/cashew tree gum for the controlled release of water and plant nutrients," *Molecules*, vol. 26, no. 9, p. 2680, May 2021, doi: 10.3390/molecules26092680.

[267] A. Azimi, A. Azari, M. Rezakazemi, and M. Ansarpour, "Removal of Heavy Metals from Industrial Wastewaters: A Review," *ChemBioEng Rev.*, vol. 4, no. 1, pp. 37–59, Feb. 2017, doi: 10.1002/cben.201600010.

[268] Q. Wu et al., "One-step synthesis of Cu(II) metal–organic gel as recyclable material for rapid, efficient and size selective cationic dyes adsorption," *J. Environ. Sci.*, vol. 86, pp. 203–212, Dec. 2019, doi: 10.1016/j.jes.2019.06.006.

[269] M. Ranjbar-Mohammadi, M. Rahimdokht, and E. Pajootan, "Low cost hydrogels based on gum Tragacanth and TiO_2 nanoparticles: characterization and RBFNN modelling of methylene blue dye removal," *Int. J. Biol. Macromol.*, vol. 134, pp. 967–975, Aug. 2019, doi: 10.1016/j.ijbiomac.2019.05.026.

[270] S. Mallakpour and F. Tabesh, "Green and plant-based adsorbent from tragacanth gum and carboxyl-functionalized carbon nanotube hydrogel bionanocomposite for the super removal of methylene blue dye," *Int. J. Biol. Macromol.*, vol. 166, pp. 722–729, Jan. 2021, doi: 10.1016/j.ijbiomac.2020.10.229.

[271] S. Mitura, A. Sionkowska, and A. Jaiswal, "Biopolymers for hydrogels in cosmetics: review," *J. Mater. Sci. Mater. Med.*, vol. 31, p. 50, Jun. 2020, doi: 10.1007/s10856-020-06390-w.

[272] S. K. Singh, S. Dey, M. P. Schneider, and S. Nandi, "D-Mannitol based surfactants for cosmetic and food applications and hydrogels to produce stabilized Ag nanoparticles," *New J. Chem.*, vol. 46, no. 13, pp. 6193–6200, 2022, doi: 10.1039/d2nj00463a.

[273] Z. Fan et al., "Understanding the rheological properties of a novel composite salecan/gellan hydrogels," *Food Hydrocoll.*, vol. 123, no. September 2021, p. 107162, 2022, doi: 10.1016/j.foodhyd.2021.107162.

[274] A. Mensah et al., "Bioactive Icariin/β-CD-IC/Bacterial Cellulose with Enhanced Biomedical Potential," *Nanomaterials*, vol. 11, no. 2, p. 387, Feb. 2021, doi: 10.3390/nano11020387.

[275] U. Amin et al., "Potentials of polysaccharides, lipids and proteins in biodegradable food packaging applications," *Int. J. Biol. Macromol.*, vol. 183, no. February, pp. 2184–2198, 2021, doi: 10.1016/j.ijbiomac.2021.05.182.

[276] E. Feng, G. Ma, Y. Wu, H. Wang, and Z. Lei, "Preparation and properties of organic–inorganic composite superabsorbent based on xanthan gum and loess," *Carbohydr. Polym.*, vol. 111, pp. 463–468, Oct. 2014, doi: 10.1016/j.carbpol.2014.04.031.

[277] H. M. C. de Azeredo, "Antimicrobial nanostructures in food packaging," *Trends Food Sci. Technol.*, vol. 30, no. 1, pp. 56–69, Mar. 2013, doi: 10.1016/j.tifs.2012.11.006.

[278] Y. Chen, M. Zhang, Y. Sun, and P. Phuhongsung, "Improving 3D/4D printing characteristics of natural food gels by novel additives: A review," *Food Hydrocoll.*, vol. 123, p. 107160, Feb. 2022, doi: 10.1016/j.foodhyd.2021.107160.

[279] R. S. M. Azam and M. Zhang, "Effect of Different Gums on Features of 3D Printed Object Based on Vitamin-D Enriched Orange Concentrate," pp. 250–262, 2018.

[280] A. Koyyada and P. Orsu, "Natural gum polysaccharides as efficient tissue engineering and drug delivery biopolymers," *J. Drug Deliv. Sci. Technol.*, vol. 63, no. December 2020, p. 102431, 2021, doi: 10.1016/j.jddst.2021.102431.

[281] R. K. Ramakrishnan, S. Wacławek, M. Černík, and V. V. T. Padil, "Biomacromolecule assembly based on gum kondagogu-sodium alginate composites and their expediency in flexible packaging films," *Int. J. Biol. Macromol.*, vol. 177, pp. 526–534, 2021, doi: 10.1016/j.ijbiomac.2021.02.156.

[282] A. Kumar and M. Ahuja, "Carboxymethyl gum kondagogu: Synthesis, characterization and evaluation as mucoadhesive polymer," *Carbohydr. Polym.*, vol. 90, no. 1, pp. 637–643, Sep. 2012, doi: 10.1016/j.carbpol.2012.05.089.

[283] Y. Wang et al., "Hydrogels with self-healing ability, excellent mechanical properties and biocompatibility prepared from oxidized gum arabic," *Eur. Polym. J.*, vol. 117, pp. 363–371, Aug. 2019, doi: 10.1016/j.eurpolymj.2019.05.033.

[284] V. Rana, S. Kamboj, R. Sharma, and K. Singh, *Modification of Gums: Synthesis Techniques and Pharmaceutical Benefits*, vol. 3. 2015. doi: 10.1002/9781119041450.ch10.

[285] P. Li, T. Wang, J. He, J. Jiang, and F. Lei, "Synthesis, characterization, and selective dye adsorption by pH- and ion-sensitive polyelectrolyte galactomannan-based hydrogels," *Carbohydr. Polym.*, vol. 264, p. 118009, Jul. 2021, doi: 10.1016/j.carbpol.2021.118009.

[286] N. R. Gupta et al., "Synthesis and characterization of PEPO grafted

carboxymethyl guar and carboxymethyl tamarind as new thermo-associating polymers," *Carbohydr. Polym.*, vol. 117, pp. 331–338, Mar. 2015, doi: 10.1016/j.carbpol.2014.09.073.

[287] C. Berlangieri, G. Poggi, S. Murgia, M. Monduzzi, L. Dei, and E. Carretti, "Structural, rheological and dynamics insights of hydroxypropyl guar gel-like systems," *Colloids Surfaces B Biointerfaces*, vol. 168, pp. 178–186, Aug. 2018, doi: 10.1016/j.colsurfb.2018.02.025.

[288] R. Murali, P. Vidhya, and P. Thanikaivelan, "Thermoresponsive magnetic nanoparticle – Aminated guar gum hydrogel system for sustained release of doxorubicin hydrochloride," *Carbohydr. Polym.*, vol. 110, pp. 440–445, Sep. 2014, doi: 10.1016/j.carbpol.2014.04.076.

[289] S. Thakur, G. S. Chauhan, and J.-H. Ahn, "Synthesis of acryloyl guar gum and its hydrogel materials for use in the slow release of l-DOPA and l-tyrosine," *Carbohydr. Polym.*, vol. 76, no. 4, pp. 513–520, May 2009, doi: 10.1016/j.carbpol.2008.11.012.

[290] M. B. Santos, C. W. P. de Carvalho, and E. E. Garcia-Rojas, "Microencapsulation of vitamin D3 by complex coacervation using carboxymethyl tara gum (*Caesalpinia spinosa*) and gelatin A," *Food Chem.*, vol. 343, p. 128529, May 2021, doi: 10.1016/j.foodchem.2020.128529.

[291] K. K. Mali, S. C. Dhawale, and R. J. Dias, "Synthesis and characterization of hydrogel films of carboxymethyl tamarind gum using citric acid," *Int. J. Biol. Macromol.*, vol. 105, pp. 463–470, Dec. 2017, doi: 10.1016/j.ijbiomac.2017.07.058.

[292] K. Khushbu, S. G. Warkar, and N. Thombare, "Zinc micronutrient-loaded carboxymethyl tamarind kernel gum-based superabsorbent hydrogels: controlled release and kinetics studies for agricultural applications," *Colloid Polym. Sci.*, vol. 299, no. 7, pp. 1103–1111, Jul. 2021, doi: 10.1007/s00396-021-04831-8.

[293] S. Pal, S. Ghorai, C. Das, S. Samrat, A. Ghosh, and A. B. Panda, "Carboxymethyl Tamarind-g-poly(acrylamide)/Silica: A High Performance Hybrid Nanocomposite for Adsorption of Methylene Blue Dye," *Ind. Eng. Chem. Res.*, vol. 51, no. 48, pp. 15546–15556, Dec. 2012, doi: 10.1021/ie301134a.

[294] D. H. Hanna and G. R. Saad, "Encapsulation of ciprofloxacin within modified xanthan gum- chitosan based hydrogel for drug delivery," *Bioorg. Chem.*, vol. 84, pp. 115–124, Mar. 2019, doi: 10.1016/j.bioorg.2018.11.036.

[295] L. Liang et al., "Carboxymethyl konjac glucomannan mechanically reinforcing gellan gum microspheres for uranium removal," *Int. J. Biol. Macromol.*, vol. 145, pp. 535–546, Feb. 2020, doi: 10.1016/j.ijbiomac.2019.12.188.

[296] G. Zhu, L. Sheng, and Q. Tong, "Preparation and characterization of carboxymethyl-gellan and pullulan blend films," *Food Hydrocoll.*, vol. 35, pp. 341–347, Mar. 2014, doi: 10.1016/j.foodhyd.2013.06.009.

[297] L. R. M. Lima et al., "Poly(N-isopropylacrylamide)/galactomannan from Delonix regia seed thermal responsive graft copolymer via Schiff base reaction," *Int. J. Biol. Macromol.*, vol. 166, pp. 144–154, Jan. 2021, doi:

10.1016/j.ijbiomac.2020.10.121.

[298] P. Dey, S. Maiti, and B. Sa, "Gastrointestinal delivery of glipizide from carboxymethyl locust bean gum-Al3+-alginate hydrogel network: In vitro and in vivo performance," *J. Appl. Polym. Sci.*, vol. 128, no. 3, pp. 2063–2072, 2013, doi: 10.1002/app.38272.

[299] S. Maiti, M. Chowdhury, A. Chakraborty, S. Ray, and B. Sa, "Sulfated locust bean gum hydrogel beads for immediate analgesic effect of tramadol hydrochloride," *J. Sci. Ind. Res.*, vol. 73, no. 1, pp. 21–28, 2014.

CHAPTER – 2

Carboxymethylated Gum Tragacanth Crosslinked POLY (Sodium Acrylate) Hydrogel: Fabrication, Characterization, Rheology and Drug-Delivery Application

2.1 Introduction

An excellent way to increase the drug's effectiveness is to deliver it using any reliable carrier in medical science. In this modern period, natural gum polysaccharides are explored as the main component in pharmaceutical formulations [1,3]. Recently, the potential of Gum Tragacanth has been explored in cosmetics, pharmaceuticals, bio and food industries [4,5]. The GT obtained from *Astragalus gummifer* is considered GRAS (Generally Recognized As Safe)[6]. GT is a heterogeneous, anionic and naturally available polysaccharide. The presence of arabinogalactan in GT was confirmed by acid hydrolysis [7]. In traditional local medications, GT act as a demulcent for gastrointestinal problems and sore throats. It may additionally have analgesic properties [8]. The property of the GT can be enhanced through chemical modifications. The reported modification methods of GT are graft-copolymerization [9] and carboxymethylation [10]. However, carboxymethylation is most widely favoured as it is cheap, quickly processed and produces versatile products with better water retention properties and strength [11] compared to natural ones [12]. In the current study, GT was carboxymethylated to synthesize CMGT and the potential of CMGT in drug delivery was further investigated by synthesizing CMGT based hydrogel.

The three-dimensional network structure of a hydrogel has been created by the chemical cross-linking of polysaccharides with suitable monomer by using a suitable

initiator and multifunctional cross-linker. In the past few years, the hydrogel has increasingly been utilized as a carrier in drug delivery application to produce sustained and controlled drug release because of its 3D web structure and excellent swelling property [13,14].

The swellability of the hydrogel can be enhanced by using sodium acrylate (SA) content in the graft polymerization [15]. Ganguly et al. also observed the same swellability of the hydrogel based on Psyllium gum copolymerized with acrylic acid and sodium acrylate [16]. The application of CMGT in the preparation of superabsorbent hydrogel has been reported by Mohammad B et al. [17]. Previous literature reveals that CMGT based hydrogel and their application in drug delivery is still to be explored. In this study, we have synthesized and characterized the novel Aceclofenac Sodium (AFS) loaded hydrogel based on graft co-polymerization of SA onto the CMGT backbone. AFS is a drug categorised in category- Non steroidal Anti-inflammatory drugs.

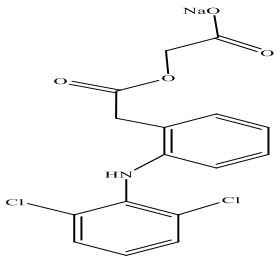

Aceclofenac Sodium

The various formulations of CMGT-co-SAH were synthesized by varying the amount of KPS as initiator and MBA as cross-linker, and their Swelling Index (SI) was assessed. Also, by changing the temperature, i.e., 27°, 37°C and 47°C, SI and network parameters of the hydrogel were determined. Modification of the GT to CMGT and

their graft copolymerization with SA was confirmed by XRD, FTIR, TGA, SEM and C^{13}-NMR. Rheological analysis of the SAH, which is considered as control hydrogel and CMGT-co-SAH were done to determine the gel characteristics. Further, the drug release behaviour of the CMGT-co-SAH was evaluated by using a model drug, AFS by applying different kinetic models such as Hixon-Crowell, Higuchi, Korsmeyer-Peppas, Zero-order and First-order kinetic model to analyse the drug release profile.

2.2 Experimental

2.2.1 Materials

GT (purchased from local market, New Delhi), Sodium monochloroacetate (SMCA, CDH, New Delhi), N,N′-methylenebis-acrylamide (MBA, CDH, New Delhi), Sodium hydroxide (NaOH, Fischer Scientific, Mumbai), Acrylic acid (AA, CDH, New Delhi), Potassium per sulphate (KPS, Fischer Scientific, Mumbai), Iso propyl alcohol (Fischer Scientific, Mumbai), methanol (Fischer Scientific, Mumbai), Aceclofenac Sodium (AFS) was gifted from Unicure India Pvt. Ltd. and all the solutions were prepared in milli-Q grade distilled water.

2.2.2 Synthesis of Carboxymethylated Gum Tragacanth (CMGT)

The CMGT was synthesized using a previously described method [12] with slight modifications in the procedure. Derivatization of the polysaccharides chain follows Williamson's synthesis reaction shown in scheme 2.1. For 0.2 degrees of substitution (0.2 DOS chosen for good swelling properties), the 1 g of GT was weighed and mixed continuously for 15 minutes in distilled water. Then (0.00775 moles) of NaOH was added to the homogeneous solution of GT. After 30 minutes of stirring, SMCA

(0.00123 moles) was gradually added. The solution was stirred at magnetic stirrer for 3 hours at 70°C to make it homogeneous. Once the CMGT solution was cooled, the precipitates of CMGT was filtered, washed at least three times with isopropyl alcohol (80%), and oven dried at 45 °C.

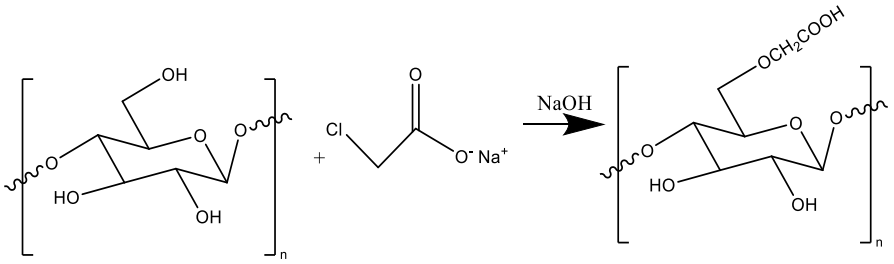

Gum SMCA Carboxymethylated gum

Scheme 2.1: Carboxymethylation

2.2.3 Estimation of Degree of Substitution (DOS) on GT

DOS of CMGT was determined by back titration [18]. CMGT (1 g) was dispersed in the required volume of HCl and Isopropyl alcohol was added as a solvent. The stirring of the solution with a glass rod was carried out for 15 minutes to avoid the formation of lumps. The solution was left undisturbed for 20 minutes. Afterwards, distilled water was added and subjected to magnetic stirring for a few minutes. Post sedimentation, water was decanted. The sediment was filtered. Multiple washing was done with distilled water to free it from excess acid. A silver nitrate test was performed to check the presence of acid in the filtrate. Finally, the residue was divided into two accurately weighed parts. One part of the residue was dispersed in 50 ml of 0.1 N NaOH and subjected to magnetic stirring for 30 minutes before back titrating with 0.1 N HCl. The dried content was calculated after drying the other part of the residue.

Equations (1 & 2) were used to calculate DOS [19].

$$\text{DOS} = \frac{0.162\text{A}}{1-0.058\text{A}} \quad (1)$$

$$\text{Where A} = \frac{(ml\ of\ NaOH\ X\ N1)-(\ ml\ of\ HCl\ X\ N2)}{gm\ of\ the\ dried\ sample} \quad (2)$$

N1 and N2 represent the normalities of NaOH and HCl, and A represents (milliequivalents of NaOH /gm of sample).

2.2.4 Synthesis of CMGT-co-SAH

CMGT-co-SAH was synthesized by taking 1 g of CMGT with DOS (0.2) (0.33% w/v) in distilled water. 7.2 ml of acrylic acid (AA) was neutralized using 13 ml of 8.07 mol/L NaOH solution and added to CMGT solution. At room temperature, KPS (0.0061 mol/L) and MBA (0.017 mol/L) were added to the aqueous mixture with continuous stirring for two hours on a magnetic stirrer. The polymerization procedure was carried out in a water bath at 60°C for two hours. The synthesized hydrogel was washed with an organic/aqueous solvent to remove the soluble components. It was then dried in the hot air oven at 45 °C, till constant weight. Reaction contents were optimized by varying the amount of reactants; KPS 0.0061 mol/L to 0.01223 mol/L and MBA 0.010 mol/L to 0.021 mol/L (Table 2.1). SAH (control hydrogel) was synthesized by opting similar method without adding CMGT. Optimal formulation of hydrogel (i.e., CMGT-co-SAH-4) was selected for further characterization based on the highest Swelling Index among various compositions (CMGT-co-SAH-1 to 11).

Table 2.1: Different formulation of CMGT-co-SAH and their swelling Index

Formulation	Polymer (CMGT)(g)	Monomer (AAc)(g)	NaOH (mol/l)	Initiator (KPS) (mol/L)	Cross-linker (MBA) (mol/L)	SwellingIndex (g/g of gel) (After 24 hours)
CMGT-co-SAH-1	0.1	7.2	8.07	0.0061	0.01	22.28±0.27
CMGT-co-SAH-2	0.1	7.2	8.07	0.0061	0.012	23.29±0.17
CMGT-co-SAH-3	0.1	7.2	8.07	0.0061	0.015	28.95±0.02
CMGT-co-SAH-4	0.1	7.2	8.07	0.0061	0.017	33.13±0.04
CMGT-co-SAH-5	0.1	7.2	8.07	0.0061	0.019	27.13±0.08
CMGT-co-SAH-6	0.1	7.2	8.07	0.0061	0.021	25.74±0.25
CMGT-co-SAH-7	0.1	7.2	8.07	0.0074	0.01	26.92±0.56
CMGT-co-SAH-8	0.1	7.2	8.07	0.0074	0.012	30.45±0.04
CMGT-co-SAH-9	0.1	7.2	8.07	0.0086	0.01	30.25±0.19
CMGT-co-SAH-10	0.1	7.2	8.07	0.0086	0.015	27.67±0.02
CMGT-co-SAH-11	0.1	7.2	8.07	0.0098	0.01	26.26±0.50

2.3 Characterization and Analysis

2.3.1 Swelling Studies

Effect of cross-linker, initiator and the temperature on hydrogel's network was analyzed by the swelling equilibrium method in buffer solution of pH 7.4. The oven dried and weighed discs of hydrogel were dipped in the solvent. After a fixed interval, the hydrogel discs were removed from the swelling medium, extra fluid was tapped with tissue paper, and weighed again until the constant weight was obtained. These studies were done in triplicate. Equation 3 was used to calculate the Swelling Index (SI) [20].

$$SI\% = \frac{Ws - Wi}{Wi} X\ 100 \quad (3)$$

Wi represents the dried hydrogel disc's weight, whereas *Ws* represents the swollen hydrogel disc's weight at a certain period.

2.3.2 Rheological Analysis

2.3.2.1 Steady Rheological Behaviour

The rheological characteristics of CMGT-co-SAH and SAH were assessed in the swollen state in PBS buffer of pH 7.4 at room temperature using an Anton Paar Modular Compact Rheometer 302 (MCR). The shear rate ranged from 0.001 to 1 s^{-1} with a PP-25 i.e., parallel plate having a diameter of 25 mm and along with 2.5 mm of the inter-platen gap. The results from the plot, shear vs. shear rate, were fitted to Power Law (PL) model to acquire the required parameters.

PL model: $\tau = K\gamma^n$ (4)

The shear stress (τ) in (Pa), consistency coefficient (K) in (Pa.s), shear rate ($\dot{\gamma}$) in (s^{-1}), and fluidity index (n) are all represented in the equation (4) [21].

2.3.2.2 Amplitude Sweep

The test for amplitude sweep was done on SAH and CMGT-co-SAH in an oscillatory condition at a frequency of 10 rad s^{-1} to optimize suitable parameters for further dynamic testing. The amplitude sweep test is conducted in a fixed strain % of 0.001 % to 10 %. The test may reveal the linear viscoelastic region (LVR), which may be used to examine sample characteristics.

2.3.2.3 Frequency Sweep

Low and high frequencies (1-100 rad s^{-1}) and (100-1000 rad s^{-1}) respectively, were used in the frequency sweep test. For CMGT-co-SAH and SAH, the loss (G″) and storage (G′) moduli are plotted against (ω) angular frequency at room temperature.

2.3.3 SEM

Morphology of four samples (GT, CMGT, SAH and CMGT-co-SAH) was compared by using JEOL JSM-6610LV Scanning Electron Microscope and all samples were coated with gold for analysis. SEM was operated at 20 kV accelerating voltage and 1,000x magnifications [22].

2.3.4 FTIR

FTIR of CMGT-co-SAH were compared with GT, CMGT and SAH. The FTIR analysis of samples was done between range 4000 to 650 cm^{-1} on Perkin-Elmer model 2000 FT-IR spectrometer [23].

2.3.5 ^{13}C-NMR

Solid state ^{13}C-NMR was done for four samples, i.e., GT, CMGT, SAH and CMGT-co-SAH with 200 mg of samples at 9T of magnetic field on a Bruker Avance 500 WB solid state NMR spectrometer using 4mm of the probe [24].

2.3.6 XRD

The samples (GT, CMGT, SAH and CMGT-co-SAH) X-Ray Diffractogram were recorded by diffracting angle from 10° to 80° at 2°/min with 40 KV generator voltage using Expert Pro MRD, Panalytical, X-Ray diffractometer [25].

2.3.7 TGA

The samples (GT, CMGT, SAH and CMGT-co-SAH) were thermally tested with a consistent heating rate of 10°C/min from 25 to 800°C in N_2 atmosphere, using a PerkinElmer TGA, 4000 [26].

2.3.8 Analysis of network parameters of CMGT-co-SAH

The AFS amount released from the hydrogel matrix is determined by the hydrogel's swelling, which is directly related to the network parameters like Molecular weight of the segments between two neighbouring crosslinks of the network hydrogel ($\overline{Mc}$), the volume fraction of the swollen hydrogel (ϕ), mesh size (ξ), Flory Huggins interaction parameter (χ) and crosslink density (ρ). These parameters were calculated by Flory-Rehner equation given in equation 5[27].

$$\overline{Mc} = -D_H + Vm + \phi^{\frac{1}{3}} [\ln(1-\phi) + \phi + \chi\phi^2]^{-1} \quad (5)$$

Here, , ϕ represents the swollen hydrogel's volume fraction, Vm represents the molar volume of the swelling agent, which determine the amount of solvent absorbed by the hydrogel and the Flory Huggins interaction parameter is represented by χ.

ϕ, for swollen hydrogel, was calculated using equation (6).

$$\phi = \left[\left(\frac{D_H}{D_S}\right)\left(\frac{\mathrm{Ws}-\mathrm{Wi}}{\mathrm{Wi}}\right) + 1\right]^{-1} \quad (6)$$

Here, D_S and D_H are the densities of the solvent (g/cm^3) and hydrogel, respectively; Wi and Ws are the weight of initial and swollen state of the hydrogel.

The Flory Huggins interaction parameter (χ) was determined by using the equation (7)

$$\chi = \left(\phi\left({}^{1}/_{1-\phi}\right) + \mathrm{Z}\ln(1-\phi) + \mathrm{Z}\phi\right)[2\phi - \phi^2\mathrm{Z} - \phi^2\mathrm{T}^{-1}(d\phi/dT)^{-1}]^{-1} \quad (7)$$

where $\mathrm{Z}=\left[\left(\frac{\phi^{\frac{2}{3}}}{3}-\frac{2}{3}\right)\left(\phi^{\frac{1}{3}}-\frac{2\phi}{3}\right)\right]^{-1}$ and $d\phi/dT$ is the slope calculated by plotting a graph between temperature in °C and volume fraction (ϕ). 24 h swelling of hydrogel was determined at 27°, 37° and 47°C in buffer of pH 7.4. Mesh size and Crosslink density were determined by using the given equation (8,9) [28,29].

$$\rho = \frac{D_H}{\overline{Mc}} \quad (8)$$

$$\xi = \left[\left(\frac{71}{1000}\right)(\phi)^{-\frac{1}{3}}\right](\overline{Mc})^{\frac{1}{2}} \quad (9)$$

2.3.9 Drug Loading and Release Profile of Aceclofenac Sodium (AFS)

The AFS loading and release profile of CMGT-co-SAH was determined in pH 7.4 buffer solution at 37°C. The swelling equilibrium approach was used to load the drug

into the hydrogel [30]. For 24 hours, the hydrogel was immersed in a drug solution with a fixed concentration (1.25 mg/ml). The drug-loaded hydrogel was immersed in 100 ml buffer solution of pH 7.4 and placed in a water bath shaker, set at 80 rpm and 37°C, to analyze the release profile of hydrogel. At every hour, 1ml of the drug containing solution was taken out and replaced by a fresh buffer solution. The process was continued for 24 hours. The withdrawn samples were analyzed by a UV -visible spectrometer at 274 nm. The amount of AFS was measured by comparing the absorbance value from the calibration curve. The Experiment was conducted in triplicates and drug release kinetics was analyzed by applying various drug release models. The Encapsulation Efficiency (EE) was calculated by using equation 10 [31].

$$\% \text{ of EE} = \left(\frac{\text{Actual loading}}{\text{Theoretical loading}}\right) * 100 \quad (10)$$

Actual loading is determined by using UV-Visible Spectrophotometer. Where, loading of the drug into the hydrogel determine by using the initial concentration of the drug in the solution and the drug present in the supernatant after absorption [32]. Theoretical loading is the weight of the dried hydrogel disc after swelling in drug solution.

2.3.10 Kinetic Models for Drug Release Profile

To determine the drug release profile of AFS loaded CMGT-co-SAH, Higuchi, Hixon-Crowell, Korsmeyer-Peppas, First-order and Zero-order kinetic models were employed [20,33]. Mathematical equations of the models have been given in table 2.2.

Table 2.2: Mathematical expression of kinetic models

Models	Mathematical Equation	Parameter
Zero Order	$F_t = K_o t$	F_t=Amount of drug release in time t K_o= Zero-order constant
First Order	$(1 - F_t) = K_1 t$	K_1= First order constant
Higuchi	$F_t = K_H t^{1/2}$	K_H= Higuchi constant
Hixon-Crowell	$W_o^{1/3}$-$W_t^{1/3} = K_{HC} t$	W_o=Initial amount of drug present in hydrogel W_t=Amount of drug release at time t K_{HC}= Hixon-crowell constant
Korsmeyer-Peppas	$\frac{M_t}{M_\infty} = K_{KP} t^n$	$\frac{M_t}{M_\infty}$=Fraction of drug release in time *t.* M_t= Amount of drug release at time t and M_∞= initial amount of drug. K_{KP}=Rate constant n= Release exponent

2.3.11 Hemo-Compatibility Studies

The hemolytic potential of hydrogel was determined by an *in vitro* hemolysis in %. The blood sample (1 ml) was collected from healthy human in EDTA treated tubes and centrifuged for 5 minutes, at 3000 rpm. Supernatant of blood plasma was discarded, and separated RBCs were, washed in 1x PBS (pH 7.4), further re-suspended in 1 ml of 1x PBS. For use in experiments this stock solution was diluted to 4% v/v in 1x PBS. The sample was added to 96 well plates in increasing amount from 0.125 mg/ml to 2.5 mg/ml. The 100 ul of RBC solution was added to each well. Final volume was made up to 200 ul in each well with 1x PBS (pH 7.4). Triton X-100 was used as the positive control (0.1%w/v) and 1x PBS (pH 7.4) act as negative control. The 96 well plate was incubated at 37℃ for 1 h with shaking in an incubator

shaker. After incubation the plate was centrifuged at 3000 rpm for 5 min. The 100 ul of the supernatant was collected in another 96 well plate and measured the absorbance (A) at 540 nm on Elisa plate reader [34].

The hemolysis in % was calculated by using equation 11.:

$$\text{Hemolysis in \%} = \left(\frac{A_{CMGT-co-SAH} - A_{1xPBS}}{A_{\text{triton X}-100} - A_{1xPBS}}\right) X100 \quad (11)$$

Hemolysis in % was evaluated on average of two replicates[35].

2.4 Results and Discussions

Synthesis of the CMGT-co-SAH was based on the free radical polymerization technique. Where, formation of the free radicals and crossing between the generated free radicals is the key point for the formation of a cross-linked hydrogel. Here the free radicals were generated by using the initiator KPS and the NN-MBA acting as cross-linker which enhances the cross- linking and strengthen the hydrogel. The given below scheme 2.2 shows the free radical formation and crosslinking within the presursors.

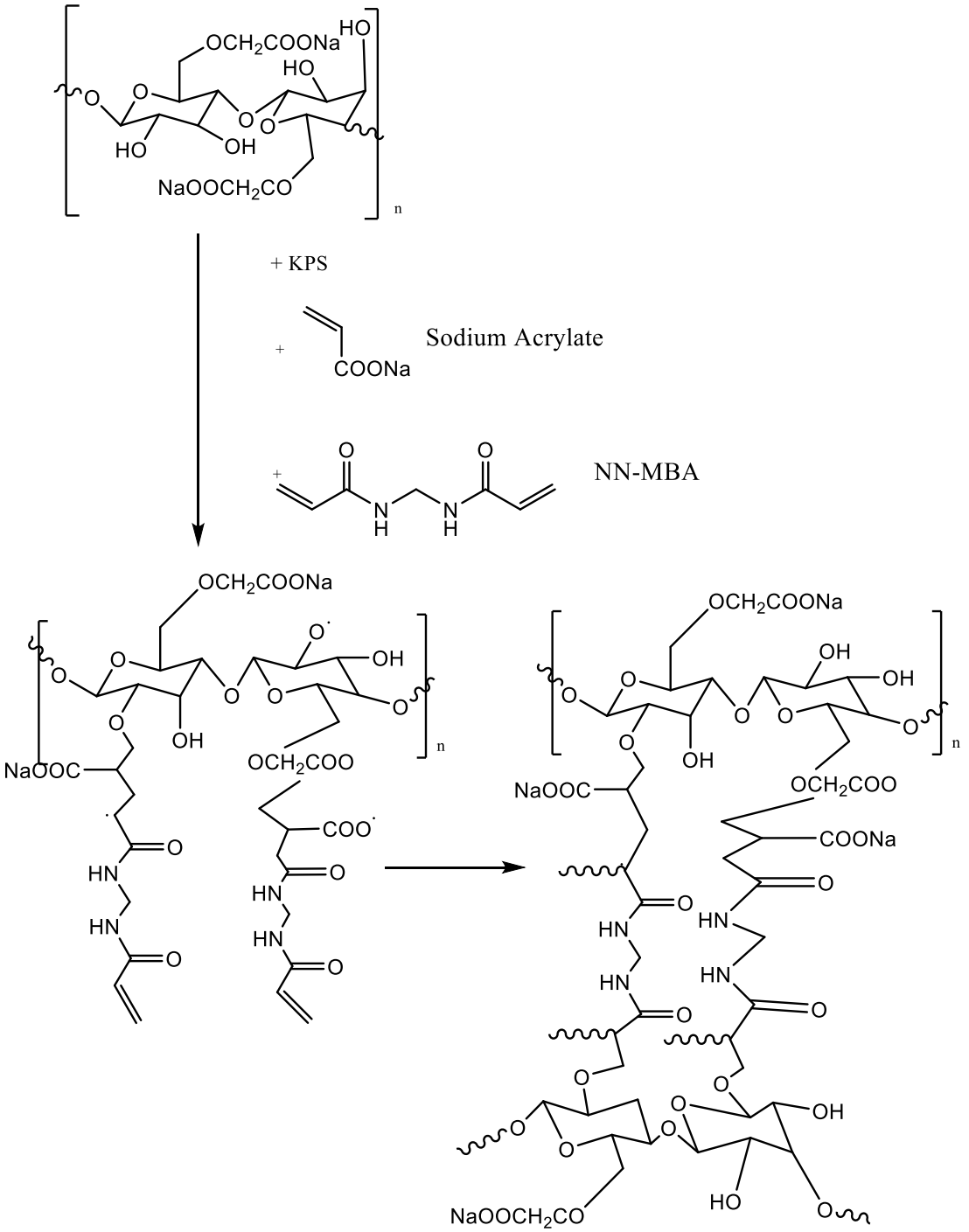

Scheme 2.2: Synthesis of CMGT-co-SAH

2.4.1 Swelling Studies

CMGT-co-SAH formulations 1-11 were synthesized by varying concentrations of KPS and MBA where monomer and polysaccharides concentrations were not

changed. Their Swelling Index was determined. The formulation which is having maximum SI has been used to determine the effect of change in temperature on swelling of the hydrogel.

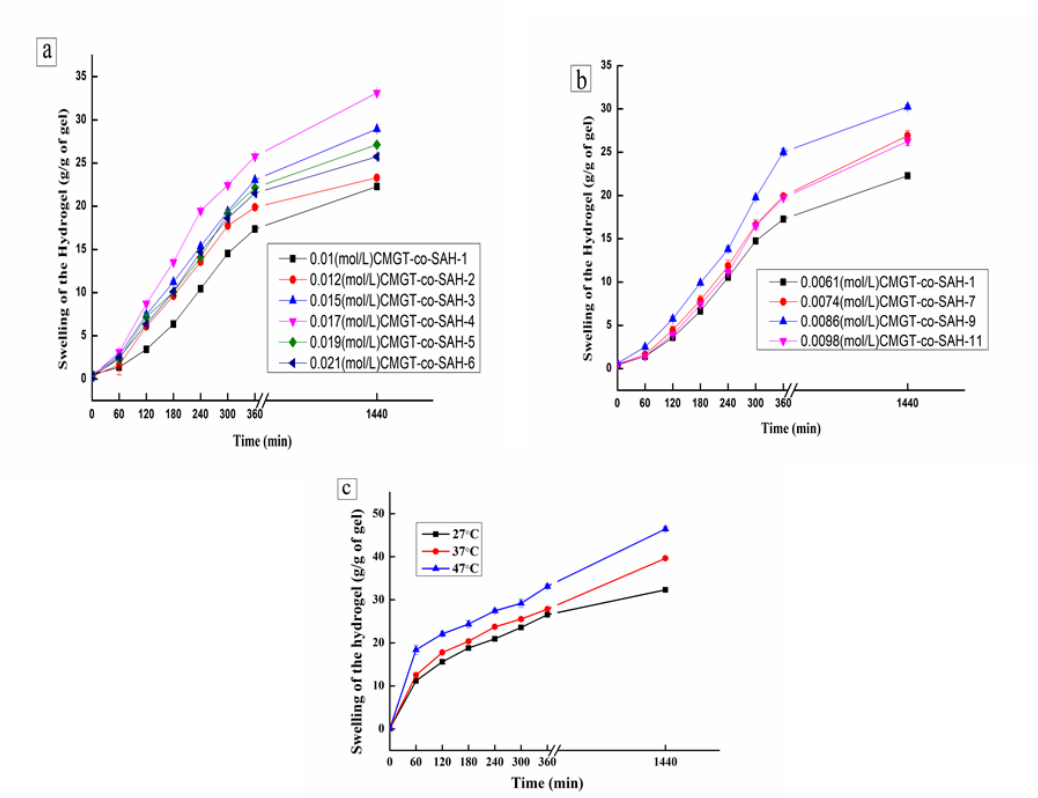

Figure 2.1: (a) Effect of cross-linker on hydrogel's swelling, (b) Effect of initiator on hydrogel's swelling and (c) Effect of temperature on hydrogel's swelling

2.4.1.1 Effect of Cross-Linker on Hydrogel's Swelling

The effect of cross-linker's concentration was observed in samples (CMGT-co-SAH-1 to 6 listed in table 2.1, shown in figure 2.1(a). Swelling Index increases when the cross-linker concentration increases from 0.01mol/L to 0.017 mol/L due to a rise in cross-linked density beyond which the Swelling Index decreases. This may be due to the occurrence of rigid structure, beyond cross-linker concentration of 0.017 ml/L which causes a reduction in polymer stretching.

2.4.1.2 Effect of Initiator on Hydrogel's Swelling

According to figure 2.1 (b), as the initiator concentration increases, the anionic radical increases. Anionic radical will increase macro-radicals in the parent chain, which raises the Swelling Index to 30.25±0.19 g/g (CMGT-co-SAH-1, 7, 9 and 11) listed in table 2.1 (where cross-linker concentration is constant). Further, with increase in the concentration of initiator beyond 0.0086 mol/L, Swelling Index decreases due to termination of the chain through the biomolecular collision.

2.4.1.3 Effect of Temperature on Hydrogel's Swelling

The SI (g/g of gel) at 27°, 37° and 47° was found to be 32.30±0.12, 39.63±0.30, 46.47±0.54 respectively. It was observed from results that as the temperature increases, hydrogel's swelling increases (figure 2.1(c)) due to increase in movement of the segments of the polymerized chains. This confirms that the rate of absorption/diffusion of solvent molecules by CMGT-co-SAH is temperature dependent.

2.4.2 Rheological Analysis

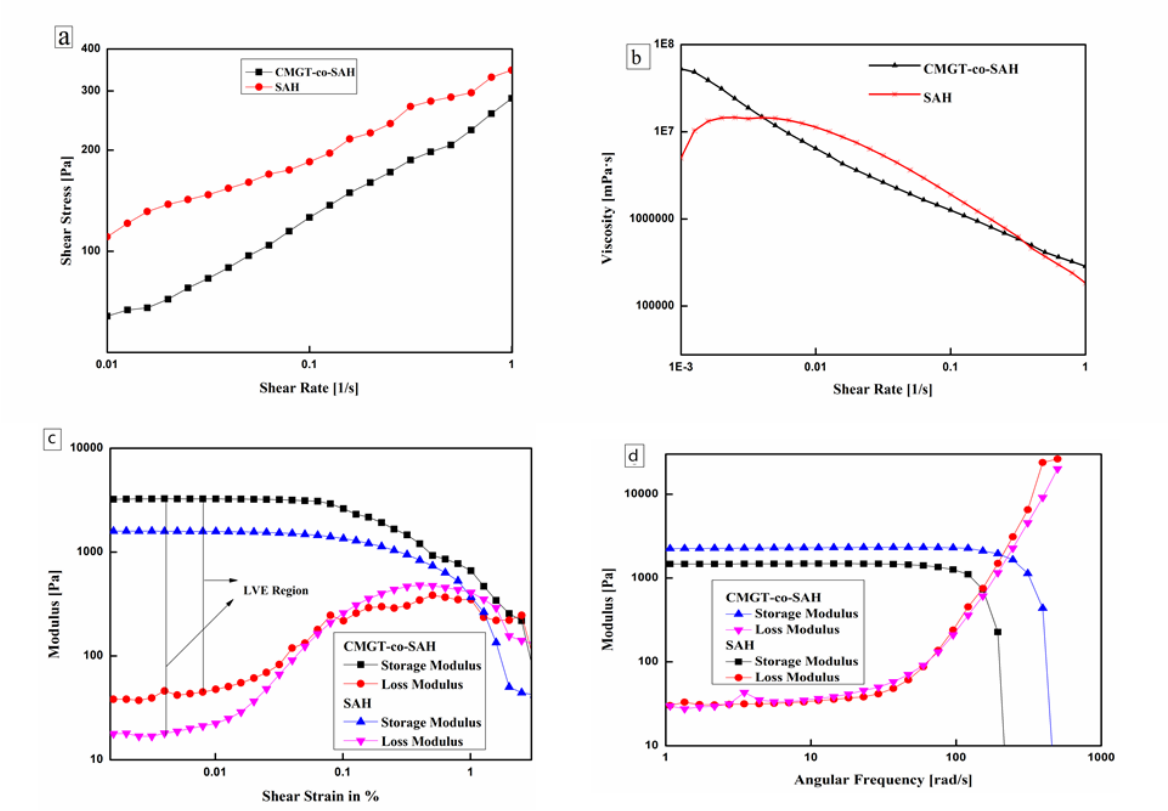

Figure 2.2: (a) Shear rate vs Shear stress graph for CMGT-co-SAH and SAH, (b) Viscosity profile of CMGT-co-SAH and SAH with varying shear rate, (c) Amplitude sweep with LVE and (d) frequency sweep graphs

The gel strength and rigidity of the swollen hydrogel were determined by using rheological analysis. From figure 2.2(a), in which the graph was plotted against shear stress and shear rate, for both hydrogels (CMGT-co-SAH and SAH), it was observed that the shear stress is directly proportional to shear rate. For data (shear rate vs. shear stress graph), the PL model was fitted to calculate the consistency coefficient (K) and fluidity index (N). The value of R^2 obtained from the PL model indicates that both the hydrogels have high consistency and correlated with reported results in the previous literature [36]. The value of 'n' shows flow characteristics, when obtained results of

shear rate vs. shear stress was fitted to the PL model. The value of 'n' in table 2.3 is more for CMGT-co-SAH than SAH, representing the intermolecular interaction of the monomer and the CMGT. The value of n for both hydrogel is less than one, which means pseudo-plastic behaviour of the hydrogel. This behaviour was also determined by the shear viscosity test, figure 2.2(b). The hydrogel showed a steady decrease in shear-dependent viscosity with an increase in shear rate, which might indicate the time-dependent rupturing of the hydrogel matrix's intrinsic bonding, thus representing the shear thinning behaviour of hydrogel.

Table 2.3: Parameters according to Power law Model in steady rheological behaviour (shear stress vs. shear rate)

	Power law Model		
Hydrogel	K	N	R^2
SAH	11.70	0.23	0.9907
CMGT-co-SAH	11.35	0.33	0.9946

2.4.2.1 Amplitude Sweep

The whole strain was divided into two regions. One is the Linear Viscoelastic Region (LVR), a shear region, which is not affected by applied stress. The other area is non-linear and it was observed from figure 2.2(c) that the G' and G" values change when the strain exceeds 0.01%. Above this LVR, the storage and the loss modulus dropped due to rupturing of the hydrogel matrix. By increasing the stress %, intermolecular interaction deformed, reducing the moduli values. Samples act as viscoelastic solid when G'>G". Below 0.01% strain, the shape of CMGT-co-SAH & SAH was retained. Above 0.01% strain, intermolecular chains start to disentangle. The yield strain of CMGT-co-SAH is more than SAH due to the addition of CMGT, which shows

intermolecular interaction of CMGT and SA. Similar properties were observed by Ganguly et al. in psyllium grafted with poly acrylic acid and sodium acrylate hydrogel [16]. The viscoelastic sweep should be analyzed within the LVE range [36].

2.4.2.2 Frequency Sweep

For this analysis, the frequency ranged from 1 to 1000 rad s^{-1}. Storage and loss moduli were plotted against (ω) i.e., angular frequency figure 2.2(d). The graph shows viscoelastic solid behaviour, where the loss modulus is dominant at high frequencies and the storage modulus is prominent at low frequencies. Therefore the structure of the hydrogel is stable at low frequency and deformed at high frequency. CMGT-co-SAH has a greater storage modulus than SAH because there may be crosslinking between SA and CMGT. It shifts the cross-over point toward a higher frequency[16,37].

2.4.3 Scanning Electron Micrograph (SEM)

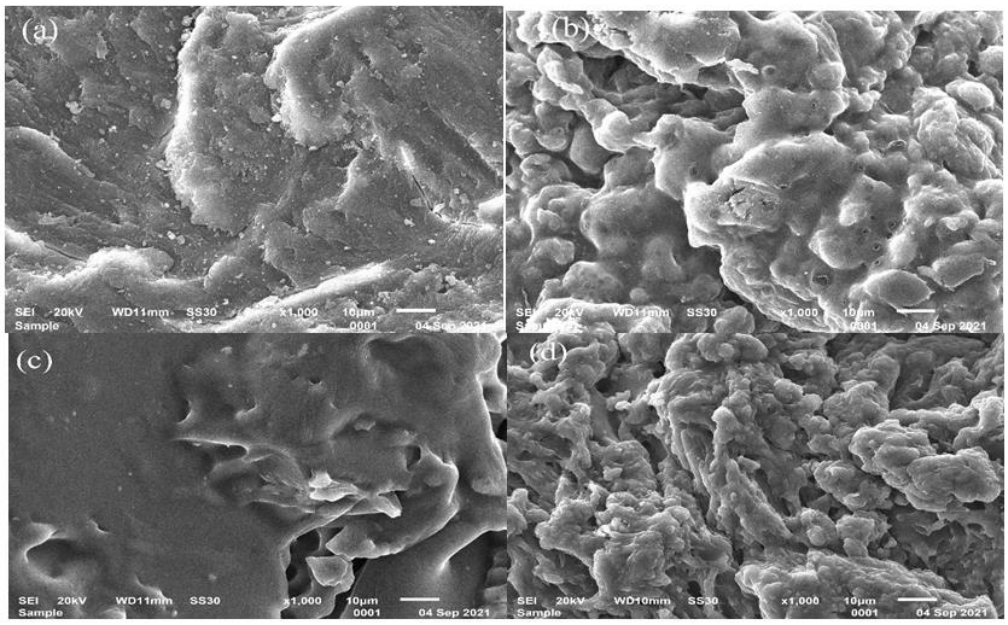

Figure 2.3: SEM at (1000x) for (a) GT, (b) CMGT, (c) SAH and (d) CMGT-co-SAH

The surface morphology of GT, CMGT, SAH and CMGT-co-SAH has been analyzed by SEMs, which are represented in figure 2.3. It has been observed from the SEMs that GT and SAH have a smooth and homogeneous morphology, whereas CMGT and CMGT-co-SAH have structural heterogeneity and porous morphology. The change in surface morphology of the CMGT and its hydrogel is due to the cross-linked networks confirmed by SEMs taken at 1000x magnification[6,38].

2.4.4 FTIR Analysis

Absorption bands observed in FTIR spectra were compared with previously published literature as given in figure 2.4 (a). A broad absorption band at 3311 cm^{-1} was observed in GT, representing an overlapped peak indicating H-bond due to -OH groups of polysaccharides. Absorption bands at 1720 cm^{-1} in GT represent a stretch of acidic and ester carbonyl groups and at 1602 cm^{-1} represent C-O and COO^- groups of D-Glacturonic acid. The peak at 1247 cm^{-1} represents the esteric skeleton group. Stretch at 1029 cm^{-1} corresponds to C-O and C-C group present in GT's pyranose rings [12].

The broad absorption band at 3329 cm^{-1} in CMGT and GT, but band intensity is lower in GT than CMGT, suggests that carboxymethylation may reduce the number of –OH groups. A band at 1600 cm^{-1} represents the extension vibration of the COO^- groups, which confirms the carboxymethylation process. Other absorption bands at 1244 cm^{-1} and 1029 cm^{-1} are corresponding to the similar vibrations of GT as explained above [39].

SAH's FTIR spectrum represents absorption bands at 1556 $cm^{-1}$and 1400 cm^{-1}due to the bending vibrations of the CH_2 group of sodium acrylate parts [40].

In the CMGT-co-SAH's spectrum, the absorption band at 3329 cm^{-1} corresponds to the acidic -OH group overlapped with the amide -NH group. Absorption bands at 1722 cm^{-1} represent the stretch of acidic and ester carbonyl groups and at 1606 cm^{-1} are due to the amide carbonyl group. Absorptions at 1244 $cm^{-1}$and 1028 cm^{-1} are assigned as of CMGT. A little shift in absorptions confirms the crosslinking of CMGT with sodium acrylate [38]**.**

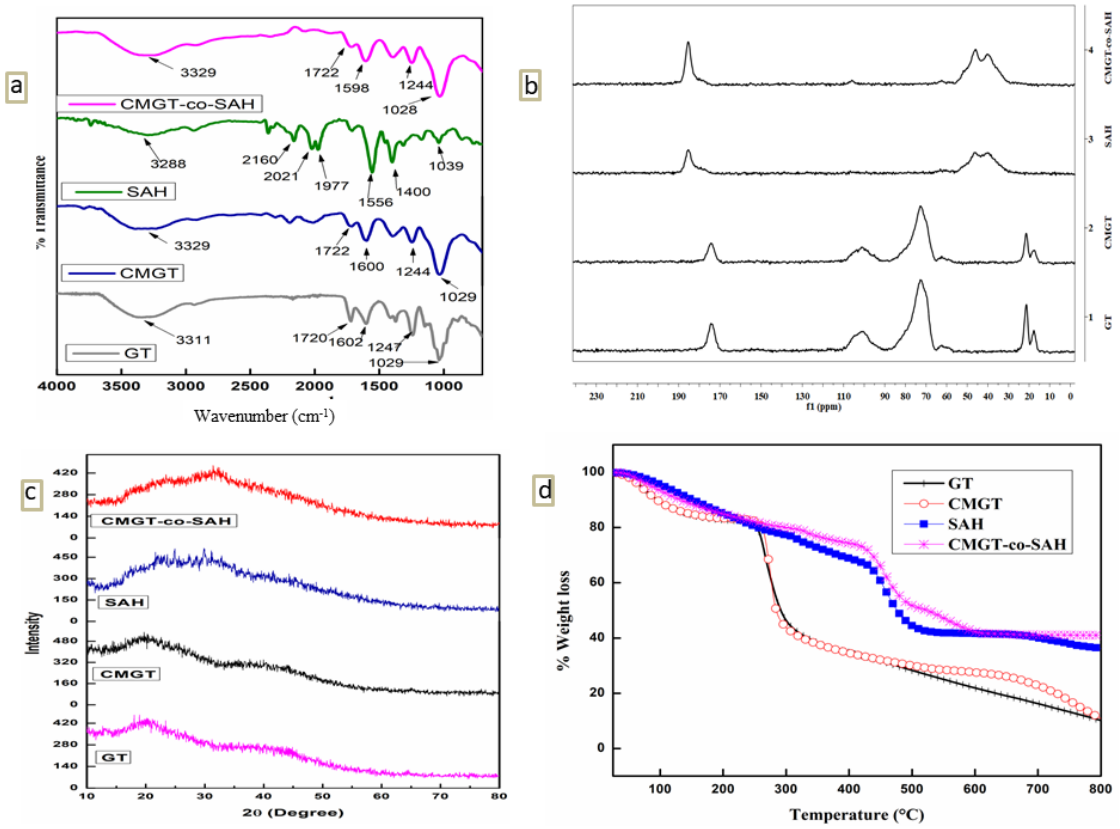

Figure 2.4: (a) FTIR, (b) 13C-NMR, (c) XRD and (d) TGA spectra of GT, CMGT, SAH and CMGT-co-SAH

2.4.5 ^{13}C-NMR Studies

The result of solid-state ^{13}C-NMR spectra of GT, CMGT, SAH and CMGT-co-SAH are shown in figure 2.4 (b). At 174.24 ppm, characteristic peaks have been identified in GT due to the -COOH group of galacturonic acid in the GT[33]. At 100.59 ppm (represents anomeric carbon of polysaccharides), at 72.56 ppm (due to C attached to-

OH group of polymeric chain), 17-22 ppm (assigned to -CH_2 group of polysaccharides). NMR spectrum of CMGT represents characteristic peaks at 174.26 ppm (carbonyl carbon of CMGT), at 101.04 ppm (anomeric carbon of polysaccharides). This peak shifted to a higher ppm value than GT may be due to carboxymethylation. Peak at 72.71 ppm due to –C-OH group, peak intensity lower down as compared to GT, confirms carboxymethylation. In SAH, characteristic peaks from 40-47 ppm and 185.51 ppm assigned to -CH and -COOH group, respectively. In CMGT-co-SAH, characteristics peaks from 40-47 ppm assigned to -CH of sodium acrylate and little shift in frequency confirmed crosslinking of CMGT with SA. At 106.05 ppm small intensity peak was identified, representing anomeric carbon of polysaccharides. At 185.38 ppm (-COOH of SA and CMGT, a shift in frequency due to crosslinking of CMGT with SA) [6, 33].

2.4.6 XRD Studies

Figure 2.4(c) represents the crystallinity/amorphous characteristics of the samples, analyzed by XRD. The GT showed a broad diffraction peak at ≈20°, indicating that it is an amorphous polysaccharide, and there is little shift in the 2θ value due to carboxymethylation. The diffraction pattern of SAH and CMGT-co-SAH show the amorphous nature. The shift in the diffraction peak of CMGT-co-SAH was observed, may be due to cross-linking of CMGT and SA[41, 42].

2.4.7 TGA

Figure 2.4(d) represents the thermal degradation of GT, CMGT, SAH and CMGT-co-SAH. GT demonstrates two-step weight loss, with an initial loss of around 18% between 39 - 234°C due to the loss of moisture from the gum. The decomposition of

GT's highly branched heterogeneous structure results in a 72 % weight loss from temperature 234°C to 800°C, with a residual weight of about 10%.

CMGT decomposes in three stages, 35-240°C, the range shows 16% loss due to humidity. The second stage ranges from 240-620°C due to decomposition of polysaccharide rings, breaking of C-O-C bond in CMGT chain and elimination of CO_2, which is around 74%. 620-800°C range shows weight losses due to breakdown of CMGT backbone and 10% were residual weight.

Thermal decomposition of SAH occurs in four stages, 30-299°C, 299-427°C, 427-548°C, 672-800°C and were about 23%, 11%, 25% and 5% respectively. The first stage weight loss was result of loss of moisture. The second stage of weight loss was due to carboxyl group decomposition of the SAH and the last two stages show the breakage of cross-linking in SAH network. 36% is the residual weight at 800°C.

CMGT-co-SAH decomposed in four stages 44-322°C, 322-411°C, 411-521°C, and 521-629°C. The first stage shows 21% loss due to moisture content. The second stage of 6% loss represents the decomposition of polysaccharide rings along with the elimination of CO_2. The latter two stages represent breakage of the CMGT backbone and SA chain with 23% and 9% weight loss respectively. The residual weight at 800°C was 41%. From the decomposition of all samples, it was concluded that modified gum and its hydrogel were more thermally stable than GT and SAH [17,43].

2.4.8 Network Parameters of Hydrogel

The network parameters like (Molecular weight of the segments between two neighbouring crosslinks ($\bar{M}_c$), the volume fraction of the hydrogel in the swollen state

(ϕ), mesh size (ξ), Flory Huggins interaction parameter (χ), and crosslink density (ρ)) of CMGT-co-SAH were determined as a function of temperature and given in table 2.4. When a hydrogel is immersed in a liquid for swelling, it expands until the osmotic forces that aid in the polymer's dissolution is counterbalanced by the elastic forces caused by stretched polymer chains. High $\bar{M}_c$ value shows that the network is highly elastic and expands quickly when exposed to a liquid solvent [27]. As the temperature increases, $\bar{M}_c$ and ξ of the hydrogel network increases along with that ρ and χ decreases [44].

Table 2.4: Network parameters of CMGT-co-SAH as a function of temperature

Temperature	Φ	X	$\bar{M}_c$ (g/mol)	ρ (mol/cm^3)	ξ (nm)
27°C	0.042079	0.217329772	8458	8.3578	18.773
37°C	0.034604	0.239979899	12807	5.5194	24.657
47°C	0.028767	0.261771407	19100	3.7010	32.024

2.4.9 AFS Loading, Release and Kinetics

The encapsulation efficiency of the loaded hydrogel found out to be 63.8% and the release studies of AFS from AFS-loaded-CMGT-co-SAH were determined in a buffer solution of pH 7.4, AFS is soluble in buffer of pH 7.4 therefore 7.4 pH buffer was selected for release study. Also, the swelling of the hydrogel is maximum in pH 7.4 buffer. Here, the two factors, the solubility of the drug and swelling of the hydrogel are responsible for the diffusion of the drug. Generally, the release/swelling of drug/hydrogel is co-related with the cross-linked matrix of monomer and polysaccharides, nature of the solvent, density and composition of the hydrogel [28]. The rate was reasonably rapid during the early phases of drug release from the hydrogel, as shown in figure 2.5(a). After

that, it demonstrated controlled and sustained release. The rate of drug release decreases with an instant of time. It was observed from the release data that 52.2% of the loaded drug was released from the matrix in early time interval. It might be because the drug on the surface of the polymer matrix releases faster than the drug integrated into the polymeric matrix, allowing for controlled drug delivery from the hydrogel. The results reveals that the release of the drug from the hydrogel is related to the swelling of the hydrogel and follows the fickian mechanism [45]. The kinetics were further investigated by fitting the obtained drug release data to several mathematical models. Figure 2.5(b) and table 2.5, shows that the highest correlation coefficient (R^2) value was found in the Korsmeyer-Peppas model, representing drug release from a polymeric system. The measured Release Exponent i.e., 'n' is 0.4176 given in table 2.5, less than 0.5 and corresponds to the fickian mechanism of drug release [46], in which the driving force is a chemical gradient and the release mechanism is diffusion-controlled [31]. The Higuchi model also supports the fickian diffusion of the drug from the hydrogel polymeric matrix.

Table 2.5: Different models to study drug release kinetics of AFS from CMGT-co-SAH

Models	**R^2**	**K**	**n**
Zero-order	0.9344	K_o (min^{-1}) 0.03251±0.0024	
First-order	0.9292	K_1 (min^{-1}) 0.11515±0.0040	
Hixon-Crowell	0.9344	K_{HC} ($min^{-1/2}$) 0.002±1.5500	
Higuchi	0.9919	K_H($min^{-1/3}$) 1.48271±0.038	
Korsmeyer-Peppas	0.9933	K_{KP}(min^{-n}) 0.029348±0.005	0.4176

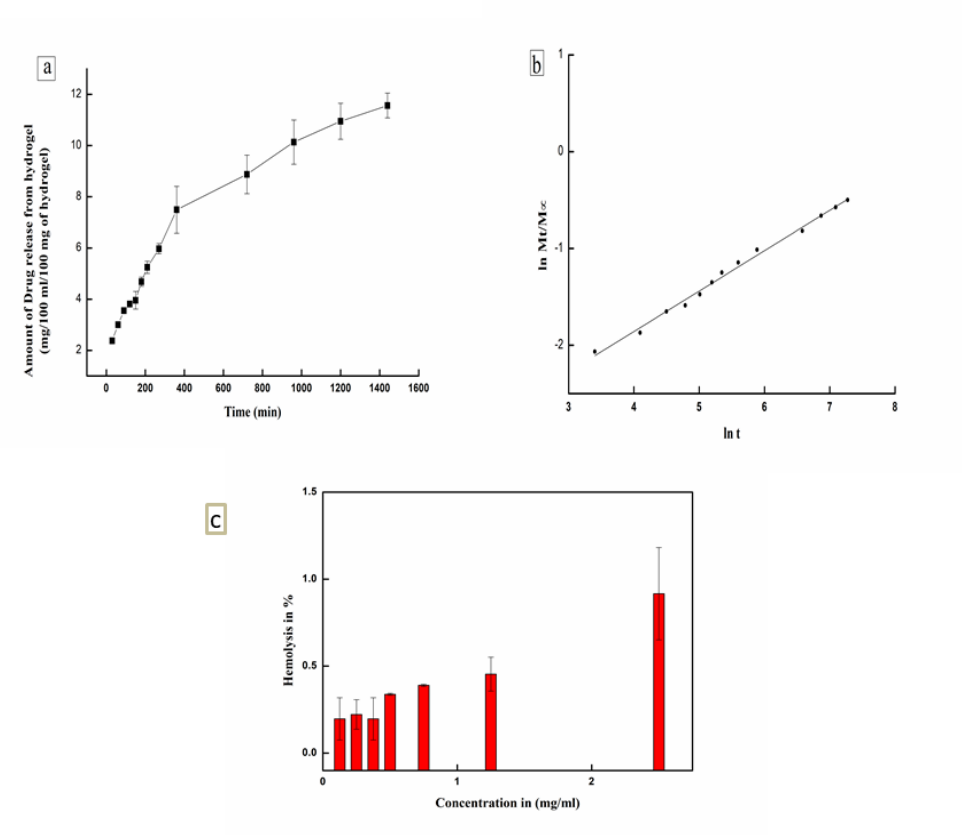

Figure 2.5: (a) Release profile of AFS from CMGT-co-SAH (b) Graph between ln M_t/M_∞ & ln t for determination of the rate constant and rate exponent and (c) Hemo-compatability studies

2.4.10 Hemo-Compatibility studies

Hemolytic potential of CMGT-co-SAH was evaluated (Table 2.6) and results was plotted shown in figure 2.5(c). The evaluated results show that % hemolysis is less than 1 at every concentration. In general, the sample shows % hemolysis less 5 is highly hemo-compatible and may be good for pharmaceutical application[47].

Table 2.6: Hemocompatibility studies result

CMGT-co-SAH Concentration(mg/ml)	Haemolysis in %	Remarks
0.125	0.1965±0.12	Highly hemocompatible
0.250	0.2223±0.08	Highly hemocompatible
0.375	0.1965±0.12	Highly hemocompatible
0.500	0.3381±0.006	Highly hemocompatible
0.750	0.3895±0.006	Highly hemocompatible
1.250	0.4539±0.09	Highly hemocompatible
2.500	0.9164±0.26	Highly hemocompatible

The results obtained from Hemolysis test show that CMGT-co-SAH is highly hemocompatible shown in figure 2.5(c) and table 2.6 and all the reactants used to synthesize CMGT-co-SAH previously been reported as safe and non-toxic to the environment. Recently, cytocompatibilities of GT and Acrylic acid based hydrogel by MTT assay was confirmed by Sayadnia et al.[42]. Khan and Anwar have proven that carboxymethylation does not have any cytotoxic effects [48]. N,N′-methylenebis(acrylamide) used in the synthesis of CMGT-co-SAH is also safe for drug delivery [49].

2.5 Conclusion

The current investigation focused on the structural modification of natural gum into its carboxymethylated derivative and the subsequent fabrication of CMGT-co-SA Hydrogel by graft copolymerization technique. The synthesized CMGT-co-SAH shows more stability than SAH, revealed by characterization performed by using an optimum formulation (CMGT-co-SAH-4). The investigation reveals that cross-linker

and initiator concentration affect the swelling of the hydrogel. Molecular weight and mesh size between two neighbouring crosslinks increase with the increase in temperature. The elasticity of SAH was less than CMGT-co-SAH as (G'/G") was raised with the addition of CMGT to the hydrogel. The Hemolysis test result confirms the hemocompatible nature of the hydrogel. The drug release from the hydrogel loaded with the non-steroidal anti-inflammatory drug- Aceclofenac sodium follows the fickian diffusion mechanism. It is best fitted in Korsmeyer-Peppas and Higuchi models. Thus it can be concluded that synthesized hydrogel is suitable for the controlled release of drug molecules.

2.6 References

[1] A. Bajpai and V. Raj, "Hydrophobically modified guar gum films for wound dressing," *Polym. Bull.*, vol. 78, no. 8, pp. 4109–4128, Aug. 2021, doi: 10.1007/s00289-020-03302-4.

[2] B. Sharma, R. Bharti, and R. Sharma, "Controlled drug delivery: 'A review on the applications of smart hydrogel,'" *Mater. Today Proc.*, vol. 65, pp. 3657–3664, 2022, doi: 10.1016/j.matpr.2022.06.237.

[3] B. Singh, V. Sharma, R. Kumar, and M. Mohan, "Development of dietary fiber psyllium based hydrogel for use in drug delivery applications," *Food Hydrocoll. Heal.*, vol. 2, no. November 2021, p. 100059, 2022, doi: 10.1016/j.fhfh.2022.100059.

[4] M. Nejatian, S. Abbasi, and F. Azarikia, "Gum Tragacanth: Structure, characteristics and applications in foods," *Int. J. Biol. Macromol.*, vol. 160, pp. 846–860, Oct. 2020, doi: 10.1016/j.ijbiomac.2020.05.214.

[5] E. Nazarzadeh Zare, P. Makvandi, and F. R. Tay, "Recent progress in the industrial and biomedical applications of Tragacanth gum: A review," *Carbohydr. Polym.*, vol. 212, no. January, pp. 450–467, 2019, doi: 10.1016/j.carbpol.2019.02.076.

[6] B. Singh and V. Sharma, "Crosslinking of poly(vinylpyrrolidone)/acrylic acid with Tragacanth gum for hydrogels formation for use in drug delivery applications," *Carbohydr. Polym.*, vol. 157, pp. 185–195, Feb. 2017, doi: 10.1016/j.carbpol.2016.09.086.

[7] C. A. Tischer, M. Iacomini, and P. A. J. Gorin, "Structure of the

arabinogalactan from gum tragacanth (*Astralagus gummifer*)," *Carbohydr. Res.*, vol. 337, no. 18, pp. 1647–1655, 2002, doi: 10.1016/S0008-6215(02)00023-X.

[8] R. T. Polez et al., "Biological activity of multicomponent bio-hydrogels loaded with Tragacanth gum," *Int. J. Biol. Macromol.*, vol. 215, no. April, pp. 691–704, 2022, doi: 10.1016/j.ijbiomac.2022.06.153.

[9] C. Verma, P. Negi, D. Pathania, V. Sethi, and B. Gupta, "Preparation of pH-sensitive hydrogels by graft polymerization of itaconic acid on tragacanth gum," *Polym. Int.*, vol. 68, no. 3, pp. 344–350, Mar. 2019, doi: 10.1002/pi.5739.

[10] Rimpy, Abhishek, and M. Ahuja, "Evaluation of carboxymethyl Moringa gum as nanometric carrier," *Carbohydr. Polym.*, vol. 174, pp. 896–903, Oct. 2017, doi: 10.1016/j.carbpol.2017.07.022.

[11] A. G. Sullad, L. S. Manjeshwar, and T. M. Aminabhavi, "Microspheres of carboxymethyl guar gum for in vitro release of abacavir sulfate: Preparation and characterization," *J. Appl. Polym. Sci.*, vol. 122, no. 1, pp. 452–460, Oct. 2011, doi: 10.1002/app.34173.

[12] A. K. Veeramachineni, T. Sathasivam, R. Paramasivam, S. Muniyandy, and J. Pushpamalar, "Synthesis and Characterization of a Novel pH-Sensitive Aluminum Crosslinked Carboxymethyl Tragacanth Beads for Extended and Enteric Drug Delivery," *J. Polym. Environ.*, vol. 27, no. 7, pp. 1516–1528, Jul. 2019, doi: 10.1007/s10924-019-01448-5.

[13] Q. Wang et al., "Injectable DNA Hydrogel-Based Local Drug Delivery and

Immunotherapy," *Gels*, vol. 8, no. 7, p. 400, 2022, doi: 10.3390/gels8070400.

[14] C. Chang and L. Zhang, "Cellulose-based hydrogels: Present status and application prospects," *Carbohydr. Polym.*, vol. 84, no. 1, pp. 40–53, 2011, doi: 10.1016/j.carbpol.2010.12.023.

[15] E. Jabbari and S. Nozari, "Swelling behavior of acrylic acid hydrogels prepared by γ-radiation crosslinking of polyacrylic acid in aqueous solution," *Eur. Polym. J.*, vol. 36, no. 12, pp. 2685–2692, 2000, doi: 10.1016/S0014-3057(00)00044-6.

[16] S. Ganguly et al., "Design of psyllium-g-poly(acrylic acid-co-sodium acrylate)/cloisite 10A semi-IPN nanocomposite hydrogel and its mechanical, rheological and controlled drug release behaviour," *Int. J. Biol. Macromol.*, vol. 111, pp. 983–998, 2018, doi: 10.1016/j.ijbiomac.2018.01.100.

[17] M. Behrouzi and P. N. Moghadam, "Synthesis of a new superabsorbent copolymer based on acrylic acid grafted onto carboxymethyl Tragacanth," *Carbohydr. Polym.*, vol. 202, pp. 227–235, Dec. 2018, doi: 10.1016/j.carbpol.2018.08.094.

[18] M. B. Santos, C. H. C. dos Santos, M. G. de Carvalho, C. W. P. de Carvalho, and E. E. Garcia-Rojas, "Physicochemical, thermal and rheological properties of synthesized carboxymethyl tara gum (*Caesalpinia spinosa*)," *Int. J. Biol. Macromol.*, vol. 134, pp. 595–603, Aug. 2019, doi: 10.1016/j.ijbiomac.2019.05.025.

[19] S. Verma and M. Ahuja, "Carboxymethyl Sesbania gum: Synthesis, characterization and evaluation for drug delivery," *Int. J. Biol. Macromol.*,

vol. 98, pp. 75–83, May 2017, doi: 10.1016/j.ijbiomac.2017.01.070.

[20] M. Suhail, P.-C. Wu, and M. U. Minhas, "Development and characterization of pH-sensitive chondroitin sulfate-co-poly(acrylic acid) hydrogels for controlled release of diclofenac sodium," *J. Saudi Chem. Soc.*, vol. 25, no. 4, p. 101212, Apr. 2021, doi: 10.1016/j.jscs.2021.101212.

[21] Z. Fan et al., "A novel multifunctional Salecan/κ-carrageenan composite hydrogel with anti-freezing properties: Advanced rheology, thermal analysis and model fitting," *Int. J. Biol. Macromol.*, vol. 208, pp. 1–10, May 2022, doi: 10.1016/j.ijbiomac.2022.03.054.

[22] S. Tanpichai, F. Phoothong, and A. Boonmahitthisud, "Superabsorbent cellulose-based hydrogels cross-liked with borax," *Sci. Rep.*, vol. 12, no. 1, pp. 1–12, 2022, doi: 10.1038/s41598-022-12688-2.

[23] R. Kannaujia et al., "Facile synthesis of $CuFe_2O_4$ doped polyacrylic acid hydrogel nanocomposite and its application in dye degradation," *Mater. Lett.*, vol. 252, pp. 198–201, Oct. 2019, doi: 10.1016/j.matlet.2019.05.094.

[24] B. Singh, V. Sharma, and R. and A. Kumar, "Designing Moringa gum-Sterculia gum-polyacrylamide hydrogel wound dressings for drug delivery applications," *Carbohydr. Polym. Technol. Appl.*, vol. 2, p. 100062, Dec. 2021, doi: 10.1016/j.carpta.2021.100062.

[25] S. Malik and M. Ahuja, "Gum kondagogu-g-poly (acrylamide): Microwave-assisted synthesis, characterisation and release behaviour," *Carbohydr. Polym.*, vol. 86, no. 1, pp. 177–184, Aug. 2011, doi: 10.1016/j.carbpol.2011.04.027.

[26] H. R. Badwaik, K. Sakure, A. Alexander, Ajazuddin, H. Dhongade, and D. K. Tripathi, "Synthesis and characterisation of poly(acryalamide) grafted carboxymethyl xanthan gum copolymer," *Int. J. Biol. Macromol.*, vol. 85, pp. 361–369, Apr. 2016, doi: 10.1016/j.ijbiomac.2016.01.014.

[27] A. R. Kulkarni, K. S. Soppimath, T. M. Aminabhavi, A. M. Dave, and M. H. Mehta, "Glutaraldehyde crosslinked sodium alginate beads containing liquid pesticide for soil application," *J. Control. Release*, vol. 63, no. 1–2, pp. 97–105, 2000, doi: 10.1016/S0168-3659(99)00176-5.

[28] B. Singh and B. Singh, "Influence of graphene-oxide nanosheets impregnation on properties of Sterculia gum-polyacrylamide hydrogel formed by radiation induced polymerization," *Int. J. Biol. Macromol.*, vol. 99, pp. 699–712, Jun. 2017, doi: 10.1016/j.ijbiomac.2017.03.037.

[29] J. T. Chung, K. D. F. Vlugt-Wensink, W. E. Hennink, and Z. Zhang, "Effect of polymerization conditions on the network properties of dex-HEMA microspheres and macro-hydrogels," *Int. J. Pharm.*, vol. 288, no. 1, pp. 51–61, 2005, doi: 10.1016/j.ijpharm.2004.09.011.

[30] B. Singh and B. Singh, "Influence of graphene-oxide nanosheets impregnation on properties of sterculia gum-polyacrylamide hydrogel formed by radiation induced polymerization," *Int. J. Biol. Macromol.*, vol. 99, pp. 699–712, Jun. 2017, doi: 10.1016/j.ijbiomac.2017.03.037.

[31] H. Goel, N. Gupta, D. Santhiya, N. Dey, H. B. Bohidar, and A. Bhattacharya, "Bioactivity reinforced surface patch bound collagen-pectin hydrogel," *Int. J. Biol. Macromol.*, vol. 174, pp. 240–253, 2021, doi:

10.1016/j.ijbiomac.2021.01.166.

[32] H. Bera, S. Mothe, S. Maiti, and S. Vanga, "Carboxymethyl fenugreek galactomannan-gellan gum-calcium silicate composite beads for glimepiride delivery," *Int. J. Biol. Macromol.*, vol. 107, pp. 604–614, Feb. 2018, doi: 10.1016/j.ijbiomac.2017.09.027.

[33] B. Singh and V. Sharma, "Designing galacturonic acid /arabinogalactan crosslinked poly(vinyl pyrrolidone)- co-poly(2-acrylamido-2-methylpropane sulfonic acid) polymers: Synthesis, characterization and drug delivery application," *Polymer (Guildf).*, vol. 91, pp. 50–61, May 2016, doi: 10.1016/j.polymer.2016.03.037.

[34] V. Suryadevara, S. R. Lankapalli, B. Thalamanchi, A. Patcha, and L. H. Danda, "Design and evaluation of verapamil hydrochloride controlled release hydrogel-based matrix tablets," *Asian J. Pharm.*, vol. 10, no. 1, pp. 51–58, 2016.

[35] K. Pal and S. Pal, "Development of porous hydroxyapatite scaffolds," *Mater. Manuf. Process.*, vol. 21, no. 3, pp. 325–328, 2006, doi: 10.1080/10426910500464826.

[36] Z. Fan et al., "Understanding the rheological properties of a novel composite Salecan/Gellan hydrogels," *Food Hydrocoll.*, vol. 123, no. September 2021, p. 107162, 2022, doi: 10.1016/j.foodhyd.2021.107162.

[37] R. Yadav and R. Purwar, "Influence of metal oxide nanoparticles on morphological, structural, rheological and conductive properties of mulberry silk fibroin nanocomposite solutions," *Polym. Test.*, vol. 93, no. July 2020, p.

106916, 2021, doi: 10.1016/j.polymertesting.2020.106916.

[38] Y. Bachra, A. Grouli, F. Damiri, M. Talbi, and M. Berrada, "A Novel Superabsorbent Polymer from Crosslinked Carboxymethyl Tragacanth Gum with Glutaraldehyde: Synthesis, Characterization, and Swelling Properties," *Int. J. Biomater.*, vol. 2021, pp. 1–14, Nov. 2021, doi: 10.1155/2021/5008833.

[39] A. M. A. Hasan, M. Keshawy, and M. E. S. Abdel-Raouf, "Atomic force microscopy investigation of smart superabsorbent hydrogels based on carboxymethyl guar gum: Surface topography and swelling properties," *Mater. Chem. Phys.*, vol. 278, no. August 2021, p. 125521, 2022, doi: 10.1016/j.matchemphys.2021.125521.

[40] F. B. Santos, N. T. Miranda, M. I. R. B. Schiavon, L. V. Fregolente, and M. R. Wolf Maciel, "Thermal degradation kinetic of poly(acrylamide-co-sodium acrylate) hydrogel applying isoconversional methods," *J. Therm. Anal. Calorim.*, vol. 146, no. 6, pp. 2503–2514, 2021, doi: 10.1007/s10973-020-09899-y.

[41] B. Singh, L. Varshney, S. Francis, and Rajneesh, "Designing tragacanth gum based sterile hydrogel by radiation method for use in drug delivery and wound dressing applications," *Int. J. Biol. Macromol.*, vol. 88, pp. 586–602, 2016, doi: 10.1016/j.ijbiomac.2016.03.051.

[42] S. Sayadnia, E. Arkan, R. Jahanban-Esfahlan, S. Sayadnia, and M. Jaymand, "Tragacanth gum-based pH-responsive magnetic hydrogels for 'smart' chemo/hyperthermia therapy of solid tumors," *Polym. Adv. Technol.*, vol. 32, no. 1, pp. 262–271, 2021, doi: 10.1002/pat.5082.

[43] W. Wang and A. Wang, "Synthesis, swelling behaviors, and slow-release characteristics of a guar gum-g-poly(sodium acrylate)/sodium humate superabsorbent," *J. Appl. Polym. Sci.*, vol. 112, no. 4, pp. 2102–2111, May 2009, doi: 10.1002/app.29620.

[44] B. Singh and B. Singh, "Graft copolymerization of polyvinylpyrollidone onto *Azadirachta indica* gum polysaccharide in the presence of crosslinker to develop hydrogels for drug delivery applications," *Int. J. Biol. Macromol.*, vol. 159, pp. 264–275, Sep. 2020, doi: 10.1016/j.ijbiomac.2020.05.091.

[45] B. Singh and Rajneesh, "Gamma radiation synthesis and characterization of gentamicin loaded polysaccharide gum based hydrogel wound dressings," *J. Drug Deliv. Sci. Technol.*, vol. 47, pp. 200–208, Oct. 2018, doi: 10.1016/j.jddst.2018.07.014.

[46] K. Mukherjee, P. Dutta, and T. K. Giri, "Al3+/Ca2+ cross-linked hydrogel matrix tablet of etherified Tara gum for sustained delivery of tramadol hydrochloride in gastrointestinal milieu," *Int. J. Biol. Macromol.*, vol. 232, p. 123448, Mar. 2023, doi: 10.1016/j.ijbiomac.2023.123448.

[47] ASTM F 756-13, "Standard practice for assessment of hemolytic properties of materials. Philadelphia," *Am. Soc. Test. Mater.*, pp. 1–5, 2000, doi: 10.1520/F0756-13.

[48] S. Khan and N. Anwar, "Gelatin/carboxymethyl cellulose based stimuli-responsive hydrogels for controlled delivery of 5-fluorouracil, development, in vitro characterization, in vivo safety and bioavailability evaluation," *Carbohydr. Polym.*, vol. 257, no. September 2020, p. 117617, 2021, doi:

10.1016/j.carbpol.2021.117617.

[49] M. M. Lakouraj, M. Rezaei, and V. Hasantabar, "Synthesis, characterization and in-vitro prolonged release of L-DOPA using a novel amphiphilic hydrogel based on Sodium alginate-polypyrrole," *Int. J. Biol. Macromol.*, vol. 193, no. PA, pp. 609–618, 2021, doi: 10.1016/j.ijbiomac.2021.10.171.

CHAPTER – 3

Synthesis and Characterization of Carboxymethylated Locust Bean Gum-*co*-poly(SA)-*cl*-poly(MBA) pH Responsive Hydrogel for Controlled Drug Delivery of Metformin Hydrochloride

3.1 Introduction

Locus bean gum (LB) is obtained from the endosperm of the seeds of *Ceratonia siliqua Linn*. It is also known as galactomannan because it contains galactose and mannose in a 1:4 ratio [11],[15],[16] and has a high M Wt (960,000–1,100,000 g/mol). LB gum also has excellent potential as an emulsifier, gelling, thickening, stabilising agent and as an additive (E410) [4]. The US Food and Drug Administration (FDA) has given this gum approval for use in food [5]. Metformin hydrochloride (MFH) is an anti-hyperglycemic agent used to treat type II diabetes mellitus [6].

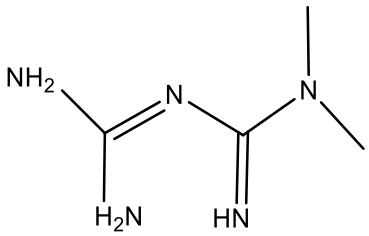

H-Cl

Structure of Metformin Hydrochloride

It is low in bioavailability (50–60%) and requires a high dose frequently through immediate release tablets due to its short half-life (0.9–2.6 hours) [7]. A good compliance of the extended release system is useful to reduce the side effects of conventional immediate release systems. The oral absorption of MFH is reported to be

mainly restricted to the small intestine. Therefore, it is necessary to create an appropriate drug delivery system that initiates the partial release of the drug into the stomach and completes it in jejunum, so that at this particular transit time all the drugs must be released through the system. pH-dependent polymers have been used in this site-specific drug delivery system to improve the therapeutic effectiveness of MFH [8].

The sustained release of MFH from a new drug delivery system is discussed in this chapter. For this, firstly, natural locust bean gum has been derivatized to carboxymethylated locust bean gum (CMLB). Afterward, the novel hydrogel was synthesized by using CMLB co- polymerized with poly Sodium Acrylate which were cross-linked with N,N′-methylenebis(acrylamide) (MBA). For the first time, CMLB-*co*-poly(SA)-*cl*-poly(MBA) Hydrogel's swelling behaviour and network parameters were analysed, and characterized by XRD, SEM, ^{13}C-NMR, TGA and FT-IR. Hemolysis test was done to analyse the bio-compatible nature of the hydrogel. The drug release behaviour of the hydrogel was analysed in buffer pH 2.2, 7.4 and distilled water (DW) by using model drug, MFH. In order to determine drug encapsulation and controlled drug release behaviour, various kinetic models were applied to drug release data to consider synthesized hydrogel as an effective drug delivery carrier.

3.2 Experimental

3.2.1 Materials

Sodium monochloroacetate (SMCA, CDH, New Delhi), Locust bean gum (LB) (purchased from local market, Acrylic acid (AA, CDH, New Delhi), N,N′-methylenebis(acrylamide) (MBA, CDH, New Delhi, Iso propyl alcohol (Fischer Scientific, Mumbai), Sodium hydroxide (NaOH, Fischer Scientific, Mumbai),

Potassium per sulphate (KPS, Fischer Scientific, Mumbai) and milli-Q grade Distilled water for preparation of solution.

3.2.2 Synthesis of Carboxymethyl Locust Bean Gum (CMLB)

The CMLB was synthesized using the previously described procedure in chapter-2 [9]. The mechanism adopted for the polysaccharide chain derivatization was Williamson's synthesis of ether. To achieve the necessary substitution level, weighed 10 g of LB was dispersed in 35 ml of DW and stirred continuously on magnetic stirrer. After 30 minutes of stirring, added 0.00775M NaOH to the solution, and slowly added SMCA (0.00123M). The final reaction mixture was stirred at 70°C to obtain a homogenous solution. After cooling, the precipitate was filtered and washed with isopropyl alcohol (80%) at least three times and dried in a hot oven at 45° C.

3.2.3 Estimation of Degree of Substitution (DOS) on LB

Back titration method was used to determine the DOS on LB [9]. CMLB (1g) is distributed into 3-5 ml 0.1 N HCl and stirred for 15 minutes to avoid lump formation and 1 ml of isopropyl alcohol was used as solvent. Then added 25 ml of DW and stirred for a few minutes. After sedimentation, supernatant was discarded and sediments were filtered through a muslin cloth, and the residue was washed with DW multiple times till the filtrate gives negative silver nitrate test. Finally, the dried residue was dispersed in 50 ml of NaOH solution of 0.1 N and back titrated with 0.1 N HCl.

Equations (1 and 2) were used to calculate DOS [10].

$$\mathrm{DOS} = 0.162\mathrm{A}/1 - 0.058\mathrm{A} \quad (1)$$

Where, $A = \frac{(ml\ of\ NaOH\ X\ N1) - (ml\ of\ HCl\ X\ N2)}{gram\ of\ the\ dried\ sample}$ (2)

A is the milliequivalents of NaOH needed per gram of sample, while N1 and N2 stand for the normalities of NaOH and HCl respectively.

3.2.4 Synthesis of CMLB-*co*-poly(SA)-*cl*-poly(MBA) Hydrogels

CMLB-*co*-poly(SA)-*cl*-poly(MBA) Hydrogel (1-5) was synthesized by taking CMLB in DW with DOS (0.2) (0.33% w/v). 7.2 g of AA was neutralized using 13 ml 8.07 mol/L of NaOH. KPS (0.0098 mol/L). MBA (0.012 mol/L, 0.015 mol/L, 0.017 mol/L, 0.019 mol/L and 0.021 mo/L) was added to the aqueous reaction in a conical flask and stirred for 2 hours at room temperature and then at 60 °C for 2 hours in the water bath. To eliminate the soluble chemical compounds, the hydrogel was washed using aqueous and organic solvents and cut in thin discs before being dried in an oven at 45 °C for constant weight. The sample for characterization was selected on the basis of highest Swelling Index given in table 3.1.

Table 3.1: Swelling Index of the CMLB-*co*-poly(SA)-*cl*-poly(MBA) hydrogels after 24 hours at different concentration of cross-linker

Sr. No.	Formulation on the basis of Concentration of Cross-linker(MBA)	Swelling Index of Hydrogel(g/g) after 24 hours		
		pH 2.2	pH 7.4	DW
1	0.012 mol/L	19.06±0.27	25.59±0.29	33.91±0.43
2	0.015 mol/L	19.99±0.20	26.76±0.29	34.94±0.08
3	0.017 mol/L	19.97±0.23	25.32±0.64	34.12±0.40
4	0.019 mol/L	19.87±0.21	25.24±0.27	33.53±0.38
5	0.021 mol/L	19.38±0.38	24.64±0.30	33.22±0.37

3.3 Characterizations of LB, CMLB and CMLB-*co*-poly(SA)-*cl*-poly(MBA) Hydrogel

3.3.1 Swelling Studies

The swelling studies were carried out by varying (i) concentration of cross-linker MBA (0.012 mol/L, 0.015 mol/L, 0.017 mol/L, 0.019 mol/L and 0.021 mo/L) at temperature 37 °C and in DW and pH 7.4 and 2.2 buffer solution, (ii) temperature (27°, 37° and 47°) in pH 7.4 buffer solution with MBA 0.015 mol/L. Swelling index of the hydrogels was analysed by swelling equilibrium method. Calculation for the swelling index(SI) was given in Equation 3[11].

$$SI\% = \frac{Ws - Wd}{Wd} \; X \; 100 \qquad (3)$$

At a certain period of time interval, W_d represents the weight of dried hydrogel, whereas W_s for swollen hydrogel.

3.3.2 Network Parameters

Using the Flory-Rehner equation, hydrogel network characteristics were assessed using data on hydrogel swelling at 27 °C, 37 °C and 47 °C. In our previous studies [9], we provided a brief procedure for assessing the hydrogels' mesh size (ξ) and Flory-Huggins interaction parameter (χ), the volume fraction of the swollen hydrogel (ϕ), Molecular weight of the segments between two neighbouring crosslinks of the network hydrogel ($\overline{Mc}$), and crosslink density (ρ). Also, the impact of different parameters on the network characteristics was studied.[12,13]

3.3.3 SEM

Scanning electron microscopic (SEM) studies of LB, CMLB and CMLB-*co*-poly(SA)-*cl*-poly(MBA) Hydrogel were conducted using (Model: JEOL JSM-

6610LV). Gold coated samples were analysed at SEM, at accelerating voltage 20 kV and at 1,000 X magnifications.

3.3.4 FTIR

The IR spectra of powdered samples of LB, CMLB and CMLB-*co*-poly(SA)-*cl*-poly(MBA) Hydrogel were analyzed on Perkin-Elmer model 2000 FT-IR spectrometer.

3.3.5 ^{13}C-NMR

^{13}C-NMR of samples LB, CMLB and CMLB-*co*-poly(SA)-*cl*-poly(MBA) Hydrogel were done on Bruker Avance 500 WB solid state NMR spectrometer.

3.3.6 TGA

The thermo-gravimetric analysis (TGA) was recorded using a PerkinElmer thermo-gravimetric analyzer, TGA 4000, in N_2 atmosphere with 10 °C/min of uniform heating rate from 25° to 800°C.

3.3.7 XRD

X-ray diffraction patterns were analyzed using Expert Pro MRD,Panalytical, X-Ray diffractometer by analyzing the diffraction by analyzing the diffraction angle from 10° to 80° at 40 keV.

3.3.8 Rheology

Rheological analysis was performed on swollen disc of hydrogel in three different solvent using an Anton Paar Modular Compact Rheometer 302 (MCR).

3.3.9 Drug loading and Release profile of Metformin Hydrochloride (MFH)

The anti-diabetic drug MFH was loaded onto the hydrogel. The loading of the drug was done by the swelling equilibrium method. The hydrogel disc (0.1 g) was emerged in a fixed proportion of the drug and buffer solution (2mg/ml) for 24 hours at 37°C. The loading and release profile of the drug were evaluated by using a calibration curve of MFH in different buffer solution at 232 nm [14]. MFH loaded samples were dried and weighed for drug release study. In 50 ml solution of (2.2, 7.4 and DW), drug loaded samples were placed at 37 °C and samples were collected at interval of 30 minutes up to 4 hours and after that different time interval up to 24 hours. The data obtained from the drug release profile was applied in different kinetic models [15]. Encapsulation Efficiency% (% of EE) was calculated using equation 4.

$$\% \text{ of EE} = \left(\frac{\text{Actual loading}}{\text{Theoretical loading}}\right) * 100 \quad (4)$$

Actual loading is determined by using UV-Visible Spectrophotometer. Where, loading of the drug into the hydrogel determine by using the initial concentration of the drug in the solution and the drug present in the supernatant after absorption [16]. Theoretical loading is the weight of the dried hydrogel disc after swelling in drug solution.

3.3.10 Hemo-Compatibility Test

The hemolytic potential of CMLB-*co*-poly(SA)-*cl*-poly(MBA) hydrogel was determined by an *in vitro* hemolysis in %. The blood sample (1 ml) was collected from healthy human in EDTA treated tubes and centrifuged for 5 minutes, at 3000 rpm. Supernatant of blood plasma was discarded, and separated RBCs were, washed in 1x PBS (pH 7.4), further re-suspended in 1 ml of 1x PBS. For use in experiments

this stock solution was diluted to 4% v/v in 1x PBS. The sample was added to 96 well plates in increasing amount from 0.125 mg/ml to 2.5 mg/ml. The 100 ul of RBC solution was added to each well. Final volume was made up to 200 ul in each well with 1x PBS (pH 7.4). Triton X-100 was used as the positive control (0.1%w/v) and 1x PBS (pH 7.4) act as negative control. The 96 well plate was incubated at 37℃ for 1 h with shaking in an incubator shaker. After incubation the plate was centrifuged at 3000 rpm for 5 min. The 100 ul of the supernatant was collected in another 96 well plate and measured the absorbance (A) at 540 nm on Elisa plate reader. The hemolysis in % was evaluated by using given equation 5:

$$\text{Hemolysis in \%} = \left(\frac{A_{\text{CMLB}-cl-\text{polySA}} - A_{1\text{xPBS}}}{A_{\text{triton X}-100} - A_{1\text{xPBS}}}\right) \text{X}100 \quad (5)$$

Hemolysis in % was evaluated on average of two replicates [17].

3.4 Results and Discussions

The CMLB-*co*-poly(SA)-*cl*-poly(MBA) hydrogel was fabricated by using the free radical polymerization method in the presence of CMLB, polySA, KPS and MBA. This reaction was carried out by following our previously published article [9]. The chemistry behind the synthesis of CMLB-*co*-poly(SA)-*cl*-poly(MBA) hydrogel has been shown in Scheme 3.1. The synthesized hydrogel was further used to form MFH-loaded CMLB-*co*-poly(SA)-*cl*-poly(MBA) hydrogel using the swelling equilibrium method as used in our previous study. CMLB-*co*-poly(SA)-*cl*-poly(MBA) Hydrogel with cross-linker 0.015 mol/L exhibited maximum swelling index (shown in figure 3.1a) thus selected for further studies.

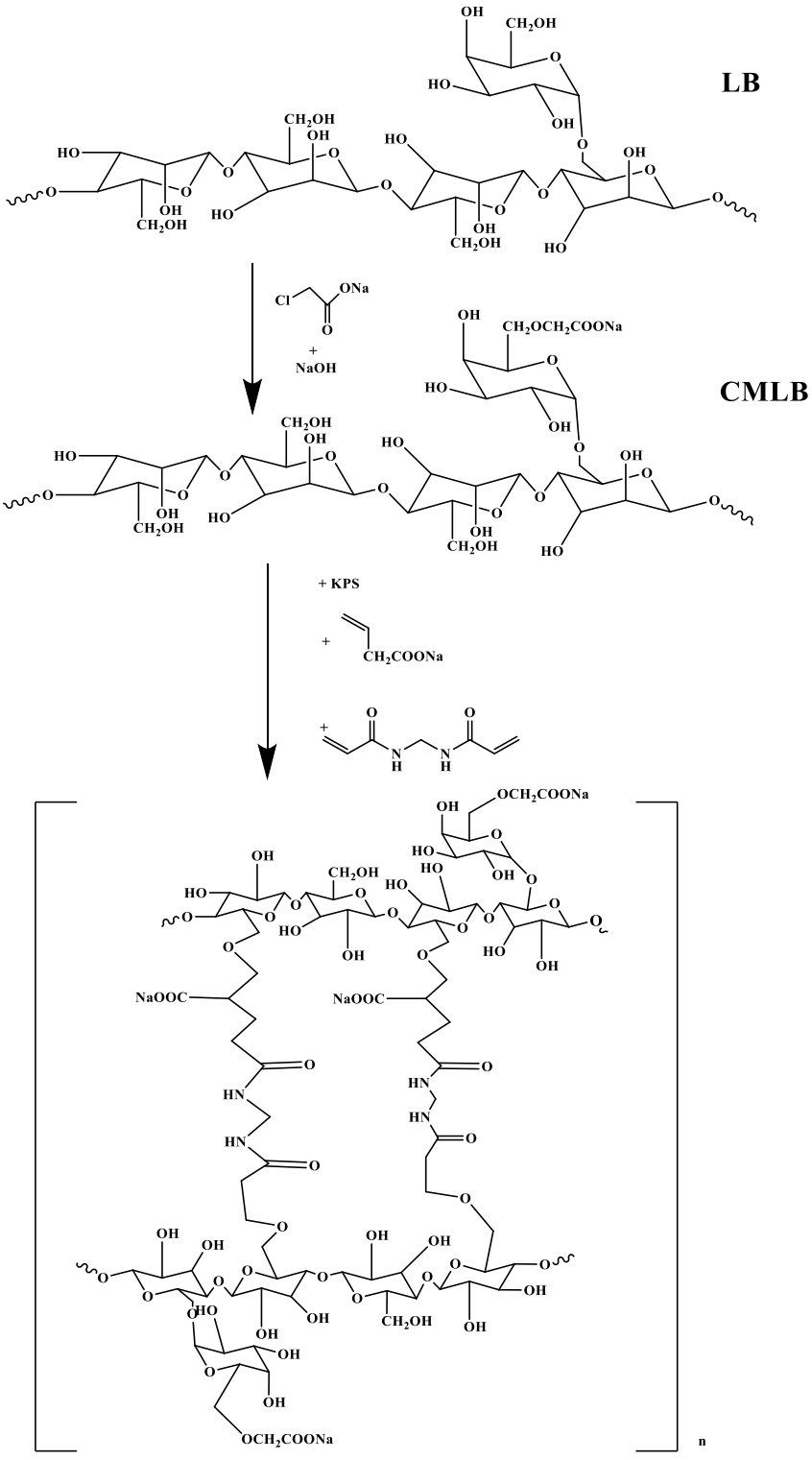

CMLB-*co*-poly(SA)-*cl*-poly(MBA)

Scheme 3.1: Synthesis of CMLB-*co*-poly(SA)-*cl*-poly(MBA) Hydrogel

3.4.1 Swelling Studies

3.4.1.1 Effect of Change in Amount of Cross-Linker on the Swelling of CMLB-*co*-poly(SA)-*cl*-poly(MBA) Hydrogel

The swelling of the hydrogel's shown in figure 3.1a, was carried out to determine the effect of the cross-linker on the cross linking density during the co-polymerization reaction. The swelling index of the hydrogel initially increases with the concentration of the cross-linker, but further increase in its concentration results in a decrease in the swelling index. Increased concentrations of cross-links promote network cross-links, but decrease laterally due to delay in the relaxation of polymer chains on the polymer network [9, 18].

3.4.1.2 Effect of Change in pH and Temperature on the Swelling of CMLB-*co*-poly(SA)-*cl*-poly(MBA) Hydrogel

It has been observed from figure 3.1b and 3.1c, that the pH and temperature of the swelling medium affect the hydrogels' potential to swell. The constituted ions (COO^-) formed at higher pH in the matrix material during partial hydrolysis may be the cause of this ionic repulsion and thus cause the opening of the pores in the polymeric web [24,25]. Swelling of the hydrogel correlated with the release of the drug. The swelling is highest in DW among three solvent, which cause abrupt release of the drug while swelling is very low in pH 2.2 buffer solution that will not release drug appropriately at the site of release. As the swelling is appropriate in pH 7.4 buffer solution cause the sustained release of the drug from the hydrogel because drug will release through swelling equilibrium method. The extent of network dissociation is depends upon the difference between pKa and pH values; therefore, a large disparity cause higher

degree of network dissociation. In an acidic medium with a pH of 2.2, protonated –COOH groups form extended hydrogen bonding thus reducing the electrostatic repulsion which cause low rate of swelling of hydrogels in pH 2.2. Suhail et al. also observed the similar results of swelling in pH 1.2 and pH 7.4 buffer solutions [21].

Swelling Index (g/g) at three different temperatures 27°, 37° and 47° were found out to be 26.26±0.13, 28.61±0.51 and 36.36±0.32 respectively. The impact of the temperature on the swelling degree can be attributed to the dynamic interplay of the hydrogen bonding between the functional groups of CMLB and poly(SA) within the hydrogel, having association and dissociation processes. Furthermore, as the temperature rises, the enhanced swelling of the polymer molecules promotes the diffusion of the water molecules within the polymer network. Notably, the flory-Huggins interaction parameter is temperature- dependent, exerting a significant influence on the hydrogel's swelling extent [22].

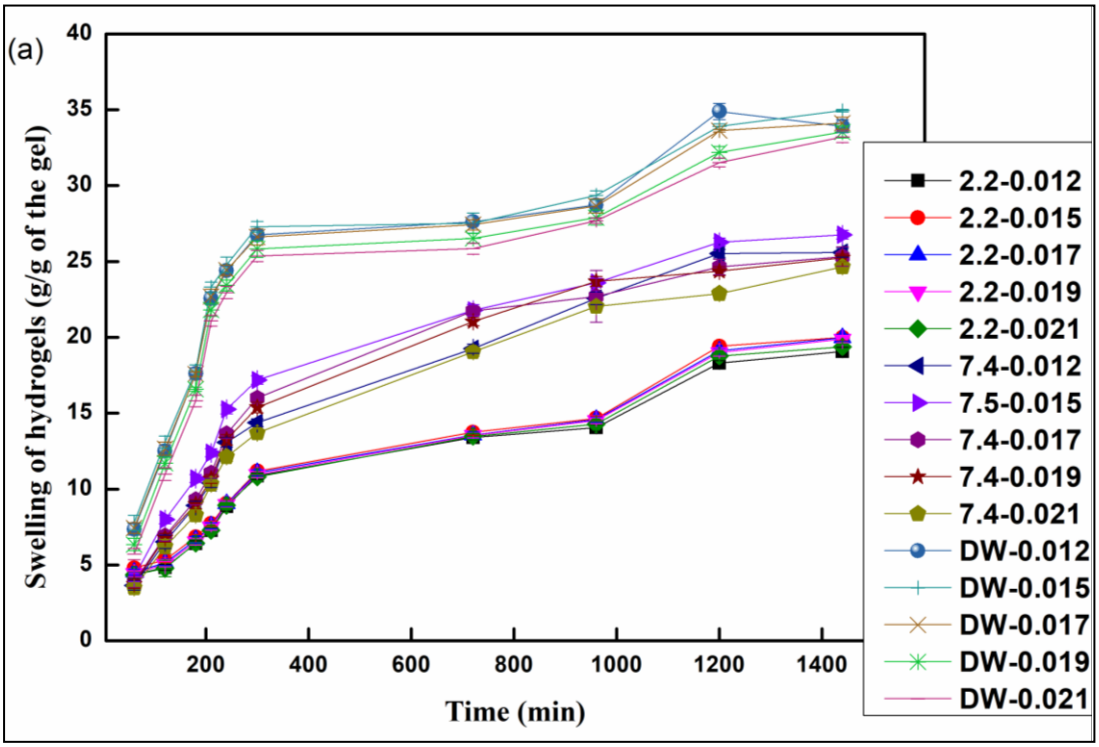

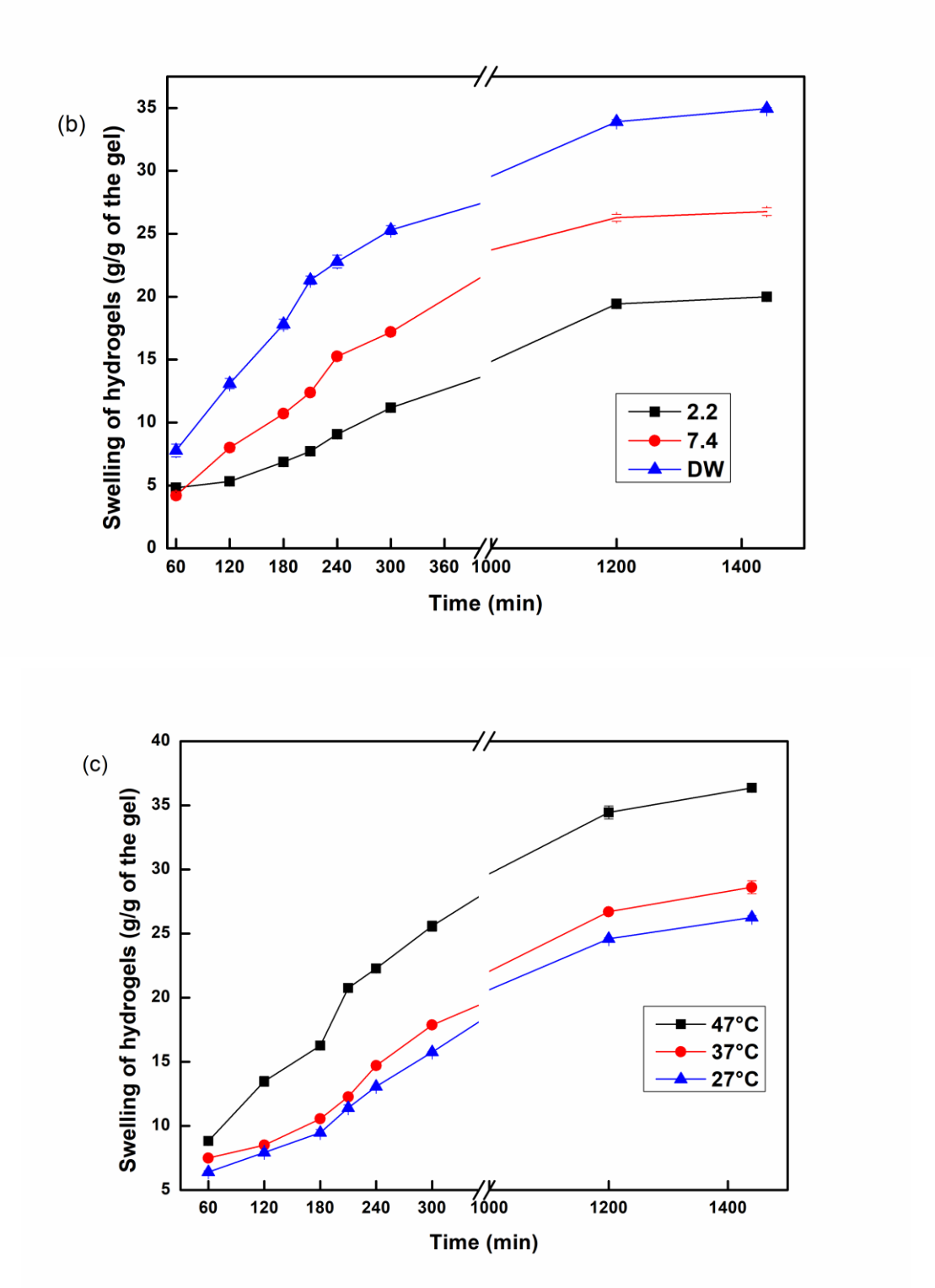

Figure 3.1: (a) Effect of cross-linker on swelling of the hydrogel, (b) effect of pH of the solvent on the swelling of the hydrogel and (c) effect of temperature of the solvent on the swelling of the hydrogel

3.4.2 Network Parameter

Table 3.2: The network parameters of CMLB-*co*-poly(SA)-*cl*-poly(MBA) hydrogel as a function of different parameters

Sr. No.	Parameters	Polymer volume fraction ϕ	Flory Huggins interaction parameter χ	Molecular weight in (g/mol) of the segments between two neighbouring crosslinks $\overline{Mc}$	crosslink density (ρ) x10^{-4} (mol/cm3)	mesh size ξ (nm)
			Effect of solvent			
1.	2.2	0.023	0.284	28941	0.24	41.97
2.	7.4	0.019	0.305	45972	0.16	56.31
3.	DW	0.0104	0.372	195093	0.03	143.39
			Effect of temperature			
4.	27 °C	0.019	0.306	43946	0.15	55.17
5.	37 °C	0.019	0.305	45972	0.16	56.31
6.	47 °C	0.011	0.373	202576	0.03	146.85
			Effect of cross-linker concentration (mol/L)			
10.	0.012	0.053	0.191	5173	1.35	13.58
11.	0.015	0.049	0.198	5901	1.19	14.80
12.	0.017	0.052	0.193	5362	1.30	13.92
13.	0.019	0.053	0.192	5208	1.34	13.65
14.	0.021	0.055	0.186	4593	1.48	12.60

According to the results shown in table 3.2, when MBA was raised during polymerization, the effect on network characteristics demonstrated that mesh size (ξ) initially grew from 13.58 to 14.80 nm and then decreased (14.80 to 12.60 nm). Increase in the temperature and pH of the swelling medium raise the swelling. The findings showed that temperature and swelling media had an impact on the hydrogel matrix's mesh size. At higher pH buffers and higher temperatures, Mc and ξ values were found to be greater; however, ρ values showed the opposite patterns. The partial hydrolysis that led to the production of ions and their repulsion caused the crosslinked hydrogel's swelling to rise in the pH 7.4 buffer solution. Similar findings were reported by Singh et al. on *Azadirachta indica* gum based hydrogel used for drug delivery [23].

3.4.3 SEM

The surface morphology of LB gum, CMLB gum and CMLB-*co*-poly(SA)-*cl*-poly(MBA) hydrogel has been analyzed by SEMs at 1000X, shown in figure 3.2. The SEM images shown that LB gum have homogeneous, compact, and smooth morphology [15,29], whereas CMLB gum and CMLB-*co*-poly(SA)-*cl*-poly(MBA) hydrogel have coarse and porous morphology and also structural heterogeneity. Changes in surface morphology of the CMLB and its hydrogels are more favourable for drug diffusion [25].

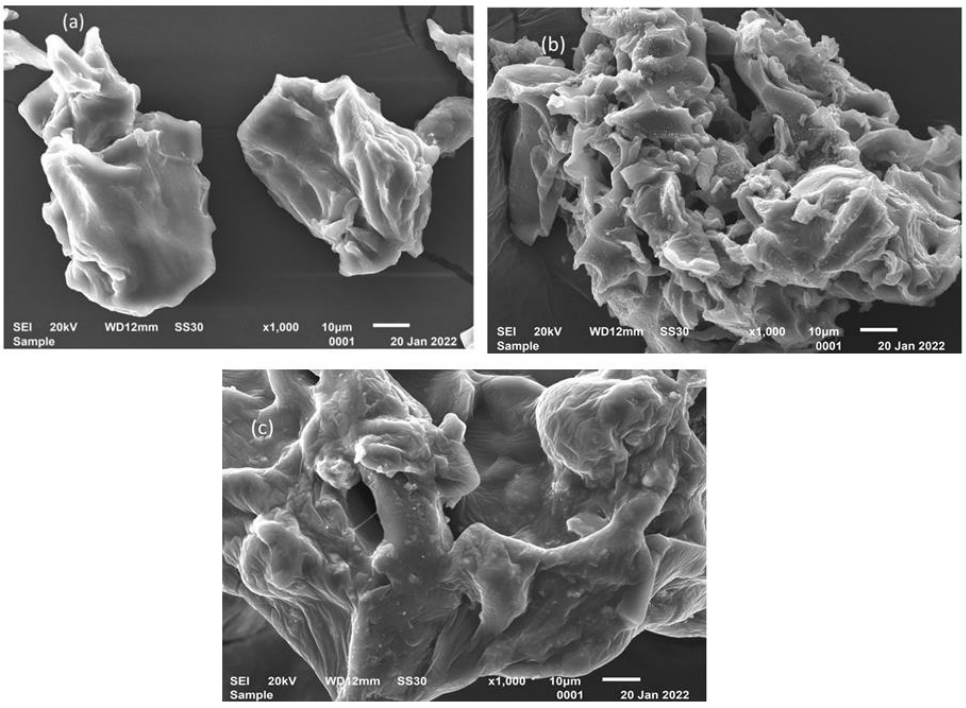

Figure 3.2: Scanning electron micrographs of (a) LB, (b) CMLB and (c) CMLB-*co*-poly(SA)-*cl*-poly(MBA)

3.4.4 FTIR

The peak observed from the FTIR spectrum is compared to previous publications, as shown in figure 3.3. In LB a broad absorption band at 3304 cm^{-1} was observed, indicating an overlapped peak of H-bond due to the -OH present in polysaccharides. The peak at 1375 cm^{-1} confirms the CH_2 bend. Stretch at 1020 cm^{-1} was due to C-O and C-C group present in LB gum pyranose rings [1].

The FTIR absorption peak at 3275 cm^{-1} was observed in CMLB and at 3304 cm^{-1} in LB, but peak intensity is higher in LB than CMLB, may confirms that reduction in the number of –OH groups due to carboxymethylation of LB gum. A peak at 1593 cm^{-1} represents the presence of COO^-, which may confirms the carboxymethylation of LB gum and form CMLB. Other absorption peak at 1406 cm^{-1} and 1014 cm^{-1} are

corresponding to the similar vibrations of LB but a little shift in peaks due to carboxymethylation [26].

In the CMLB-*co*-poly(SA)-*cl*-poly(MBA) hydrogel spectrum, the stretching frequency at 3305 cm^{-1} represents the -OH group (acidic) which may overlapped with the -NH present in the crosslinked structure. Absorptions at 1581 cm^{-1}, 1398 cm^{-1} and 1026 cm^{-1} are similar to CMLB but a little shift in peak absorption frequency confirms the synthesis of the hydrogel by crosslinking of CMLB with poly(SA).

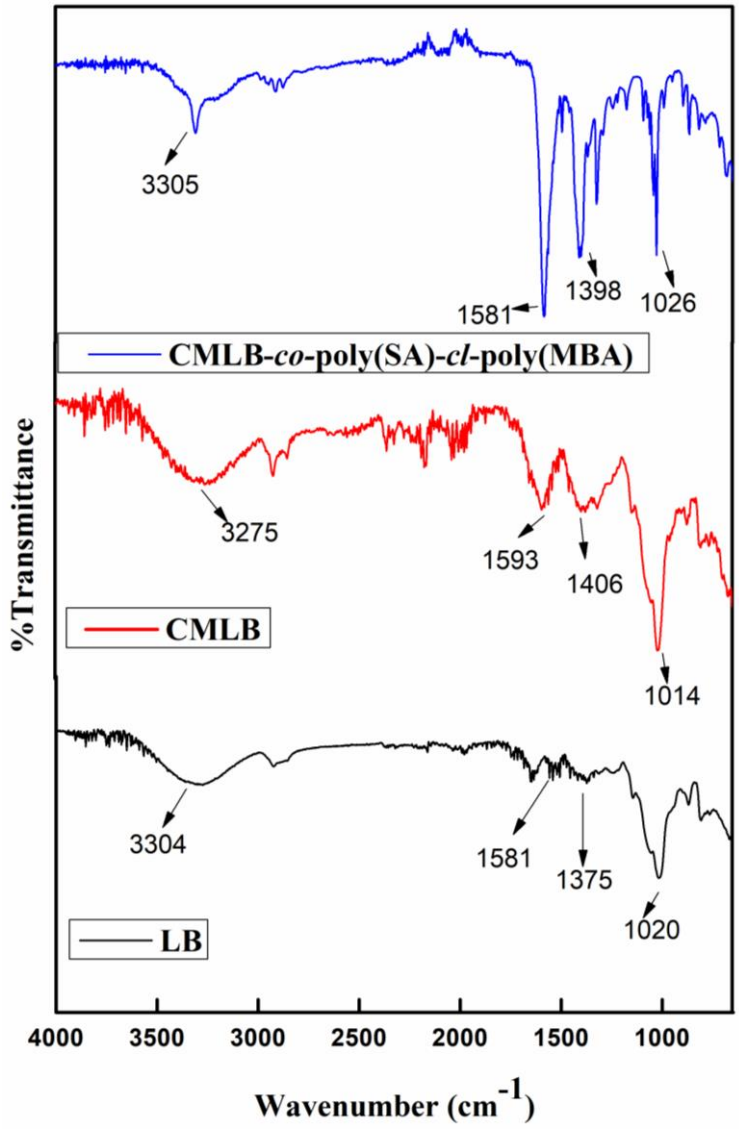

Figure 3.3: FTIR of LB, CMLB and CMLB-*co*-poly(SA)-*cl*-poly(MBA)

3.4.5 ^{13}C-NMR

The solid-state ^{13}C-NMR spectra of LB, CMLB and CMLB-*co*-poly(SA)-*cl*-poly(MBA) hydrogel are shown in figure 3.4. In 3.4 (a) At 101.62 ppm (represents anomeric carbon of polysaccharides), at 95.27 (C-4), 79.90, 75.61, 71.45, 62.51 (C-5, C-3, C-2, C-6) (due to -C- attached to -OH present in polymeric Chain). Peak at 178.95 ppm was due to carbonyl carbon of CMLB. In 3.4 (b) a merged Peak at 72.33 for (C2, C3, C5) ppm due to –C-OH group, confirms carboxymethylation. A peak at 101.35 ppm was due to anomeric carbon of polysaccharides chain. There is shift in the peak in CMLB is due to carboxymethylation. A peak at 62.45 ppm corresponds to C-6.

In fig 3.4 (c), CMLB-*co*-poly(SA)-*cl*-poly(MBA) hydrogel, peaks at 40.69 ppm and 46.99 ppm assigned to -CH of sodium acrylate, a new peak at 60.78 ppm was observed close to the peak of C-6 as in CMLB show that –OH of C-6 participates in graft polymerization. A merged peak at 72.60 ppm corresponds to Carbon 2, 3 and 5 as in CMLB, a little shift in frequency confirmed crosslinking of CMLB with polySA. At 101.97 ppm a low intensity peak was observed, confirmed the presence of anomeric carbon of polysaccharides. It also confirmed the cross-linking of CMLB and polySA. At 185.74 ppm (-COO^- of SA and CMLB), a shift in frequency due to crosslinking of CMLB with SA [27]–[29].

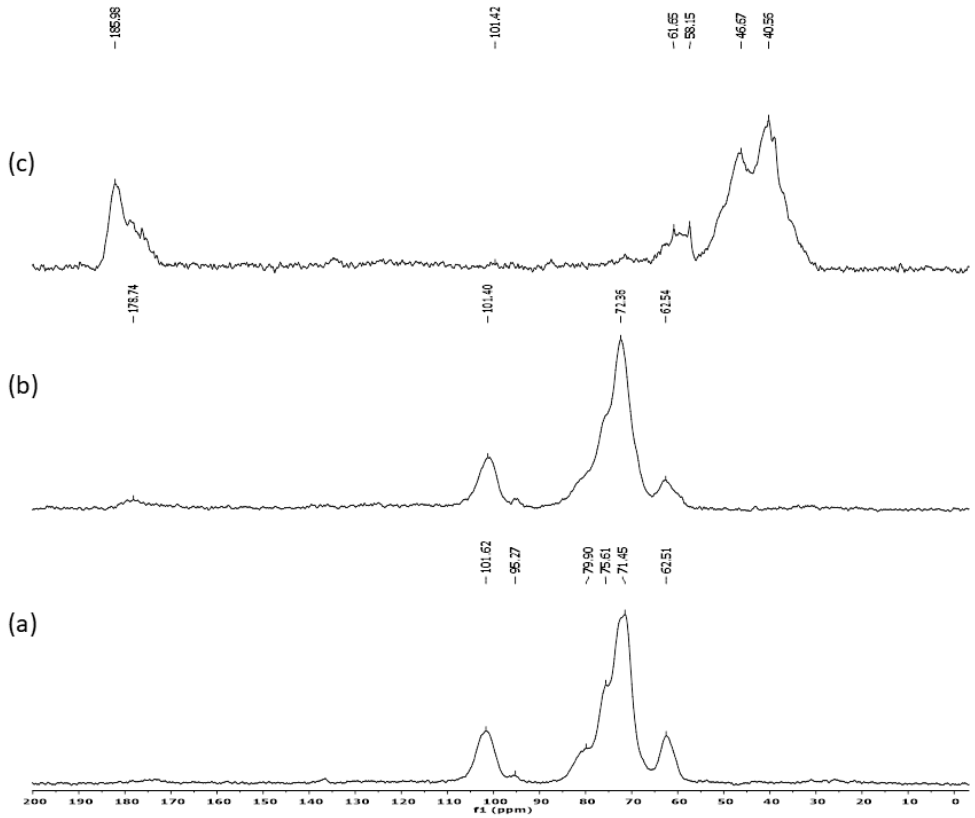

Figure 3.4: ^{13}C-NMR spectra of (a) LB, (b) CMLB and (c) CMLB-*co*-polySA-*cl*-poly(MBA)

3.4.6 TGA

Figure 3.5, represents the thermal degradation of LB, CMLB and CMLB-*co*-poly(SA)-*cl*-poly(MBA) hydrogel. LB demonstrates 3-step weight loss process, with an initial loss of 11% between 25 - 192°C due to the moisture loss. The 79.9 % weight loss was due to decomposition of highly branched heterogeneous structure of LB gum from temperature 192°C to 800°C. Maximum weight loss occurs between 300 °C to 550 °C i.e. 80%. The residual weight of LB gum was about 9.1% [25].

CMLB shown three stages of decomposition, 25-159°C, the first range shows 8.7% moisture loss. The second stage i.e., from 159 to 342 °C which is around 46.5%. It was due to decomposition of polysaccharide chain, elimination of CO_2 and breaking of C-O-C

bond in CMLB chain. 342-800°C range demonstrates weight losses of 32.2% caused by degradation-related random chain scission and 12.6% were residual weight [30].

CMLB-*co*-poly(SA)-*cl*-poly(MBA) hydrogel decomposed in four stages 25-151 °C, 151-300 °C, 300-550 °C, and 550-800 °C. The first decomposition stage has shown 5.3% loss due to moisture content. 11.5% loss represent second stage of the decomposition due to polysaccharide rings along with chain scission with elimination of CO_2. The last two stages represent CMLB backbone and SA chain breakdown with 27.7% and 11.5% weight loss respectively. The residual weight at 800°C was 44% [31]. From the decomposition stages of LB, CMLB and CMLB-*co*-poly(SA)-*cl*-poly(MBA) hydrogel, it was concluded that CMLB gum based hydrogels were more thermally stable than LB gum and CMLB gum.

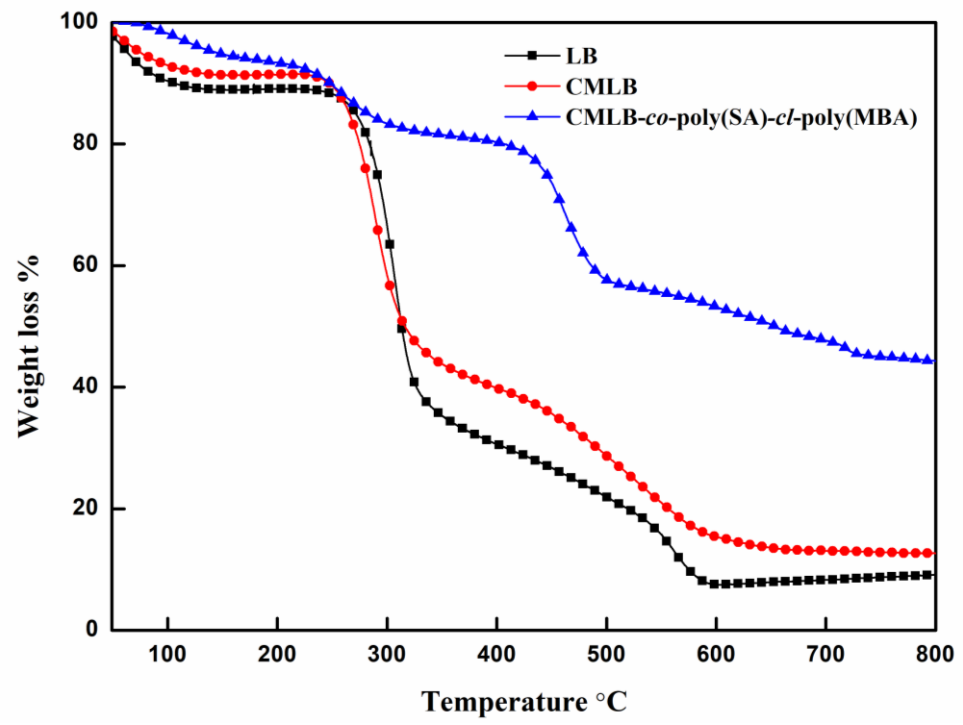

Figure 3.5: TGA of LB, CMLB, CMLB-*co*-polySA-*cl*-poly(MBA)

3.4.7 XRD

Native locust bean gum exhibited a broad peak shown in figure 3.6 at around 2θ= 19.3° but CMLB had a weakened diffraction peak at 19.9°, which was attributed to the carboxymethylation that distorted the structure of LB [28]. While for the cross-linked hydrogel, CMLB-*co*-poly(SA)-*cl*-poly(MBA) a new broad peak was observed which shows that original structure of CMLB was destroyed due to cross-linking between CMLB and SA and thus new structure was generated [32,33].

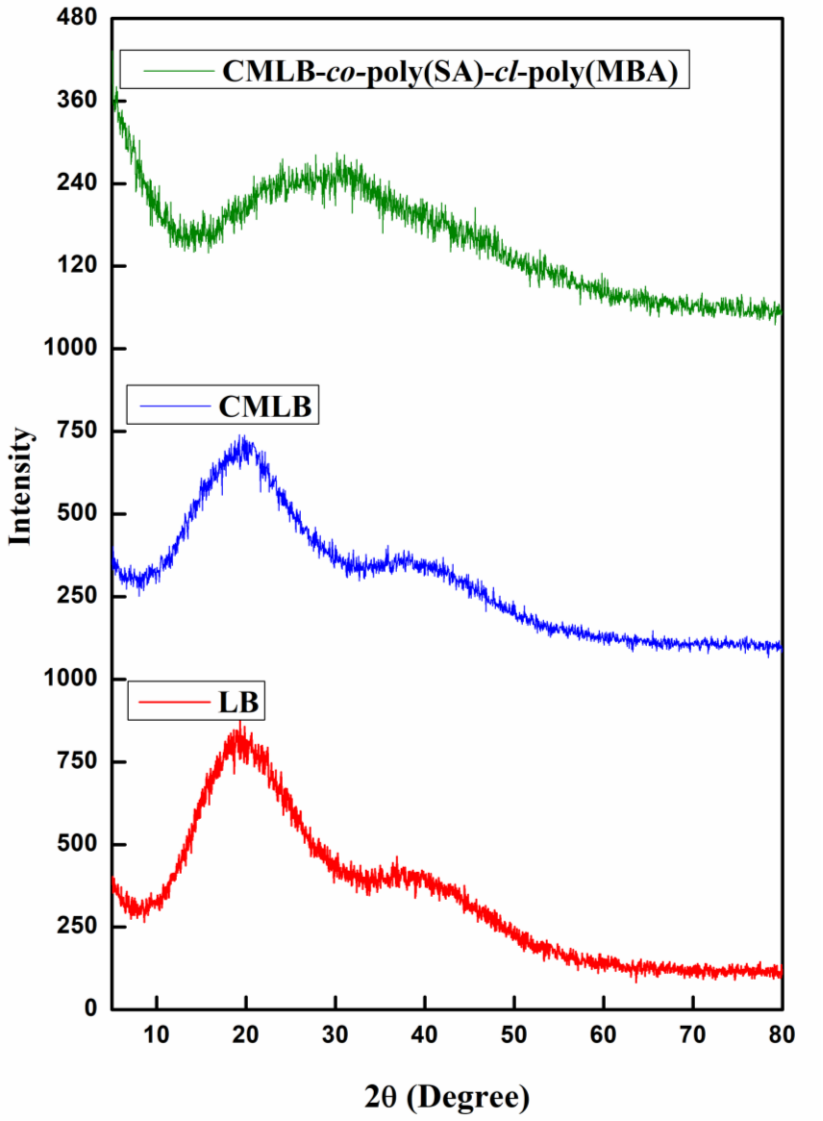

Figure 3.6: XRD of LB, CMLB, CMLB-*co*-polySA-*cl*-poly(MBA)

3.4.8 Rheological Analysis

The rheological analysis of all samples was done by oscillatory sweep test at 25°C, of the loss modulus (G″) and storage modulus (G′) as a function of amplitude and frequency in the linear domain and the determination of flow behaviour by viscosity (η) vs. shear rate plot. Measurements were performed on swollen hydrogel samples at different pH solutions to analyse the effect of pH on the hydrogel strength and flow behaviour.

3.4.8.1 Viscosity

The speed at which intermediate layers moves relative to one another measured by viscosity. During the flow, the material is sheared. This shearing is caused by shear stress, which is the force per unit area required for a material to start flowing. The substance under study is Newtonian if viscosity doesn't vary when the shear rate increases. The material exhibits non-Newtonian behaviour if it changes with the applied shear rate. A typical shear thinning behaviour of hydrogels swollen in three different pH solvent displayed by viscosity as a function of shear rate shown in figure 3.7(a). The initial increase in viscosities with shear rate is due to the hydrogels' ability to resist the flow as a result of their high inter-particle interactions. With an increase in shear rate, the hydrogel showed a steady decrease in shear-dependent viscosity due to a decrease in intermolecular attraction by the microstructural distortion.

3.4.8.2 Amplitude Sweep

Prior to a frequency sweep test, the amplitude sweep test has traditionally been employed just to identify the linear region. The two divided regions of strain were Linear Viscoelastic Region (LVR), a shear region, which was unaffected by applying

stress. The other one is non-linear region. It was observed from figure 3.7(b) that the G' (storage modulus) and G" (lose modulus) values change when the strain exceeds 0.005%, up to which LVR exists. Up to a certain strain, where G" rises, the complex structure resists deformation. The complex structure is completely destroyed by substantial deformation exceeding the critical strain, which is followed by the alignment of the polymer chains with the fluid flow and a reduction in G" [34].

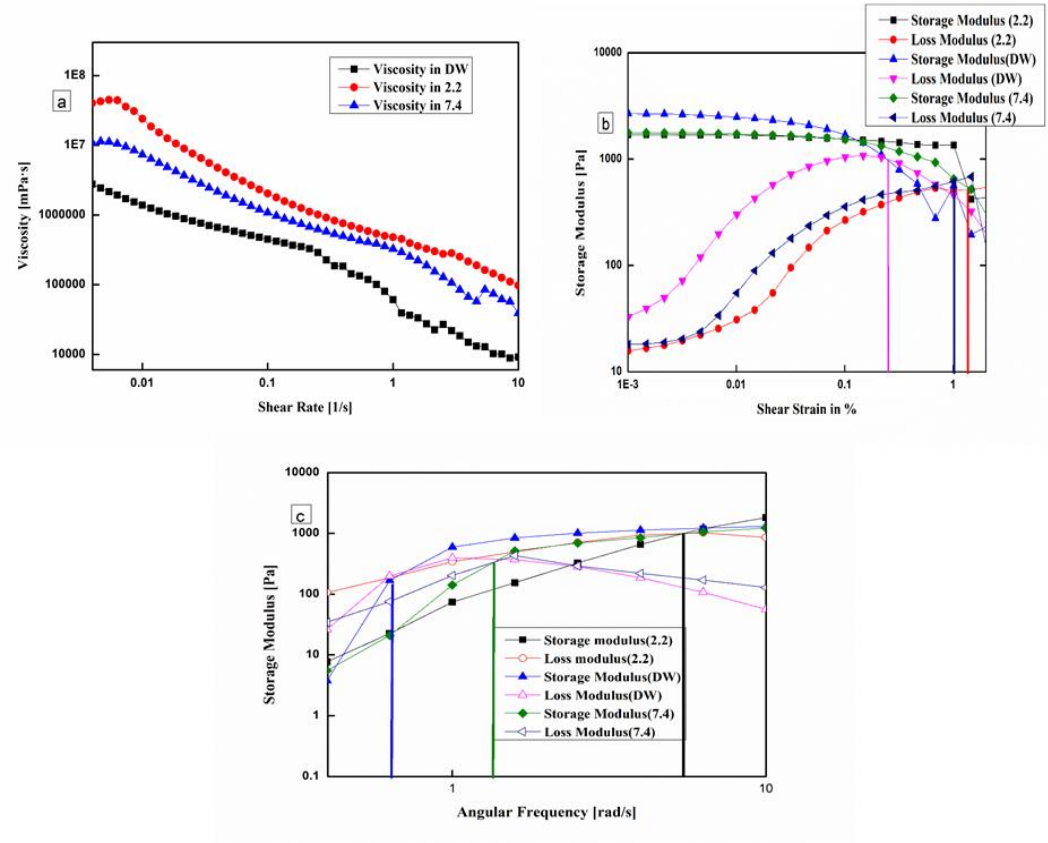

Figure 3.7: (a) Viscosity profile with varying shear rate, (b) Amplitude sweep with LVE and (c) frequency sweep graphs of CMLB-*co*-poly(SA)-*cl*-poly(MBA) hydrogel in buffer solution of pH 2.2, pH 7.4 and DW

3.4.8.3 Frequency Sweep

By increasing the stress percentage, intermolecular interaction is deformed and moduli values are reduced. When G' > G" the sample acts as a viscoelastic solid.

Below 0.005% strain, the structure and shape of swollen hydrogels in pH 2.2 and pH 7.4 buffer solutions were retained, but above 0.005% strain, disentanglement of intermolecular chains. This pattern was not followed by hydrogels swollen in DW. They were continuously deformed from 0.001% strain. The weak intermolecular interaction occurs due to excess of swelling [35].

For this analysis, the frequency ranged from 0.1 to 10 rad s^{-1}. G' and G" were plotted against angular frequency (ω) in figure 3.7(c). The frequency sweep was performed on hydrogel samples swollen in different pH solvents therefore initially at low frequency the swollen hydrogel behave as a solution. Further increase in frequency shows the viscoelastic behaviour of the samples, loss moduli decrease and storage moduli increases at cross-over point. Hydrogel swell more in distilled water and less in pH 2.2 buffer than pH 7.4 buffer thus cause weak networking in DW and strong network in pH 2.2 and crossover point shifts towards at higher frequency in DW and at low frequency in 2.2 pH [36].

3.4.9 Drug loading and Release Profile of Metformin Hydrochloride

Loading of the drug onto the hydrogel matrix was done by using swelling equilibrium method. The EE% of the MFH is found out to be 79.94±0.24% in 2.2 buffer, 90.53±0.096% in 7.4 buffer and 88.33±0.518 % in DW. Release of the drug was also analysed in 2.2 buffer, 7.4 buffer and Distilled water (DW). Release of anti-diabetic drug from drug loaded hydrogel (CMLB-*co*-poly(SA)-*cl*-poly(MBA)) was found to be 73.3±1.8 mg/100mL in 2.2 buffer, 78.46±0.34 mg/100mL in DW and 84.96±1.27 mg/100mL in 7.4 buffer solution. The results represent release of drug, more in pH 7.4 buffer than pH 2.2 buffer solution. The behaviour of the hydrogel for drug release was

similar to the swelling properties of the hydrogel. The pH dependent release can be brought on by the different levels of hydrogen bonding interaction and electrostatic attraction between the two species at various pH values. As the pH level was raised, there was a concurrent increase in both swelling and osmotic pressure within the polymeric network, leading to an enhanced release of drugs at higher pH solution[37]. Singh et al. also observed the fast release of the drug in high pH solution than neutral and low pH solutions.[15] The MFH enters the polymer network and spreads through the aqueous channel to the surface of the CMLB-*co*-poly(SA)-*cl*-poly(MBA) hydrogel and thus sustained release occurs. Dave N.P. et al. also observed the similar results for sustained release of Metformin Hydrochloride by using gum ghatti based hydrogel [38].

The release pattern of the drug was best described by Korsmeyer-Peppas (KP) model according to regression coefficient (R^2) value shown in table 3.3. The diffusion exponent (n) obtained from the KP model (Figure 3.8b) was >0.5, (0.898±0.011 in 2.2 pH buffer, 0.599±0.004 in 7.4 pH buffer and 0.584±0.003 in DW), which indicate that release of the drug from the CMLB-*co*-poly(SA)-*cl*-poly(MBA) hydrogel follows non-fickian diffusion mechanism. Other models results were enlisted in table 3.3.

Table 3.3: Different kinetic models to study drug release behaviour of MFH from CMLB-*co*-poly(SA)-*cl*-poly(MBA)

pH	Zero order		First order		Hixon-crowell		Higuchi		korsmeyer-Peppas		
	R^2	K_o (min^{-1})	R^2	K_1 (min^{-1})	R^2	K_{HC} ($min^{-1/3}$)	R^2	K_H ($min^{-1/2}$)	R^2	K_{KP} (min^{-n})	n
2.2	0.9849	0.055±0.001	0.9847	0.001±0.00	0.9908	0.0002±0.0	0.8841	1.695±0.028	0.9922	0.121±0.101	0.898±0.011
7.4	0.8427	0.070±0.001	0.9941	0.001±0.00	0.9338	0.0004±0.0	0.9743	2.240±0.017	0.9931	1.150±0.029	0.599±0.004
DW	0.8286	0.063±0.00	0.9608	0.001±0.00	0.9744	0.0003±0.0	0.9802	2.031±0.007	0.994	1.153±0.021	0.584±0.003

Through non- fickian diffusion mechanism, the drug was released from the drug loaded samples by the process of diffusion. The drug's diffusion was under swelling control and released in a sustained and controlled manner. The drug continued to release slowly after maintaining a particular concentration. This could be caused by the solvent diffusion into the polymer matrix, which causes the polymer chain to relax and swell.

Furthermore, the drug release profile of MFH (figure. 8a) also confirms the controlled and sustained drug release characteristics of the hydrogel. The water-soluble MFH is released from the polymer sample in a regulated manner as a result of supra-molecular interactions between ionic and non-ionic functional moieties like, -OH, – CH_3COONa and -COOH of CMLB and poly(SA) contained in CMLB-*co*-poly(SA)-*cl*-poly(MBA) hydrogel.

3.4.10 Hemolysis Test

Hemolytic potential of CMLB-*co*-poly(SA)-*cl*-poly(MBA) hydrogel was evaluated and results were plotted against hemolysis in % and concentration in mg/mL as shown in figure 3.8(c). The hemolysis test shown that % hemolysis of blood cells is less than 3 at every concentration. In general, samples with a percentage of less than 5 hemolysis are very hemocompatible and can be used in pharmaceutical application [39].

The results analysed from Hemolysis test show that CMLB-*co*-poly(SA)-*cl*-poly(MBA) hydrogel is very hemocompatible as shown in figure 3.8(c).

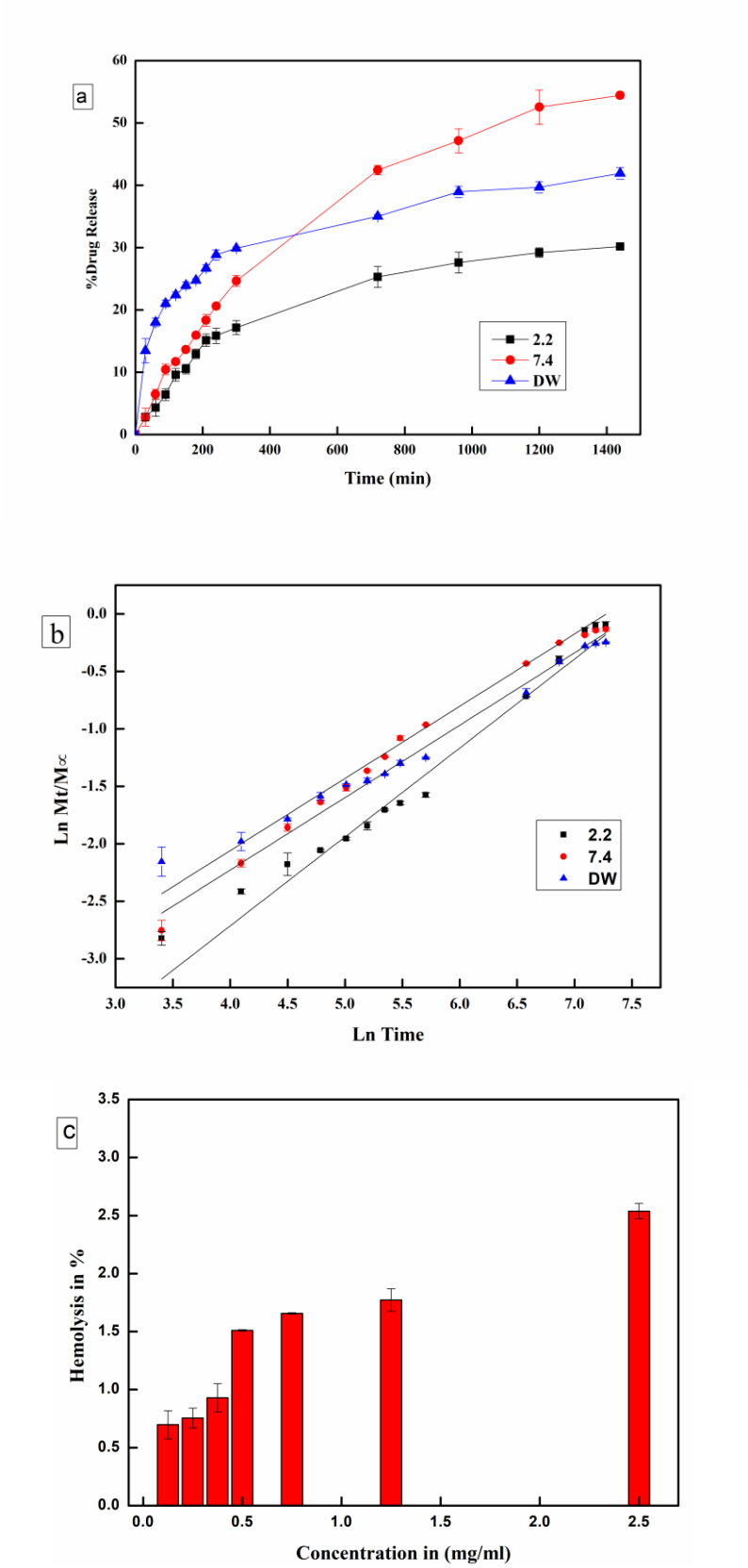

Figure 3.8: **(a) Release profile of MFH from CMLB-*co*-poly(SA)-*cl*-poly(MBA) (b) Graph between ln M_t/M_∞ and ln Time for determination of the rate constant and rate exponent and (c) Hemo-compatability studies**

3.5 Conclusion

The present work reveals the successful development of a Metformin Hydrochloride loaded hydrogel using carboxymethylated locust bean gum. The swelling studies at different pH and temperature, reveals that hydrogel is stimuli sensitive. Increase in the concentration of cross-linker, swelling index decreases. The rheology results shows that viscosity and mechanical strength of the swollen hydrogels are more in pH 2.2 than pH 7.4 buffer solution. The network parameters results also confirm the result of rheology as mesh size of hydrogel is higher and cross-linked density is lesser in pH 7.4 than pH 2.2. The hemolysis test where, hemolysis found out to be less than 3 % confirms the hemocompatibility potential of the hydrogel. Drug release data of loaded hydrogel were fitted to korsemeyer-peppas model and confirms the non-fickian drug release mechanism. The achievement of the work give insightful information regarding use of the CMLB-*co*-poly(SA)-*cl*-poly(MBA) hydrogel for controlled drug delivery carrier.

3.6 References

[1] S. Kaity, J. Isaac, P. M. Kumar, A. Bose, T. W. Wong, and A. Ghosh, "Microwave assisted synthesis of acrylamide grafted locust bean gum and its application in drug delivery," *Carbohydr. Polym.*, vol. 98, no. 1, pp. 1083–1094, 2013, doi: 10.1016/j.carbpol.2013.07.037.

[2] E. Jin, S. Wang, C. Song, and M. Li, "Influences of monomer compatibility on sizing performance of locust bean gum-g-P(MA-co-AA)," *J. Text. Inst.*, vol. 113, no. 6, pp. 1083–1092, 2022, doi: 10.1080/00405000.2021.1915572.

[3] P. Dey, B. Sa, and S. Maiti, "Carboxymethyl Ethers of Locust Bean Gum a Review," *Int. J. Pharm. Pharm. Sci.*, vol. 3, no. 2, pp. 4–7, 2011.

[4] R. S. Singh et al., "Carbamoylethyl locust bean gum: Synthesis, characterization and evaluation of its film forming potential," *Int. J. Biol. Macromol.*, vol. 149, pp. 348–358, 2020, doi: 10.1016/j.ijbiomac.2020.01.261.

[5] S. Maiti, P. Dey, A. Banik, B. Sa, S. Ray, and S. Kaity, "Tailoring of locust bean gum and development of hydrogel beads for controlled oral delivery of glipizide," *Drug Deliv.*, vol. 17, no. 5, pp. 288–300, 2010, doi: 10.3109/10717541003706265.

[6] B. Y. Swamy and Y. S. Yun, "In vitro release of metformin from iron (III) cross-linked alginate-carboxymethyl cellulose hydrogel beads," *Int. J. Biol. Macromol.*, vol. 77, pp. 114–119, 2015, doi: 10.1016/j.ijbiomac.2015.03.019.

[7] F. Martínez-Gómez, J. Guerrero, B. Matsuhiro, and J. Pavez, "In vitro release of metformin hydrochloride from sodium alginate/polyvinyl alcohol hydrogels," *Carbohydr. Polym.*, vol. 155, pp. 182–191, 2017, doi:

10.1016/j.carbpol.2016.08.079.

[8] M. Ubaid and G. Murtaza, "Fabrication and characterization of genipin cross-linked chitosan/gelatin hydrogel for pH-sensitive, oral delivery of metformin with an application of response surface methodology," *Int. J. Biol. Macromol.*, vol. 114, no. 2017, pp. 1174–1185, 2018, doi: 10.1016/j.ijbiomac.2018.04.023.

[9] M. Tanwar, R. K. Gupta, and A. Rani, "Carboxymethylated gum tragacanth crosslinked poly(sodium acrylate)hydrogel: Fabrication, characterization, rheology and drug-delivery application," *Indian J. Chem. Technol.*, vol. 30, pp. 308–319, 2023, doi: 10.56042/ijct.v30i3.70100.

[10] S. Verma and M. Ahuja, "Carboxymethyl sesbania gum: Synthesis, characterization and evaluation for drug delivery," *Int. J. Biol. Macromol.*, vol. 98, pp. 75–83, May 2017, doi: 10.1016/j.ijbiomac.2017.01.070.

[11] S. Kaur and R. Jindal, "Synthesis of interpenetrating network hydrogel from (gum copal alcohols-collagen)-co-poly(acrylamide) and acrylic acid: Isotherms and kinetics study for removal of methylene blue dye from aqueous solution," *Mater. Chem. Phys.*, vol. 220, pp. 75–86, Dec. 2018, doi: 10.1016/j.matchemphys.2018.08.008.

[12] M. F. Akhtar, N. M. Ranjha, and M. Hanif, "Effect of ethylene glycol dimethacrylate on swelling and on metformin hydrochloride release behavior of chemically crosslinked pH–sensitive acrylic acid–polyvinyl alcohol hydrogel," *DARU J. Pharm. Sci.*, vol. 23, no. 1, p. 41, Dec. 2015, doi: 10.1186/s40199-015-0123-8.

[13] A. R. Kulkarni, K. S. Soppimath, T. M. Aminabhavi, A. M. Dave, and M. H. Mehta, "Glutaraldehyde crosslinked sodium alginate beads containing liquid pesticide for soil application," *J. Control. Release*, vol. 63, no. 1–2, pp. 97–105, 2000, doi: 10.1016/S0168-3659(99)00176-5.

[14] Hariyanti, Erizal, E. Mustikarani, I. Lestari, and F. Lukitowati, "In Vitro Release of Metformin HCl from Polyvinyl Alcohol (PVA) - Gelatin Hydrogels Prepared by Gamma Irradiation," *Atom Indones.*, vol. 48, no. 1, pp. 37–43, Apr. 2022, doi: 10.17146/aij.2022.1123.

[15] B. Singh, A. Dhiman, and S. Kumar, "Polysaccharide gum based network hydrogels for controlled drug delivery of ceftriaxone: Synthesis, characterization and biomedical evaluations," *Results Chem.*, vol. 5, no. September 2022, p. 100695, 2023, doi: 10.1016/j.rechem.2022.100695.

[16] H. Bera, S. Mothe, S. Maiti, and S. Vanga, "Carboxymethyl fenugreek galactomannan-Gellan gum-calcium silicate composite beads for glimepiride delivery," *Int. J. Biol. Macromol.*, vol. 107, pp. 604–614, Feb. 2018, doi: 10.1016/j.ijbiomac.2017.09.027.

[17] K. Pal and S. Pal, "Development of porous hydroxyapatite scaffolds," *Mater. Manuf. Process.*, vol. 21, no. 3, pp. 325–328, 2006, doi: 10.1080/10426910500464826.

[18] M. Behrouzi and P. N. Moghadam, "Synthesis of a new superabsorbent copolymer based on acrylic acid grafted onto carboxymethyl Tragacanth," *Carbohydr. Polym.*, vol. 202, pp. 227–235, Dec. 2018, doi: 10.1016/j.carbpol.2018.08.094.

[19] S. M. H. Bukhari, S. Khan, M. Rehanullah, and N. M. Ranjha, "Synthesis and Characterization of Chemically Cross-Linked Acrylic Acid/Gelatin Hydrogels: Effect of pH and Composition on Swelling and Drug Release," *Int. J. Polym. Sci.*, vol. 2015, pp. 1–15, 2015, doi: 10.1155/2015/187961.

[20] B. Singh and B. Singh, "Influence of graphene-oxide nanosheets impregnation on properties of Sterculia gum-polyacrylamide hydrogel formed by radiation induced polymerization," *Int. J. Biol. Macromol.*, vol. 99, pp. 699–712, Jun. 2017, doi: 10.1016/j.ijbiomac.2017.03.037.

[21] M. Suhail, P. C. Wu, and M. U. Minhas, "Development and characterization of pH-sensitive chondroitin sulfate-co-poly(acrylic acid) hydrogels for controlled release of diclofenac sodium," *J. Saudi Chem. Soc.*, vol. 25, no. 4, p. 101212, 2021, doi: 10.1016/j.jscs.2021.101212.

[22] M. R. Jozaghkar, A. Sepehrian Azar, and F. Ziaee, "Synthesis and characterization of semi-interpenetrating polymer network hydrogel based on polyacrylic acid/polyallylamine and its application in wastewater remediation," *Polym. Bull.*, vol. 80, no. 2, pp. 2119–2135, 2023, doi: 10.1007/s00289-022-04162-w.

[23] B. Singh and B. Singh, "Graft copolymerization of polyvinylpyrollidone onto *Azadirachta indica* gum polysaccharide in the presence of crosslinker to develop hydrogels for drug delivery applications," *Int. J. Biol. Macromol.*, vol. 159, pp. 264–275, Sep. 2020, doi: 10.1016/j.ijbiomac.2020.05.091.

[24] W. Hadinugroho, S. Martodihardjo, A. Fudholi, and S. Riyanto, "Esterification of citric acid with Locust bean gum," *Heliyon*, vol. 5, no. 8, p.

e02337, 2019, doi: 10.1016/j.heliyon.2019.e02337.

[25] S. Pandey, J. Y. Do, J. Kim, and M. Kang, "Fast and highly efficient removal of dye from aqueous solution using natural locust bean gum based hydrogels as adsorbent," *Int. J. Biol. Macromol.*, vol. 143, no. 2, pp. 60–75, 2020, doi: 10.1016/j.ijbiomac.2019.12.002.

[26] P. Dey, S. Maiti, and B. Sa, "Gastrointestinal delivery of glipizide from carboxymethyl Locust bean gum-Al3+-alginate hydrogel network: In vitro and in vivo performance," *J. Appl. Polym. Sci.*, vol. 128, no. 3, pp. 2063–2072, 2013, doi: 10.1002/app.38272.

[27] Z. Zhang, P. Chen, X. Du, Z. Xue, S. Chen, and B. Yang, "Effects of amylose content on property and microstructure of starch-graft-Sodium acrylate copolymers," *Carbohydr. Polym.*, vol. 102, no. 1, pp. 453–459, 2014, doi: 10.1016/j.carbpol.2013.11.027.

[28] S. Kaity and A. Ghosh, "Carboxymethylation of Locust bean gum: Application in interpenetrating polymer network microspheres for controlled drug delivery," *Ind. Eng. Chem. Res.*, vol. 52, no. 30, pp. 10033–10045, Jul. 2013, doi: 10.1021/ie400445h.

[29] A. Chakravorty, G. Barman, S. Mukherjee, and B. Sa, "Effect of carboxymethylation on rheological and drug release characteristics of locust bean gum matrix tablets," *Carbohydr. Polym.*, vol. 144, pp. 50–58, 2016, doi: 10.1016/j.carbpol.2016.02.010.

[30] J. Tripathy, D. K. Mishra, A. Srivastava, M. M. Mishra, and K. Behari, "Synthesis of partially carboxymethylated guar gum-g-4-vinyl pyridine and

study of its water swelling, metal ion sorption and flocculation behaviour," *Carbohydr. Polym.*, vol. 72, no. 3, pp. 462–472, 2008, doi: 10.1016/j.carbpol.2007.09.014.

[31] B. Kumar et al., "Nanoporous sodium carboxymethyl cellulose-g-poly (Sodium acrylate)/fecl3 hydrogel beads: Synthesis and characterization," *Gels*, vol. 6, no. 4, pp. 1–11, 2020, doi: 10.3390/gels6040049.

[32] X. Ding et al., "Carboxymethyl konjac glucomannan-chitosan complex nanogels stabilized double emulsions incorporated into alginate hydrogel beads for the encapsulation , protection and delivery of probiotics," *Carbohydr. Polym.*, vol. 289, no. March, p. 119438, 2022, doi: 10.1016/j.carbpol.2022.119438.

[33] H. Tang, Y. Liu, Y. Li, and X. Liu, "Octenyl succinate acidolysis carboxymethyl Sesbania gum with high esterification degree: preparation, characterization and performance," *Polym. Bull.*, vol. 80, no. 4, pp. 3819–3841, Apr. 2023, doi: 10.1007/s00289-022-04218-x.

[34] K. Hyun, S. H. Kim, K. H. Ahn, and S. J. Lee, "Large amplitude oscillatory shear as a way to classify the complex fluids," *J. Nonnewton. Fluid Mech.*, vol. 107, no. 1–3, pp. 51–65, Dec. 2002, doi: 10.1016/S0377-0257(02)00141-6.

[35] G. Stojkov, Z. Niyazov, F. Picchioni, and R. K. Bose, "Relationship between Structure and Rheology of Hydrogels for Various Applications," *Gels*, vol. 7, no. 4, p. 255, Dec. 2021, doi: 10.3390/gels7040255.

[36] S. Wang, H. Tang, J. Guo, and K. Wang, "Effect of pH on the rheological properties of borate crosslinked hydroxypropyl guar gum hydrogel and

hydroxypropyl guar gum," *Carbohydr. Polym.*, vol. 147, pp. 455–463, Aug. 2016, doi: 10.1016/j.carbpol.2016.04.029.

[37] A. Ashames et al., "Development, characterization and In-vitro evaluation of guar gum based new polymeric matrices for controlled delivery using metformin HCl as model drug," *PLoS One*, vol. 17, no. 7 July, pp. 1–20, 2022, doi: 10.1371/journal.pone.0271623.

[38] P. N. Dave, P. M. Macwan, and B. Kamaliya, "Drug release and thermal properties of magnetic cobalt ferrite ($CoFe_2O_4$) nanocomposite hydrogels based on poly(acrylic acid-g-N-isopropyl acrylamide) grafted onto gum ghatti," *Int. J. Biol. Macromol.*, vol. 224, pp. 358–369, Jan. 2023, doi: 10.1016/j.ijbiomac.2022.10.129.

[39] ASTM F 756-13, "Standard practice for assessment of hemolytic properties of materials. Philadelphia," *Am. Soc. Test. Mater.*, pp. 1–5, 2000, doi: 10.1520/F0756-13.

CHAPTER – 4

Essential oils loaded carboxymethylated *Cassia fistula* gum-based novel hydrogel films for wound healing

4.1 Introduction

Skin is the largest organ in the human body and the first line of defense, but it is easily damaged by trauma, surgery and burns, which can cause chronic skin damage [1]. The healing of cutaneous wounds is a very sophisticated process that depends on an integrated effort of several highly regulated factors to restore the wounded skin to its original barrier function [2]. Numerous significant efforts have recently been undertaken to address chronic wounds [3]. Therefore, it is not surprising that wound healing has attracted a lot of interest from both scientific and commercial standpoint [2]. An essential step in promoting wound healing is determining the most appropriate dressings to use for specific types of wounds [4]. The choice of the ideal dressing for wounds is crucial to ensure the speed of healing and prevent microbial infections. The lack of biological functions in traditional dressings makes it difficult to maintain the healing environment of wounds, hindering the effectiveness of existing wound treatment techniques and resulting in high treatment costs. Therefore, it is crucial to create unique dressings with a range of applications [5].

Nowadays, numerous types of materials, both synthetic and natural, are being used to make wound dressings in a variety of physical forms, including typical gauze, oil-based gauze, hydrophilic fibers, semi-permeable membranes, foams, hydrocolloids, dressings incorporating silicone, and hydrogels [6]. Hydrogels are three-dimensional hydrophilic polymeric matrices with high water or bodily fluid

absorbing capacities. Hydrogels made of natural gums have variable swelling characteristics which allow them to become extremely absorbent valuable materials for biomedical purposes [7]. The demand for hydrogel-based wound dressings synthesized from sustainable and plant-based polysaccharide components has grown over the last decade. Due to their widespread availability, affordable cost, water absorption properties, lack of cytotoxicity, excellent biocompatibility, and biodegradability [6–8], they are more suitable for bio-medical applications.

Cassia fistula seed gum is a natural non-ionic polysaccharide extracted from its endosperms. This gum has a linear chain of 1,4-linked mannose residues as the backbone, and1,6-linked galactose residue as short lateral branches [9]. *Cassia fistula* gum has been used in traditional medicine and also in industries for its potential health and commercial applications. It is now well established that the chemical structure of polysaccharide gums can be modified by a chemical reaction called carboxymethylation to enhance their efficiency, stability, flexibility, and water solubility, making them more versatile and functional for different purposes [10]. Natural gum or carboxymethylated natural gum can be cross-linked using chemical and physical techniques to synthesize the hydrogel. A very flexible technique for enhancing the mechanical properties of hydrogels is chemical cross-linking [11].

According to earlier reports, hydrogels are synthesized by mixing or copolymerizing synthetic polyvinyl alcohol [12] with a number of biopolymers or by using carboxymethyl cellulose [13], chitosan [14], gelatin, and collagen. Commonly employed crosslinking agents include epichlorohydrin [15], glutaraldehyde [16], , urea derivatives [17], aldehyde-based reagents [18]. These crosslinking substances are cytotoxic and

environmentally unfriendly [11] therefore demand for natural cross-linkers increasing. Natural cross-linkers offer several advantages, such as biodegradability, biocompatibility, and non-toxicity, and thus suitable for various biomedical applications. The choice of cross-linker depends upon the specific natural polysaccharide used in the hydrogel and the desired properties of the final hydrogel-based product. One of the natural cross-linkers, citric acid (CA), a multifunctional carboxylic acids [19], which is a cost-effective cross-linker with sufficient efficiency [20].

The development of carboxymethylated natural gum-based hydrogel cross-linked with citric acid has recently attracted a lot of attention. It has been noted that after heating, a reaction known as intermolecular esterification will occur between the hydroxyl group (OH) of the polysaccharide and the carboxyl group (-COOH) of CA [21]. The plasticizing effect of glycerol may be attributed to both physical and chemical interactions with the other constituents. The physical interaction between hydroxyl groups of glycerol and polysaccharide; and chemical interaction with carboxyl group (-COOH) of CA [22] undergoing intermolecular esterification, enhancing the mechanical strength of the hydrogel. In polysaccharide-based hydrogels, essential oils are widely included as active components because essential oils are thought to be beneficial for the skin due to their anti-microbial, anti-inflammatory and antioxidant activity. They may also help with various skin issues and promote a healthy complexion [23]. Nevertheless, the practical use of essential oils is constrained due to their inherent instability as fragile volatile compounds. Essential oils are susceptible to degradation when exposed to various physicochemical factors like light, heat, and oxidation. To ensure their long-term biological effectiveness, minimum volatility, enhance utilization efficiency, and enable controlled release, various essential oils are

typically loaded within the hydrogel matrix [24,25]. Wang et al., prepared a carboxymethyl chitosan based wound dressing, which was loaded with three essential oils i.e., Eucalyptus essential oil, cumin essential oil and ginger essential oil and proved to be an effective dressing for skin burn [23].

The aim of this thesis chapter -4 work is to develop a novel essential oils (EO) loaded hydrogel film based on carboxymethylated *Cassia fistula* gum cross-linked with CA. Rosemary essential oil (REO) (*Rosmarinus officinalis*), Turmeric essential oil (TEO) (*Curcuma longa*) and Thuja essential oil (THEO) (*Thuja occidentalis L.*) were used for wound healing application as they possess anti-microbial, anti-inflammatory, antioxidant, and analgesic properties [26–28]. Glycerol is added as a plasticizer in the formulation. Moreover, thermal analysis (TGA), structural characteristics (FTIR and XRD), morphology (SEM), mechanical strength, anti-microbial activity, anti-oxidant activity, bio-degradability test, and cytotoxicity assay/MTT assay (*in vitro*), wound healing studies on Wistar rats (*in vivo)* with histological analysis were done. From the performed tests and assays we concluded that the film can be an effective, biocompatible and biodegradable source of wound healing.

4.2 Experimental

4.2.1 Materials

CCFG (Degree of substitution- 0.4 and with Mol. Wt.-200000-300000 Da) was received as a gift from Hindustan Pvt. Ltd, Bhiwadi, Haryana. CA, $CaCl_2$ and NaCl were purchased from CDH (Central Drug House (P) Ltd.), Delhi, while glycerol was purchased from Fisher Chemicals, UK. Bovine Serum Albumin (BSA) and DPPH were purchased from Sigma Aldrich, India. Rosemary essential oil (REO)

(*Rosmarinus officinalis*), Turmeric essential oil (TEO) (*Curcuma longa*) and Thuja essential oil (THEO) (*Thuja occidentalis L.*) were purchased from Avi Naturals, Delhi (Individual chemical constituents present in all essential oils were explained through GC-MS results attached in supporting file), Delhi. Milli-Q water was used for all experimental procedures. ISO grade (17556) soil was received as a gift from Uflex Pvt. Ltd, Noida, U.P., India. All other chemicals used were of analytical grade.

4.2.2 Preparation of CCFG-CA-EO Hydrogel Film

Food-grade CCFG was used for fabricating the hydrogel-based film for wound healing. CCFG (0.1 g) was dissolved in 10 ml of Milli-Q water. CA (0.1 g) was added as a cross-linker to the homogenous solution of CCFG. The ratio of CCFG to CA was 1:1. Glycerol (0.1 ml) was also added to the homogenized solution. 10µl of each essential oils (REO: TEO: THEO =1:1:1) was added to the hydrogel preparation with constant stirring for 3 h. Following this, sonication was employed to eliminate entrapped air, and the resulting mixture was poured into a petri dish, subsequently left to undergo drying in an oven at 45 °C for the duration of 24 hours. The control hydrogel film (CCFG-CA) was produced by following the identical procedure, without the addition of essential oils. The film synthesized through this process was then subjected to further characterizations.

4.3 Characterization of CCFG, CA, CCFG-CA Film and CCFG-CA-EO Film

4.3.1 FTIR-ATR Spectroscopy

The FTIR spectra were recorded on Perkin-Elmer model 2000 in Attenuated Total Reflectance mode (ATR), in the range of 4000-400 cm^{-1} to perform analysis of

functional groups in CCFG, CA, CCFG-CA film.

4.3.2 X-ray Diffraction Analysis

X-ray diffraction analysis was conducted using a wide-angle X-ray diffractometer (Bruker D8 Advance) with Cu-Kα radiations of λ = 1.5406 Aº. The scanning range was 2θ (5º–80º), and the scan rate was 1º/min, The X-ray diffraction analysis was perfomed at 20 kV and a current of 10 mA.

4.3.3 SEM

Scanning electron microscopy (SEM) (JEOL JSM-6610LV) was utilized to examine the surface morphology of the samples at 2500X magnification under an accelerating voltage of 20 kV.

4.3.4 TGA

To determine the thermal stability of the samples, PerkinElmer thermo-gravimetric analyzer, TGA 4000 was used. 4 mg of the samples were heated in an N_2 atmosphere from 25 ºC to 800 ºC at a heating rate of 10ºC/min.

4.3.5 Mechanical Properties of the Film

The mechanical properties of the CCFG-CA and CCFG-CA-EO films were analyzed using a Universal Testing Machine (LLOYD LR 5K). The load range was 1-50 N, with a 1000 mm extension range and a 25 mm gauge length. The test and approach speed were 500 mm/min with no preload. A strip measuring 15 mm in width and 150 mm in length was cut from each film for mechanical testing. Under air conditions, four readings were taken for each sample and the average result was evaluated to

determine the mechanical properties of the film.

4.3.6 Swelling Studies

The swelling equilibrium method was used to analyze the network of hydrogel in both Distilled Water (DW) and Stimulated Wound Fluid (SWF), a pH 8 buffer solution. 1 × 1 cm of CCFG-CA films with 50µm thickness was dried and weighed, immersed in 10 ml of solvents (DW and SWF). After every 60 minutes up to 8 hours, then after 24 hours the films were taken out from the swelling medium, excess fluid was removed using tissue paper, and the films were weighed again until a constant weight was achieved. The swelling studies were done in triplicate. The swelling index (SI) was calculated using equation 1 [29].

$$SI\% = \frac{Ws - Wi}{Wi} X\ 100 \quad (1)$$

Where, *Ws* is weight of the swollen CCFG-CA film and *Wi* is the initial weight of the CCFG-CA film before swelling.

4.3.7 Antioxidant Activity

A UV-vis spectrophotometer (UV-1800 SHIMADZU) was used to evaluate the antioxidant activity of the hydrogel solution by DPPH free-radical scavenging [30]. A modified method based on a previous study was used to determine the photochemical stability, in which (1.00 mg/mL) of CCFG-CA-EO film in ethanol were prepared at 37°C [31]. Equation-2 was used to determine the percentage of DPPH scavenging activity after mixing 1 mL of the solution with 3 mL of ethanol solution containing DPPH (1mg/20mL) and incubating it in the dark for 30 min at room temperature. The absorbance was measured at 517 nm.

Scavenging Activity of DPPH (%) = $\left(1 - \frac{Asample}{Acontrol}\right) x\ 100$ (2)

The value of $A_{control}$ indicates the absorbance of 1mL ethanol and 3mL of DPPH solution, while A_{sample} refers to the absorbance of 1mL CCFG-CA film (powdered) in 3mL DPPH solution, as stated in prior research [32,33].

4.3.8 Cytotoxicity Evaluation by MTT Assay

The cytotoxicity of the films using the HaCaT cell line was assessed using the MTT ("3- (4,5-dimethylthiazol-2-yl)-2,5-diphenyltetrazolium bromide") assay [34]. Initially, HaCaT cells were seeded in a 96-well plate with Dulbecco's Modified Eagle Medium (DMEM) medium supplemented with 10% Fetal Bovine Serum (FBS) and 1% antibiotic solution, reaching a density of approximately 8000 cells per well. The plate was then incubated at 37°C with 5% CO2. After 24 hours, cells were exposed to varying concentrations of the film (ranging from 0.75% to 5%), prepared in an incomplete medium. After incubation for 24 hours, MTT Solution (a final concentration of 250µg/ml) was added to cell culture and further incubated for 2 hours. At the end of the experiment, culture supernatant was removed and cell layer matrix was dissolved in 100 µl Dimethyl Sulfoxide (DMSO) and read in an Elisa plate reader (iMark, Biorad, USA) at 540 nm and 660 nm.

4.3.9 In vivo Wound Healing Studies

Wistar rats of either sex aged 2-3 months and weighing between 250-300g were selected for this study. The experimental protocol was approved by the Institutional Animal Ethics Committee of Delhi Pharmaceutical Sciences & Research University (DPSRU) and registration No. is 215/GO/ReBi/S/2000/CPCSEA. To prepare for the

experiment, the rats were sedated by inhaling an appropriate volume of diethyl ether in a saturated chamber. The sedation will be administered prior to inducing a wound. A specific area measuring approximately 2 cm in diameter, located behind the neck on the dorsal side, was selected and marked as the wound site. Using a hair clipper, the hair in this marked area was carefully removed. Subsequently, the shaved area was sterilized with a 70% v/v ethanol solution. To create the wound, a circular incision was made using a scalpel, resulting in a full-thickness excision wound that extends through the subcutaneous tissue. Once the wound site is cleaned of any blood and exudates, hydrogel films infused with and without essential oils were applied. These films were then secured in place by covering them with adhesive tape. In the control group, the wound was left untreated, providing a basis for comparison when evaluating the healing process [23]. Wound closure % was calculated by using equation 3.

$$\text{Wound closure } \% = (1 - \text{open wound}/\text{initial wound}) * 100 \quad (3)$$

Note-Diameter of the wound was measured for calculation of wound closure.

4.3.10 Histological Studies

During the in vivo studies, wound size measurements were recorded on the 0^{th}, 4^{th}, 7^{th} and 14^{th} day. However, tissue samples were excised on 4^{th}, 7^{th} and 14^{th} day for further analysis. To facilitate the sample excision, animals were euthanized using diethyl ether inhalation. The tissue samples were then obtained from the wounded area and subjected to histopathological examination. To preserve the tissue structure for analysis, the excised tissues were fixed in 10% buffered formalin. The formalin-fixed tissues underwent a series of processing steps, including dehydration, wax impregnation, and the creation of blocks using paraffin. Subsequently, thin sections

(3–5 µm thick) were obtained from the processed tissues using a microtome. For a detailed examination of cellular and structural changes, the obtained sections were stained with hematoxylin and eosin. This staining method allows for the visualization of nuclei in a deep blue-purple color (hematoxylin) and cytoplasm and extracellular matrix in a pinkish hue (eosin). Histological evaluations of these stained samples were then conducted to analyze and compare the effects of various treatments on the observed changes in the tissue [35].

4.3.11 Degradation Studies

To assess the ecological compatibility of the synthesized natural polymeric network, CCFA-CA hydrogel film, its biodegradability was investigated through soil burial method over a period of 15 days. Following the procedure outlined by K. Kaur et al., the samples were buried in soil (according to ISO 17556 standard) at a depth of 2 cm below the surface [36]. To ensure a consistent moisture level, water was periodically added to the soil container. Every 7 days, a sample was retrieved from the container, rinsed to eliminate soil residues, and subsequently dried at 50 °C in a hot air oven. The degree of degradation (DOD) at each stage was calculated using equation 4.

$$\% DOD = \frac{Wi - Wd}{Wi} * 100 \quad (4)$$

Where, *Wi* is the initial weight of the CCFG-CA film and *Wd* is the weight after every 7 days. Degradation confirmation during 15 days of CCFG-CA hydrogel film was evaluated through weight reduction and observing the visual changes in the film. The alteration in chemical structure and bond breakage was deduced by comparing TGA spectrum of film (degraded CCFG-CA) on 10^{th} day of decomposition with CCFG-CA.

4.3.12 Permeability Tests

4.3.12.1 Microbial Permeability Test

The microbial permeability test was conducted to determine the barrier characteristics of CCFG-CA-EO hydrogel film to microbial penetration. This was achieved by monitoring microbial growth (indicated by turbidity) within glass vials containing sterile nutrient broth. The hydrogel film (CCFG-CA-EO) was tied to vials containing 10 mL of nutrient broth and exposed to the surrounding environment for 48 h. For control, an open test tube containing nutrient broth was taken. The presence of any turbidity in the nutrient broth indicated potential microbial contamination.

4.3.12.2 Water Vapour Transmission Rate (WVTR)

The water vapour transmission rate of the polymeric CCFG-CA and CCFG-CA-EO hydrogel film was conducted in accordance with the procedure outlined in ASTM E 96-95 [37]. To evaluate water vapour penetration, a modified dry cup method was followed. For this, 5g of anhydrous $CaCl_2$ was placed separately in three vials (with a testing area of approximately 2.54 ± 0.05 cm^2). Two vials were sealed with test films CCFG-CA and CCFG-CA-EO and third vial remained open. These vials were then placed in a desiccator containing a saturated NaCl solution and placed in an oven at 37°C. After 24 h all the vials were weighed and water vapour permeability is determined in terms of WVTR using the equation 5 [38]. The experiment was performed in triplicate.

$$\text{WVTR} = \left[\frac{\Delta m}{A}\right] * \text{T} \quad (5)$$

WVTR is the water vapour Transmission Rate ($g/m^2.day$)

Δm represent the change in mass due to water vapour absorption in (g)

T represents time i.e., 24 h

A is the exposed surface area of the material in (m^2).

4.3.13 Protein Adsorption Test by using Bradford reagent

The protein adsorption by the hydrogel film was evaluated using Bovine Serum Albumin (BSA) as the model protein. The evaluation procedure used in this study was adapted from previous research literature [39]. BSA was dissolved at a concentration of 5% w/v in pH 7 PBS buffer.

To conduct the test, 10 mL of the protein solution (BSA) (2mg/mL) was added to hydrogel films measuring 1×1 cm in a petri dish. The samples were placed at 37°C for 24 h in an orbital shaker operating at 200 rpm. After 24 hours samples were removed from the protein solution and 100 µL of the left BSA protein solution was added with 1 ml of Bradford reagent and 2 ml distilled water. The protein concentrations were determined using a UV Spectrophotometer(UV-1800 SHIMADZU) at 595 nm and compare with the previously plotted calibration curve for BSA[40,41].

4.4 Results and Discussion

4.4.1 Synthesis of CCFG based hydrogel film

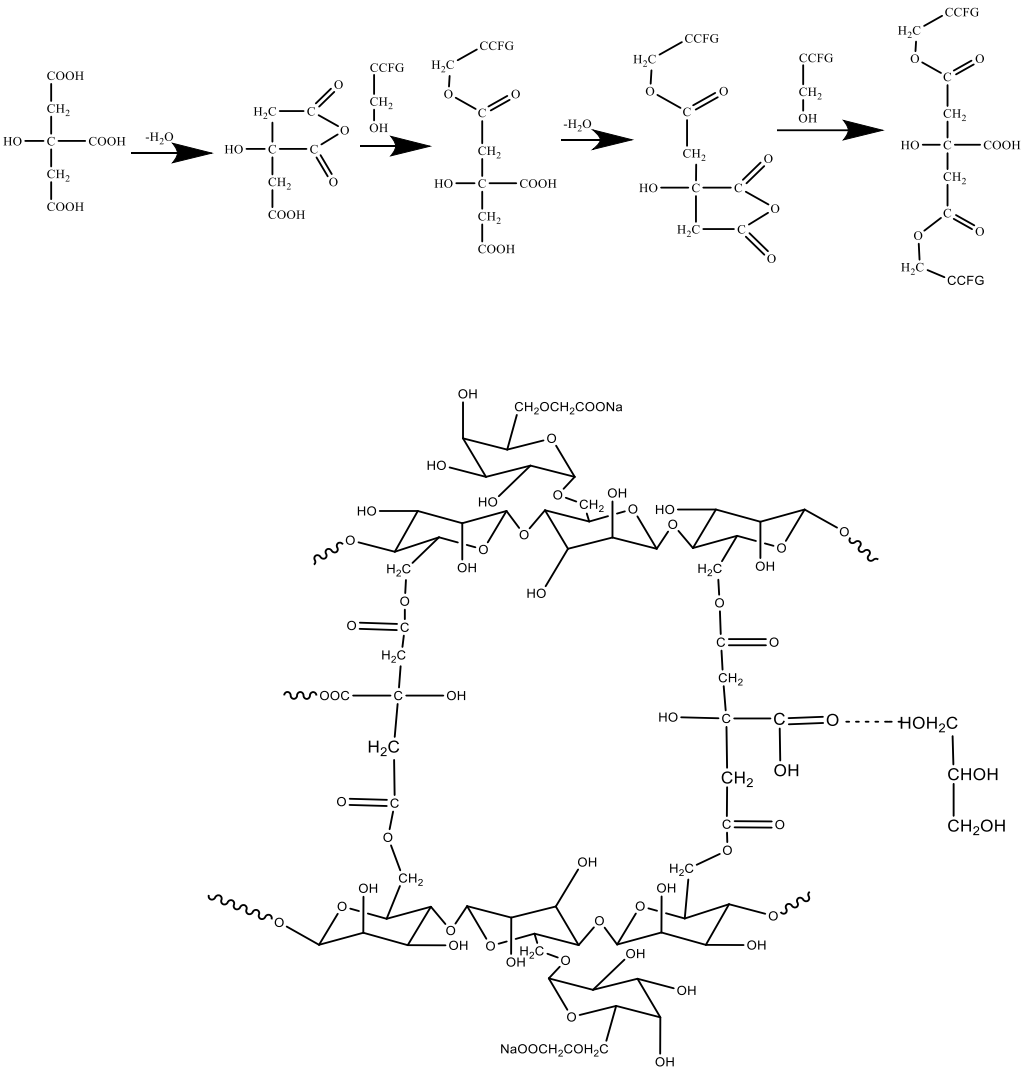

Scheme 4.1: Esterification reaction among CCFG and CA with possible Cross-linked structure

The concentration of citric acid was optimized at 0.1% w/v for the cross-linking of CCFG in order to produce a hydrogel film. Optimization studies have shown that a 5 min curing treatment at a curing temperature of 140 °C is essential to obtain a hydrogel film that has good matrix integrity. Glycerol was added to the formulation to enhance the film flexibility and the tensile strength. Glycerol, being a compact hydrophilic molecule, has

the ability to integrate between chains of polysaccharides, thereby serving as a plasticizer. This results in an increase in the gaps between polysaccharide chains, leading to a reduction in direct interactions within the cross-linked network [22].

Esterification reactions are responsible for the formation of cross-links between citric acid, glycerol and CCFG. It is possible due to the presence of the primary –OH group present in CCFG, and Glycerol and –COOH group present in CA. The possible esterification reaction is given in Scheme 4.1. When citric acid is heated to high temperature, a series of intermediate anhydrides form causing the cross-linked structure with CCFG. The cyclic anhydride formed through esterification allows the polysaccharide -OH functional group to interact, resulting in the formation of a new intra-molecular anhydride moiety with the adjacent -COOH [42,43].

4.4.2 FTIR

The FTIR spectrum of CCFG is shown in Figure 4.1. The broad peaks at 3288 cm^{-1}, 1591 cm^{-1}, 1409 cm^{-1}, and 1022 cm^{-1} are due to –OH stretching, COO^- stretching vibrations, CH_2 scissoring, and C-O-C stretching vibration, respectively. Sittikijyothin W et al., also observed the same spectra for carboxymethylated *Cassia fistula* gum [44]. In the CA spectra, the peak at 3531 cm^{-1} corresponds to –OH stretch. The peaks at 1678 cm^{-1}, 1388 cm^{-1}, and 1018 cm^{-1} correspond to –C=O stretch, -CH_2 bend, and –C-OH stretch respectively [45]. The peak at 3375 cm^{-1} corresponds to –OH stretch present in the polysaccharide rings, and 2915 cm^{-1} represents the presence of –CH_2, The CA cross-linked film shows the ester bond formation between the cyclic anhydride of CA and -OH groups of CCFG at 1713 cm^{-1}, while 1023 cm^{-1} corresponds to C-O-C stretching vibration.

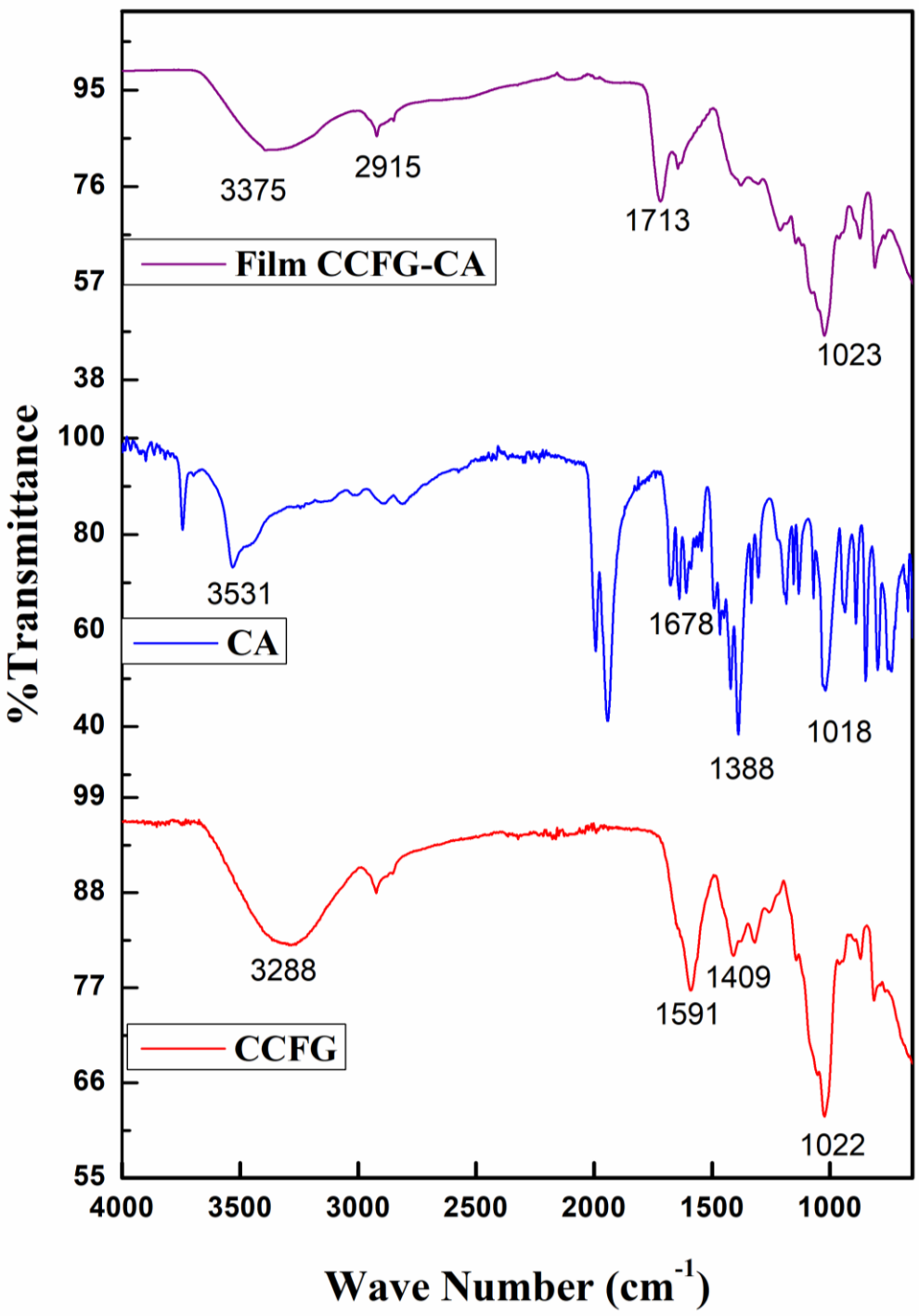

Figure 4.1: FTIR Spectra of CCFG, CA and CCFG-CA film

4.4.3 XRD

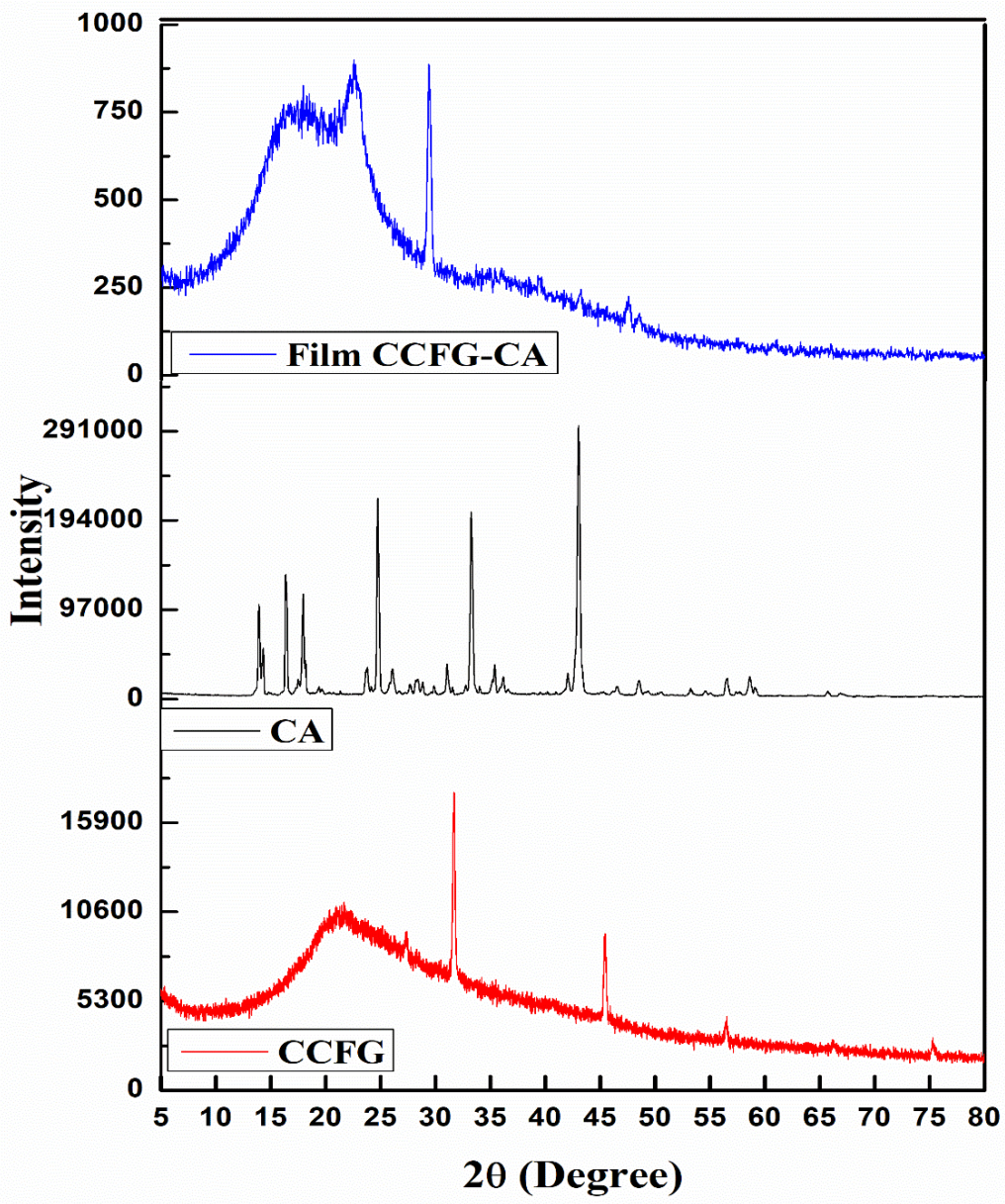

Figure 4.2: XRD pattern of CCFG, CA and CCFG-CA film

In figure 4.2, the XRD pattern of CA includes main peaks at 14°, 16°, 18°, 24.7°, 33° and 43° on the degree scale. However, these peaks are not present in the CA cross-linked CCFG hydrogel film, indicating that the crystalline structure of CA after crosslinking gets convert into an amorphous structure of hydrogel film. Crosslinking

was further confirmed by the shift in the peaks present in the XRD pattern of CCFG. Specifically, there was a shift from a broad peak at 21.2° and two sharp peaks at 31.8° and 45.5° to a broad peak at 22.5°, and a sharp peak at 29.3° in the CCFG-CA hydrogel film. The same results were observed by Huanbutta K et al. [9].

4.4.4 SEM

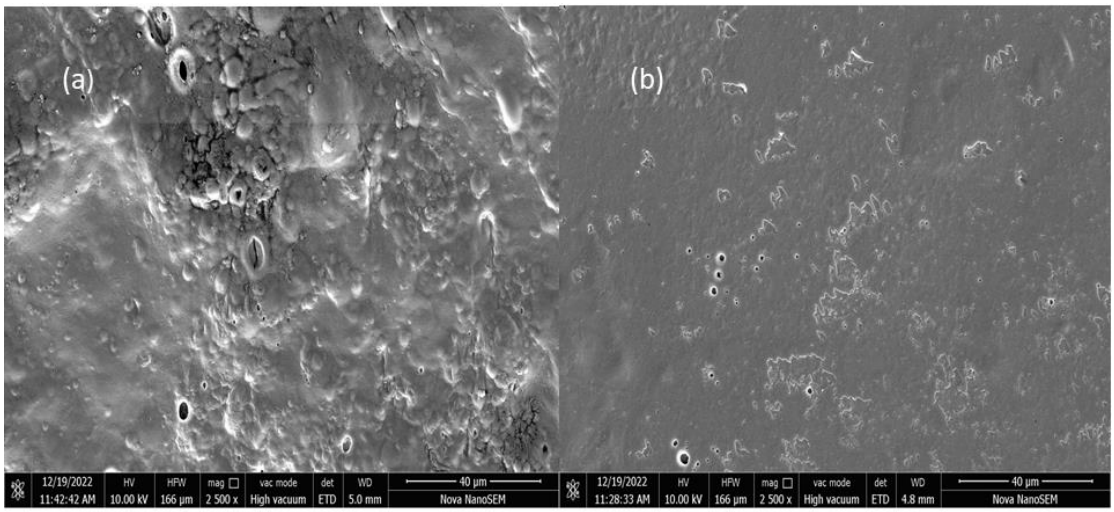

Figure 4.3: SEM at 2500X (a) CCFG-CA and (b) CCFG-CA-EO

SEM of CCFG-CA at 2500 X shows that it has more porous structure and also has homogeneity in the structure. The porous nature of the film allows the essential oils to be entrapped in the pores of the hydrogel film, which is crucial because it increases oxygen concentrations in injuries. These oxygen concentrations are required for various cell activities such as phagocytosis, mitosis, and the release of growth factors essential for damage repair [46]. SEM of CCFG-CA-EO film is given in figure 4.3(b). It has a dense and compact structure. This represents that the essential oils were incorporated in the voids present in the film, thus showing a compact structure.

4.4.5 TGA

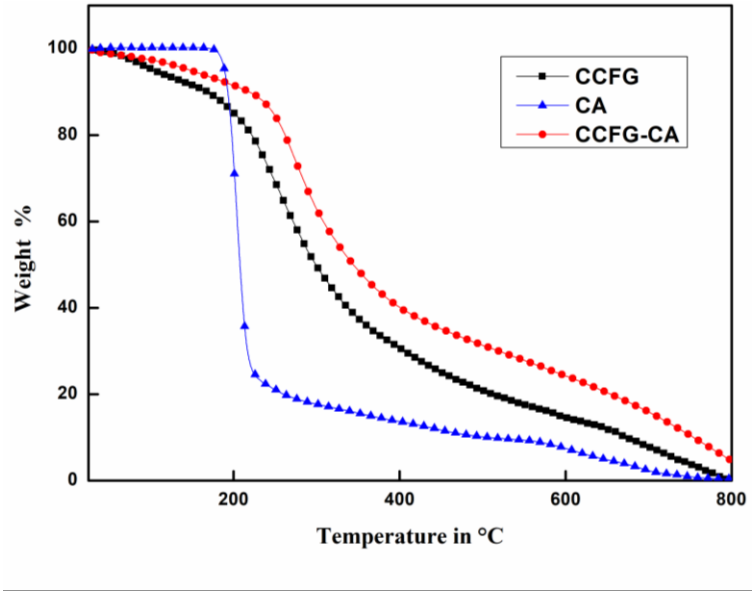

Figure 4.4 TGA of CCFG, CA and CCFG-CA film

Thermo-gravimetric analysis represents a weight loss of 82% between 171 °C and 240 °C, indicating the decomposition of CA crystals (fig. 4). Complete degradation, i.e., 100% occurs up to 800 °C [45]. CCFG shows a two-step process of decomposition. Firstly, up to 100 °C, there is a loss of moisture. Further, up to 630 °C there is a breakdown of the polysaccharide backbone. It shows complete degradation up to 800°C with no residue. CCFG-CA film shows a loss of moisture up to 125 °C. Afterwards, raised temperature causes the breakdown of the glycerol structure around 290 °C [47] and cross-linking between gum and citric acid. The film shows more stability over gum with a residue of 4.5% [48].

4.4.6 Mechanical Testing

Table 4.1, shows the results of mechanical testing for CCFG-CA and CCFG-CA-EO films. The CCFG-CA and CCFG-CA-EO films were found to be 50µm and 55µm

thick, respectively. The maximum load CCFG-CA could hold was 49.90 N, while CCFG-CA-EO could hold up to 54.1 N. The tensile strengths of CCFG-CA and CCFG-CA-EO were 39.4±0.54 MPa and 38±1.57 MPa, respectively. The results show that the tensile strength of the prepared essential oils loaded hydrogel film i.e., CCFG-CA-EO is less than the control hydrogel film, CCFG-CA. The tensile strength and elongation at break (%) can be affected by numerous factors, including the type and ratio of polymers, plasticizers, and other additives, along with their interaction with one another [49]. Chuysinuan et al, also observed the same results for gelatin based hydrogel loaded with essential oil [50].

Table 4.1: Mechanical properties of the hydrogel films

Film	Max Force(N)	Tensile Strength (MPa)	Elongation at Break (%)
CCFG-CA	49.9±0.15	39.4±0.54	9.1±0.25
CCFG-CA-EO	54.1±0.12	38±1.57	8.66±0.57

4.4.7 Swelling Studies

Swelling of the hydrogel films has been observed in distilled water (DW) and stimulated wound fluid (SWF). The results from the swelling studies have been shown in figure 4.5 and table 4.2. The hydrogel initially experienced rapid swelling, followed by a slower rate of swelling until it reached equilibrium swelling after 24 h at 37°C [51]. Subsequently, the porous network of the hydrogel became fully saturated with water, preventing further absorption of water. Similar results were observed in the SWF, but greater swelling was noted in the DW compared to SWF. This is primarily due to the presence of ions, which induced ionic repulsion between -COO^- groups, and resulted in an expansion of the mesh size. Baljit et al., also observed similar results for the swelling index of hydrogel films [52].

Table 4.2: Mechanical properties of the hydrogel films

Time	Swelling Index (DW)	Swelling Index (SWF)
60	0.84±0.09	0.74±0.03
120	1.07±0.02	1.02±0.01
180	1.21±0.02	1.15±0.01
240	1.40±0.02	1.27±0.01
300	1.54±0.03	1.41±0.02
360	1.69±0.03	1.54±0.00
420	1.82±0.03	1.61±0.00
480	1.95±0.03	1.72±0.03
1320	2.40±0.00	2.07±0.01
1380	2.51±0.03	2.17±0.03
1440	2.52±0.03	2.18±0.01

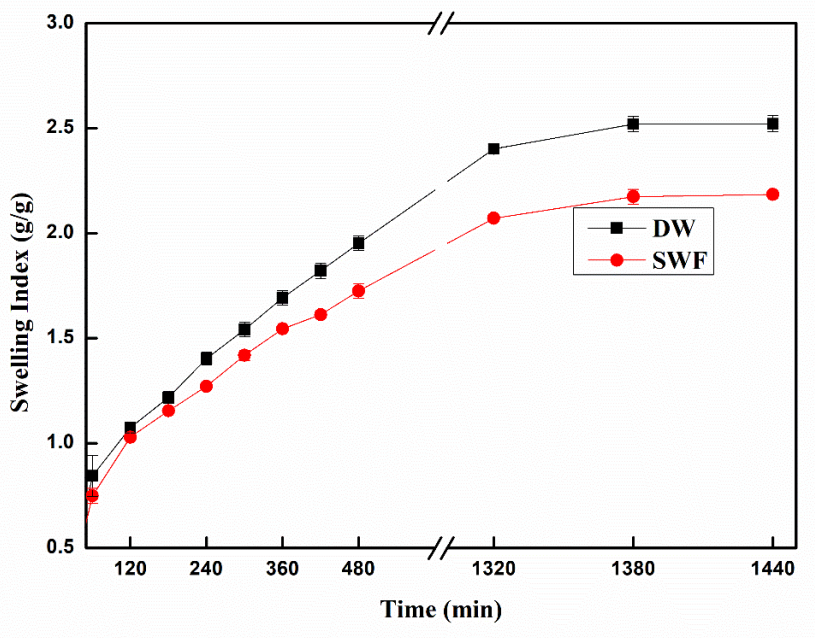

Figure 4.5: Swelling studies of hydrogel films

4.4.8 Antioxidant Activity

During the wound repair process, the body's antioxidant capacity plays a crucial role. In the initial inflammatory phase, a controlled amount of reactive oxygen species is generated to defend against invading pathogens and facilitate intracellular signalling.

In our study, we aimed to explore the antioxidant properties of CCFG-CA-EO hydrogel film. One commonly used method to assess antioxidant activity is the DPPH assay, which involves measuring the ability of a substance to neutralize DPPH, a type of free radical. This neutralization causes a change in the colour of the solution [3,53].

CCFG-CA-EO was tested to evaluate their antioxidant activity by analyzing the reduction of DPPH radicals. The absorbance (A) of control was recorded at λ_{max} 517 nm and found to be 0.914. The scavenging percentage of CCFG-CA-EO was found out to be 86.18% at concentration 1.00 mg/mL as shown in table 4.3. Antioxidants can reduce DPPH free radicals by donating hydrogen, which is essential to prevent the harmful role of free radicals in various disorders, including chronic wounds. The results suggest that all the CCFG-CA-EO samples exhibit antioxidant properties or radical scavenging activity due to their hydrogen donating or electron transfer ability.

Table 4.3: Percentage radical scavenging activity

Samples	Absorbance (after 30 min)	Percentage scavenging activity (%)
Control (DPPH+Ethanol)	0.914	0
CCFG-CA-EO (1.00 mg/mL)	0.126	86.18

4.4.9 MTT Assay

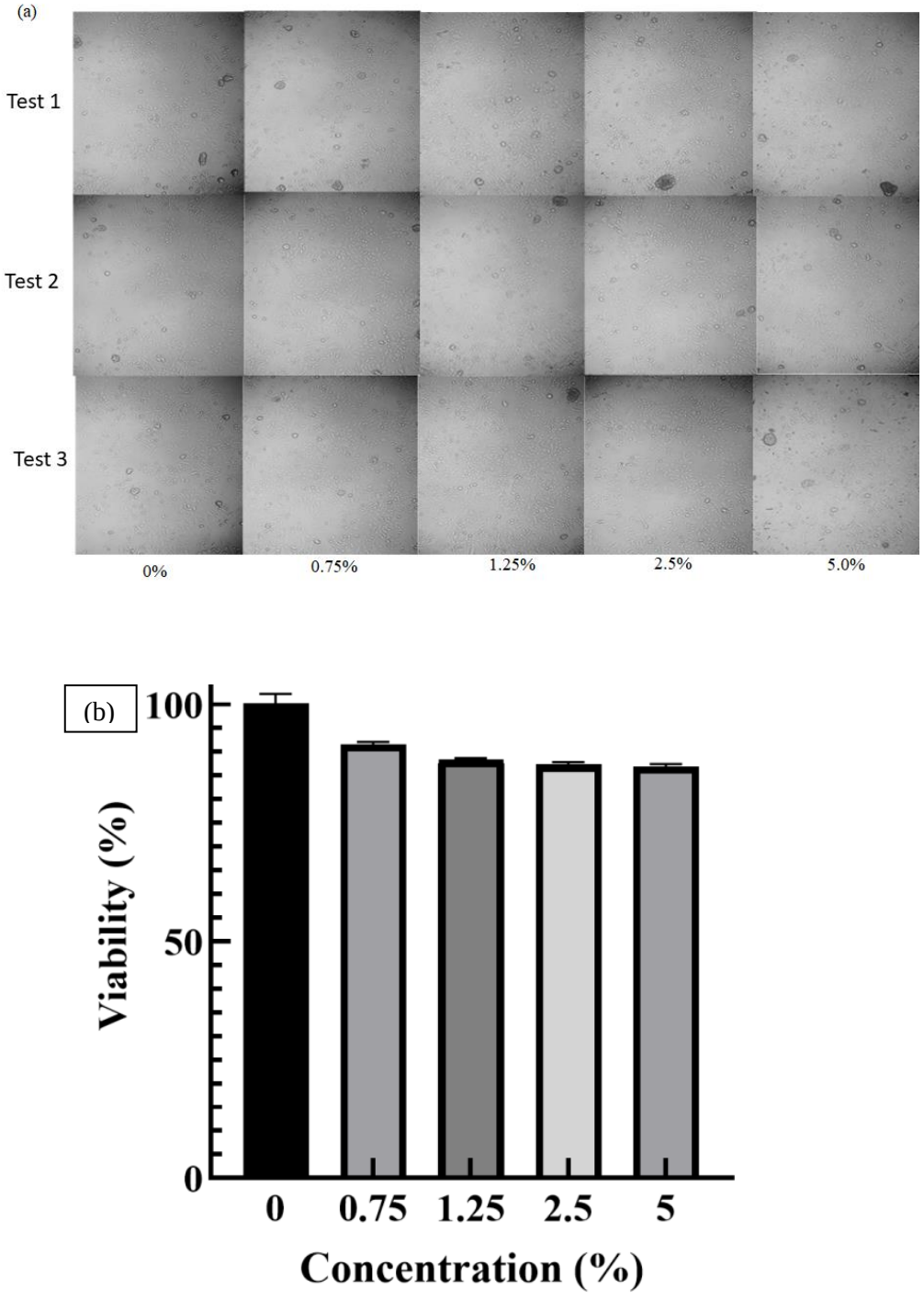

Figure 4.6: (a) HaCaT cell lines proliferation and (b) cells viability % respectively at different concentration of CCFG-CA-EO

HaCaT cell lines were used as a model cell line to evaluate the cytocompatibility of CCFG-CA-EO films. The cytotoxicity results for various concentrations are shown in Figure 4.6(a) and 7(b). It was observed that the cells were able to adhere to the film surfaces, spread, and proliferate, as shown in figure 4.6(a). Compared to the control (untreated), the cells on the CCFG-CA-EO films showed a normal shape after incubation. It can be observed that all film samples of different concentrations exhibited cell viability values of more than 85% as shown in figure 4.6(b). This indicates the good biocompatibility of the films with HaCaT cells. Cell viability of the hydrogel film CCFG-CA-EO is dose dependent as cell viability decreases with increase in concentration. Similar results were also observed by Ghatar et al. for methyl catechol based hydrogel used for skin regeneration [54].

4.4.10 *In vivo* Wound Healing Studies

Figure 4.7 illustrates the wound progression over a 14-day period for three distinct groups of animals: group 1 (Control/untreated), group 2 (CCFG-CA treated), and group 3 (CCFG-CA-EO treated). Notably, the CCFG-CA-EO treated group exhibited a remarkable acceleration in tissue regeneration and demonstrated a substantial variance in wound closure compared to the other groups.

The percentage of wound shrinkage for each group on days 4, 7, and 14 is depicted in Figure 4.7. The CCFG-CA-EO treated group displayed the most noteworthy rates of wound closure on these specified days, on 14^{th} day these group of rats show 99% of wound closure. In contrast, the CCFG-CA treated group showed wound contractions of 84%. The control group also exhibited wound contractions, albeit to a lesser extent, with 69.75%. The results emphasize the notable efficacy of CCFG-CA-EO in

promoting rapid wound closure compared to the other groups. Same results were observed by Bagher et al. with alginate/chitosan based hydrogel. [35]

Figure 4.7: *In vivo* wound-healing results representing the wound recovery at 0^{th}, 4^{th}, 7^{th} and 14^{th} day

4.4.11 Histology

One of the widely utilized staining techniques for histology is Hematoxylin and Eosin (H&E) staining. Hematoxylin imparts a deep blue-purple color to nuclei, while Eosin adds a pinkish hue to the cytoplasm and extracellular matrix. In Figure 4.8, the histology of wound healing in rats is depicted through (H&E) staining on days 4^{th}, 7^{th}, and 14^{th} day. On day 4, the epidermis in all groups was not yet well-formed, covered by acute inflammatory cells. New epithelial regeneration becomes apparent on days 7 and 14 for the group treated with CCFG-CA-EO. From day 4 to day 7 of the healing process, the epidermis grows from the wound edges toward the center. Keratinocytes,

major components of the epidermis, are responsible for epidermal formation through a process called epithelialization. Histological sections indicate a higher rate of re-epithelialization for wounds treated with CCFG-CA-EO on day 14 compared to CCFG-CA groups and the untreated group named control. Visual microscopic comparison on day 14 reveals nearly complete re-epithelialization [55,56].

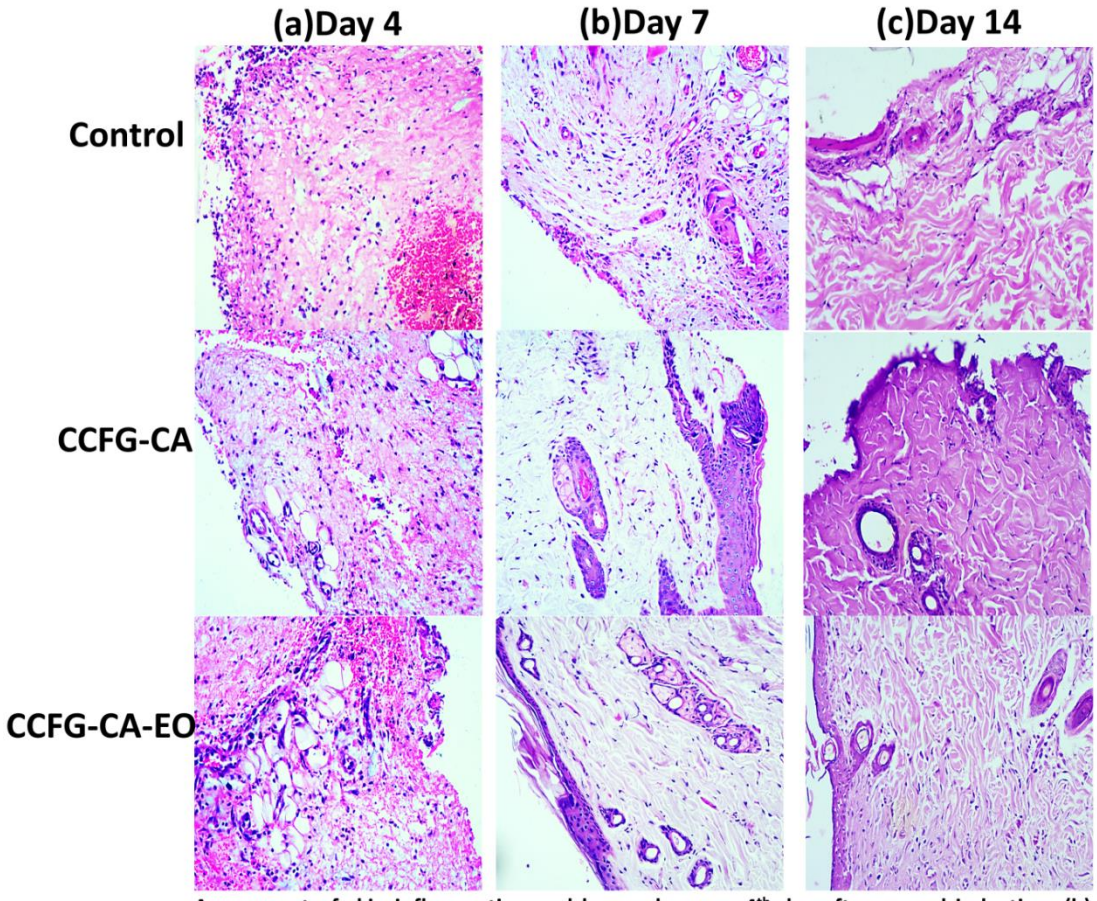

Figure 4.8: Microscopic sections of healed incisions in rats at 4th, 7th and 14th day

4.4.12 Degradation Studies

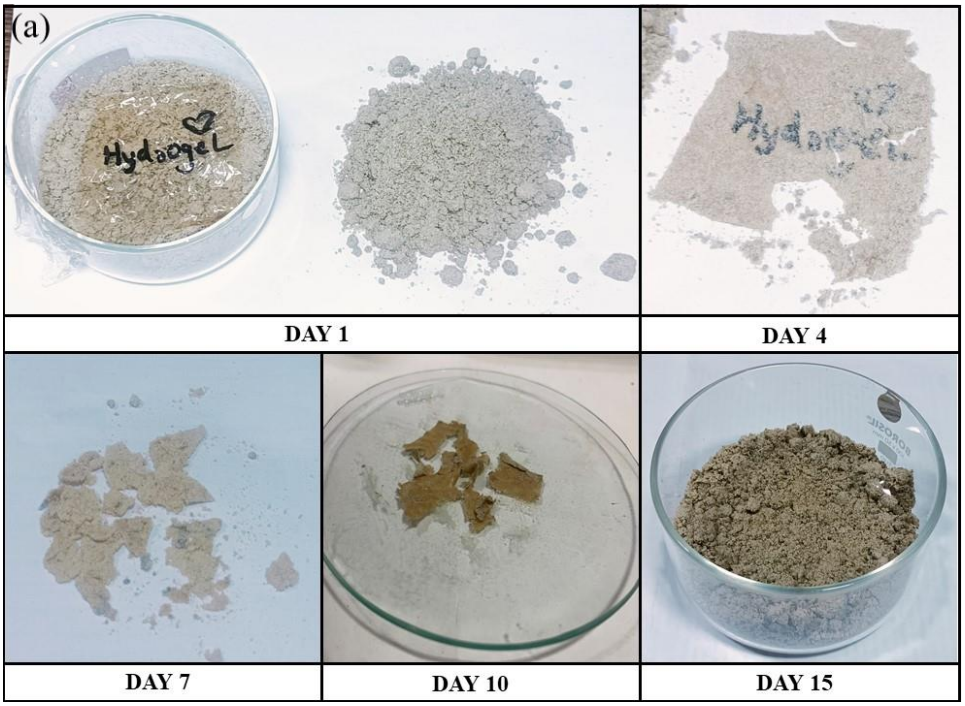

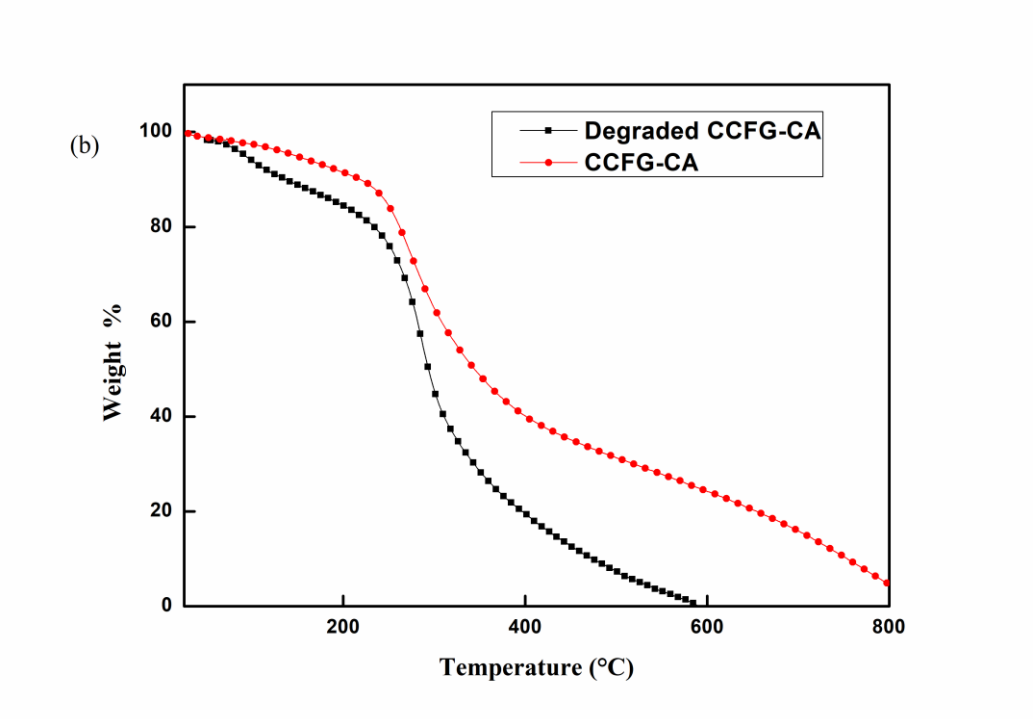

Figure 4.9: (a) Degradation studies for the film CCFG-CA by soil burial method and (b) TGA of degraded CCFG-CA film comparison with CCFG-CA film

Table 4.4: Degradation studies of CCFG-CA film

Day	weight (g)	Percentage weight loss
0	0.502	0%
4	0.345	31.27%
7	0.287	42.80%
10	0.125	75.09%
15	Not found	Can't be predicted

The hydrogel film underwent noticeable degradation starting around the 4th day of burial, as shown in figure 4.9(a) and table 4.4. Initially, the film began to exhibit cracks and a softer texture. On the 7th day, it was observed that the film had broken down into a few distinct pieces. On the 10th day, further degradation was observed as the film fragmented into smaller pieces and percentage weight loss was 75.06%. By the 15th day, the film had completely disintegrated and was no longer visible in the soil indicating complete degradation of the CCFG-CA film**.** The results were also analyzed by performing thermal degradation analysis. On the 10th day, a sample was collected, washed with distilled water, and dried at 45°C for TGA. From thermo gravimetric analysis(figure 4.9(b)), it was observed that the film had been degraded by the soil, decomposing 100% within 600 °C while the actual film showed some residual content even after 800 °C. The breakdown of the film had started under the soil and the remaining part degraded up to 600 °C during thermal analysis. Estrada-Villegas GM et al., observed similar results for degradation in 120 days for PVGA-Alginate based hydrogels [57]

4.4.13 Permeability Test

4.4.13.1 Microbial Permeability Test

The microbial penetration test was performed to assess ability of the hydrogel film CCFG-CA-EO to withstand the transmission of microbes from the surrounding environment to the upper surface of the wound. The methodology adopted was outlined by Amin et al. [58] and Mehmood et al. [59], with minor changes. After 24 h, we observed microbial growth in the uncovered vial, whereas the vial sealed with a film CCFG-CA-EO displayed no microbial growth. The results are shown in Figure 4.10, which shows that in the uncovered vial, white-colored microbial colonies grew in the nutrient medium. Conversely, the nutrient medium in the vial covered with the CCFG-CA-EO film remained clear, devoid of any microbial growth throughout the duration of the test.

Based on the outcomes of this experiment, it can be conclusively stated that the essential oil-loaded film, CCFG-CA-EO acts as a barrier against microbial penetration.

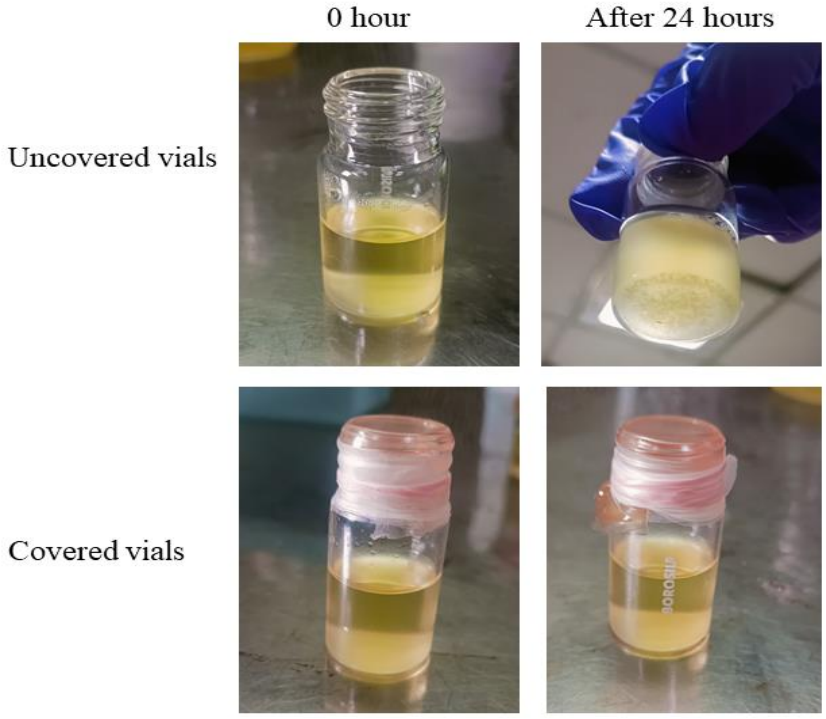

Figure 4.10: Microbial penetration test for film CCFG-CA-EO

4.4.13.2 WVTR

Hydrogel materials intended for wound healing applications must possess an optimal Water Vapour Transmission Rate (WVTR). This entails their ability to effectively regulate fluid absorption and transmission from the wound surface. The goal is to minimize the loss of bodily liquids while maintaining a high level of humidity in the surrounding environment. An ideal wound healing dressing may possess a WVTR in the range of 2000 to 2500 g/m^2.day [60]. This range ensures that it effectively maintains an environment that prevents wound dryness and water loss while also possessing the capability to inhibit the formation of excessive exudates within the wound bed [1]. It has been observed that hydrogel film CCFG-CA-EO has the appropriate WVTR required for wound healing. The WVTR for the control is notably high, measuring at 4739.24±398 g/m².day. In contrast, the hydrogel film containing

CCFG-CA-EO exhibits the lowest WVTR value, with a measurement of 2329.11±245 g/m².day. When compared to the hydrogel film without essential oils, which has a WVTR value of 2987.34±206 g/m².day, it is evident that CCFG-CA-EO possesses a more suitable WVTR value, making it effective for applications in wound healing.

4.4.14 Protein Adsorption test by using Bradford Reagent

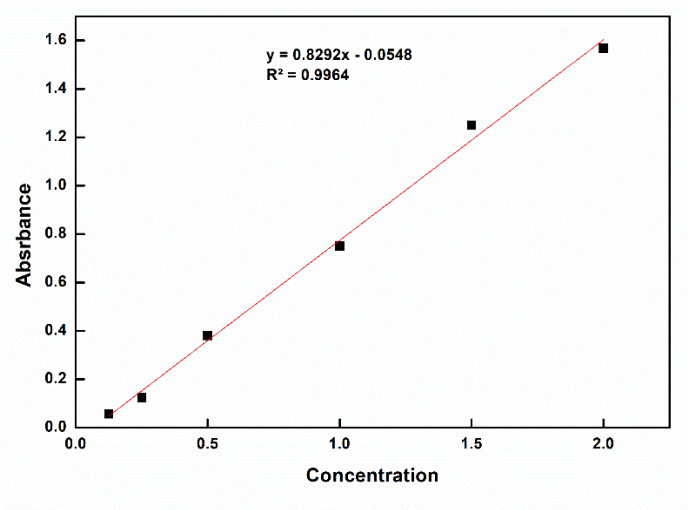

Figure 4.11: BSA calibration curve

The experimental results demonstrate that the CCFG-CA-EO-based hydrogel film's surface absorbed minimal protein. It is widely observed that a wound dressing material with low protein adsorption tendency can reduce inflammation and maintain moist wound environment at the wound site. It facilitates better interaction between the wound bed and the dressing material, thus enhancing the wound healing process and improving the patient comfort by reducing dressing adherence and minimizing pain during removal. A low-protein adsorption by hydrogel film can also help prevent the accumulation of proteins that promote the growth of bacteria and reduce the risk of secondary infection [39,41]. The hydrogel film based on CCFG-CA exhibited elevated protein adsorption i.e., 192.95 µg/mL, calculated on the basis of the obtained

calibration curve for BSA given in figure 4.11. This heightened adsorption can be attributed to the remarkably hydrophilic properties of CCFG. However, the introduction of essential oils (EO) into the CCFG-CA hydrogel film i.e., CCFG-CA-EO led to a notable reduction in protein adsorption, measuring only 12.05µg/mL. This decrease can likely be attributed to the increased hydrophobicity of the films resulting from the incorporation of essential oils.

4.5 Conclusion

The novel hydrogel-based film of CCFG, CA and glycerol which is highly biodegradable was synthesized using the solvent casting method. The film loaded with essential oils such as Turmeric, Rosemary, and Thuja, which enhanced the anti-oxidant and barrier properties of the film. The film also exhibits appropriate swelling in SWF but to a lesser extent than distilled water. To improve the thermal and mechanical properties of the film, glycerol used as plasticizing agent and citric acid as cross-linker for the polysaccharide chain. The hydrogel film allows for the permeability of water vapour, while impermeable to microorganisms. Additionally, the CCFG-CA-EO film was found to have a protein adsorption of 12.05µg/mL, indicating that it absorbs a small amount of wound exudate and maintains a moist environment for the wound. *In- vitro* studies have shown that the film is bio-compatible, and *in-vivo* and histological analysis confirm its ability to promote fast wound recovery in a rat model with CCFG-CA-EO. In conclusion, the synthesized hydrogel-based film loaded with three essential oils i.e., CCFG-CA-EO has proven to be an effective dressing for wound healing.

4.6 References

[1] M. T. Khorasani, A. Joorabloo, A. Moghaddam, H. Shamsi, and Z. MansooriMoghadam, "Incorporation of ZnO nanoparticles into heparinised polyvinyl alcohol/chitosan hydrogels for wound dressing application," *Int. J. Biol. Macromol.*, vol. 114, pp. 1203–1215, 2018, doi: 10.1016/j.ijbiomac.2018.04.010.

[2] G. Han and R. Ceilley, "Chronic Wound Healing: A Review of Current Management and Treatments," *Adv. Ther.*, vol. 34, no. 3, pp. 599–610, 2017, doi: 10.1007/s12325-017-0478-y.

[3] B. Singh, A. Sharma, N. Thakur, and R. Kumar, "Developing dietary fiber moringa gum based ciprofloxacin encapsulated hydrogel wound dressings for better wound care," *Food Hydrocoll. Heal.*, vol. 3, no. January, p. 100128, Dec. 2023, doi: 10.1016/j.fhfh.2023.100128.

[4] M. Heydari et al., "A two-layer nanofiber-Tragacanth hydrogel composite containing Lavender extract and Mupirocin as a wound dressing," *Polym. Bull.*, no. 0123456789, Feb. 2023, doi: 10.1007/s00289-022-04655-8.

[5] T. Liu et al., "Carboxymethyl Chitosan/Sodium alginate hydrogels with polydopamine coatings as promising dressings for eliminating biofilm and multidrug-resistant bacteria induced wound healing," *Int. J. Biol. Macromol.*, vol. 225, pp. 923–937, Jan. 2023, doi: 10.1016/j.ijbiomac.2022.11.156.

[6] Y. Yuan, L. Ding, Y. Chen, G. Chen, T. Zhao, and Y. Yu, "International Journal of Biological Macromolecules Nano-silver functionalized polysaccharides as a platform for wound dressings : A review," *Int. J. Biol.*

Macromol., vol. 194, no. July 2021, pp. 644–653, 2022, doi: 10.1016/j.ijbiomac.2021.11.108.

[7] M. Tanwar, R. K. Gupta, and A. Rani, "Natural gums and their derivatives based hydrogels: in biomedical, environment, agriculture, and food industry," *Crit. Rev. Biotechnol.*, pp. 1–27, Jan. 2023, doi: 10.1080/07388551.2022.2157702.

[8] M. Haghbin et al., "Fabrication and characterization of Persian gum-based hydrogel loaded with gentamicin-loaded natural zeolite: An in vitro and in silico study," *Int. J. Biol. Macromol.*, vol. 235, no. January, p. 123766, 2023, doi: 10.1016/j.ijbiomac.2023.123766.

[9] K. Huanbutta and W. Sittikijyothin, "Use of seed gums from *Tamarindus indica* and *Cassia fistula* as controlled-release agents," *Asian J. Pharm. Sci.*, vol. 13, no. 5, pp. 398–408, Sep. 2018, doi: 10.1016/j.ajps.2018.02.006.

[10] W. Sittikijyothin, B. Phonyotin, T. Sangnim, and K. Huanbutta, "Using carboxymethyl gum from *Tamarindus indica* and *Cassia fistula* seeds with Chromolaena odorata leaf extract to develop antibacterial gauze dressing with hemostatic activity," *Res. Pharm. Sci.*, vol. 16, no. 2, pp. 118–128, 2021, doi: 10.4103/1735-5362.310519.

[11] J. Maitra and V. K. Shukla, "Cross-linking in Hydrogels - A Review," *Am. J. Polym. Sci.*, vol. 4, no. 2, pp. 25–31, 2014, doi: 10.5923/j.ajps.20140402.01.

[12] H. Chopra, S. Bibi, S. Kumar, M. S. Khan, P. Kumar, and I. Singh, "Preparation and Evaluation of Chitosan/PVA Based Hydrogel Films Loaded with Honey for Wound Healing Application," *Gels*, vol. 8, no. 2, p. 111, Feb.

2022, doi: 10.3390/gels8020111.

[13] S. Nayak and S. C. Kundu, "Sericin-carboxymethyl cellulose porous matrices as cellular wound dressing material," *J. Biomed. Mater. Res. Part A*, vol. 102, no. 6, pp. 1928–1940, Jun. 2014, doi: 10.1002/jbm.a.34865.

[14] F. Aldakheel, D. Mohsen, M. El Sayed, K. Alawam, A. Binshaya, and S. Alduraywish, "Silver Nanoparticles Loaded on Chitosan-g-PVA Hydrogel for the Wound-Healing Applications," *Molecules*, vol. 28, no. 7, p. 3241, Apr. 2023, doi: 10.3390/molecules28073241.

[15] C. Winarti, M. Kurniati, A. B. Arif, K. S. Sasmitaloka, and Nurfadila, "Cellulose-based nanohydrogel from corncob with chemical crosslinking methods," *IOP Conf. Ser. Earth Environ. Sci.*, vol. 209, no. 1, 2018, doi: 10.1088/1755-1315/209/1/012043.

[16] H. S. H. Munawaroh et al., "Synthesis, modification and application of fish skin gelatin-based hydrogel as sustainable and versatile bioresource of antidiabetic peptide," *Int. J. Biol. Macromol.*, vol. 231, p. 123248, Mar. 2023, doi: 10.1016/j.ijbiomac.2023.123248.

[17] P. D. Dalton, C. Hostert, K. Albrecht, M. Moeller, and J. Groll, "Structure and Properties of Urea-Crosslinked Star Poly[(ethylene oxide)- ran -(propylene oxide)] Hydrogels," *Macromol. Biosci.*, vol. 8, no. 10, pp. 923–931, Oct. 2008, doi: 10.1002/mabi.200800080.

[18] J. Skopinska-Wisniewska, M. Tuszynska, and E. Olewnik-Kruszkowska, "Comparative Study of Gelatin Hydrogels Modified by Various Cross-Linking Agents," *Materials (Basel).*, vol. 14, no. 2, p. 396, Jan. 2021, doi:

10.3390/ma14020396.

[19] C. Demitri et al., "Novel superabsorbent cellulose-based hydrogels crosslinked with citric acid," *J. Appl. Polym. Sci.*, vol. 110, no. 4, pp. 2453–2460, Nov. 2008, doi: 10.1002/app.28660.

[20] H. Xu, L. Shen, L. Xu, and Y. Yang, "Low-temperature crosslinking of proteins using non-toxic citric acid in neutral aqueous medium: Mechanism and kinetic study," *Ind. Crops Prod.*, vol. 74, pp. 234–240, Nov. 2015, doi: 10.1016/j.indcrop.2015.05.010.

[21] A. Chang et al., "Citric acid crosslinked sphingan WL gum hydrogel films supported ciprofloxacin for potential wound dressing application," *Carbohydr. Polym.*, vol. 291, p. 119520, Sep. 2022, doi: 10.1016/j.carbpol.2022.119520.

[22] N. Suderman, M. I. N. Isa, and N. M. Sarbon, "The effect of plasticizers on the functional properties of biodegradable gelatin-based film: A review," *Food Biosci.*, vol. 24, no. June, pp. 111–119, Aug. 2018, doi: 10.1016/j.fbio.2018.06.006.

[23] H. Wang et al., "Antibacterial polysaccharide-based hydrogel dressing containing plant essential oil for burn wound healing," *Burn. Trauma*, vol. 9, p. tkab041, Jan. 2021, doi: 10.1093/burnst/tkab041.

[24] J. Cai, J. Xiao, X. Chen, and H. Liu, "Essential oil loaded edible films prepared by continuous casting method: Effects of casting cycle and loading position on the release properties," *Food Packag. Shelf Life*, vol. 26, p. 100555, Dec. 2020, doi: 10.1016/j.fpsl.2020.100555.

[25] J. Ju et al., "Application of essential oil as a sustained release preparation in

food packaging," *Trends Food Sci. Technol.*, vol. 92, pp. 22–32, Oct. 2019, doi: 10.1016/j.tifs.2019.08.005.

[26] C. O. Ogidi, A. E. Ojo, O. B. Ajayi-Moses, O. M. Aladejana, O. A. Thonda, and B. J. Akinyele, "Synergistic antifungal evaluation of over-the-counter antifungal creams with turmeric essential oil or Aloe vera gel against pathogenic fungi," *BMC Complement. Med. Ther.*, vol. 21, no. 1, pp. 1–12, 2021, doi: 10.1186/s12906-021-03205-5.

[27] N. D. Jasuja, S. Sharma, J. Choudhary, and S. C. Joshi, "Essential Oil and Important Activities of *Thuja orientalis* and *Thuja occidentalis*," *J. Essent. Oil-Bearing Plants*, vol. 18, no. 4, pp. 931–949, 2015, doi: 10.1080/0972060X.2014.884774.

[28] R. S. Borges, B. L. S. Ortiz, A. C. M. Pereira, H. Keita, and J. C. T. Carvalho, "*Rosmarinus officinalis* essential oil: A review of its phytochemistry, anti-inflammatory activity, and mechanisms of action involved," *J. Ethnopharmacol.*, vol. 229, pp. 29–45, 2019, doi: 10.1016/j.jep.2018.09.038.

[29] M. Suhail, P.-C. Wu, and M. U. Minhas, "Development and characterization of pH-sensitive chondroitin sulfate-co-poly(acrylic acid) hydrogels for controlled release of diclofenac sodium," *J. Saudi Chem. Soc.*, vol. 25, no. 4, p. 101212, Apr. 2021, doi: 10.1016/j.jscs.2021.101212.

[30] Q. Ma, Y. Ren, and L. Wang, "Investigation of antioxidant activity and release kinetics of curcumin from Tara gum/ polyvinyl alcohol active film," *Food Hydrocoll.*, vol. 70, pp. 286–292, 2017, doi: 10.1016/j.foodhyd.2017.04.018.

[31] C. Sun, C. Xu, L. Mao, D. Wang, J. Yang, and Y. Gao, "Preparation,

characterization and stability of curcumin-loaded zein-shellac composite colloidal particles," *Food Chem.*, vol. 228, pp. 656–667, 2017, doi: 10.1016/j.foodchem.2017.02.001.

[32] R. Hemalatha, P. Nivetha, C. Mohanapriya, G. Sharmila, C. Muthukumaran, and M. Gopinath, "Phytochemical composition, GC-MS analysis, in vitro antioxidant and antibacterial potential of clove flower bud (*Eugenia caryophyllus*) methanolic extract," *J. Food Sci. Technol.*, vol. 53, no. 2, pp. 1189–1198, 2016, doi: 10.1007/s13197-015-2108-5.

[33] H. Wang et al., "Characterization, release, and antioxidant activity of curcumin-loaded Sodium alginate/ZnO hydrogel beads," *Int. J. Biol. Macromol.*, vol. 121, pp. 1118–1125, Jan. 2019, doi: 10.1016/j.ijbiomac.2018.10.121.

[34] S. Kianpour et al., "Physicochemical and biological characteristics of the nanostructured polysaccharide-iron hydrogel produced by microorganism *Klebsiella oxytoca*," *J. Basic Microbiol.*, vol. 57, no. 2, pp. 132–140, 2017, doi: 10.1002/jobm.201600417.

[35] Z. Bagher et al., "Wound healing with alginate/chitosan hydrogel containing hesperidin in rat model," *J. Drug Deliv. Sci. Technol.*, vol. 55, p. 101379, 2020, doi: 10.1016/j.jddst.2019.101379.

[36] K. Kaur, R. Jindal, and D. Jindal, "International Journal of Biological Macromolecules Controlled release of vitamin B 1 and evaluation of biodegradation studies of chitosan and gelatin based hydrogels," *Int. J. Biol. Macromol.*, vol. 146, pp. 987–999, 2020, doi:

https://doi.org/10.1016/j.ijbiomac.2019.09.223.

[37] "ASTM E 96, Standard Test Methods for Water Vapor Transmission of Materials," 1996.

[38] N. Goudar, V. N. Vanjeri, D. Kasai, G. Gouripur, and R. B. Malabadi, "ZnO NPs Doped PVA / *Spathodea campanulata* Thin Films for Food Packaging," *J. Polym. Environ.*, vol. 29, no. 9, pp. 2797–2812, 2021, doi: 10.1007/s10924-021-02070-0.

[39] D. Stan et al., "Exploring the Impact of Alginate — PVA Ratio and the Addition of Bioactive Substances on the Performance of Hybrid Hydrogel Membranes as Potential Wound Dressings," pp. 1–27, 2023.

[40] N. J. Kruger, "The Bradford Method," in *Springer Protocols Handbooks*, 2009, pp. 17–24.

[41] Y. Ramdhun, M. Mohanta, T. Arunachalam, R. Gupta, and D. Verma, "Bromelain-loaded polyvinyl alcohol–activated charcoal-based film for wound dressing applications," *Macromol. Res.*, vol. 31, no. 5, pp. 469–488, 2023, doi: 10.1007/s13233-023-00119-8.

[42] K. K. Mali, S. C. Dhawale, and R. J. Dias, "Synthesis and characterization of hydrogel films of carboxymethyl tamarind gum using citric acid," *Int. J. Biol. Macromol.*, vol. 105, pp. 463–470, Dec. 2017, doi: 10.1016/j.ijbiomac.2017.07.058.

[43] S. S. Lal and S. T. Mhaske, "Old corrugated box (OCB)-based cellulose nanofiber-reinforced and citric acid-cross-linked TSP–guar gum composite film," *Polym. Bull.*, vol. 78, no. 2, pp. 885–915, Feb. 2021, doi:

10.1007/s00289-020-03138-y.

[44] W. Sittikijyothin, K. Khumduang, K. Khounvilay, and R. Mongkholrattanasit, "Physicochemical characterization of seed gum from *cassia fistula*," *Key Eng. Mater.*, vol. 818 KEM, pp. 12–15, 2019, doi: 10.4028/www.scientific.net/KEM.818.12.

[45] K. N, R. K, V. G, A. R, and R. R. C, "Structural, spectral, thermal and nonlinear optical analysis of anhydrous citric acid crystal," *Optik (Stuttg).*, vol. 192, no. March, p. 162960, 2019, doi: 10.1016/j.ijleo.2019.162960.

[46] M. M. Marin et al., "Novel Nanocomposite Hydrogels Based on Crosslinked Microbial Polysaccharide as Potential Bioactive Wound Dressings," *Materials (Basel).*, vol. 16, no. 3, p. 982, Jan. 2023, doi: 10.3390/ma16030982.

[47] M. S. Hernández, L. N. Ludueña, and S. K. Flores, "Citric acid, chitosan and oregano essential oil impact on physical and antimicrobial properties of cassava starch films," *Carbohydr. Polym. Technol. Appl.*, vol. 5, no. March, p. 100307, Jun. 2023, doi: 10.1016/j.carpta.2023.100307.

[48] R. Batool et al., "Fabrication and Characterization of Celecoxib-Loaded Chitosan/Guar Gum-Based Hydrogel Beads," *Pharmaceuticals*, vol. 16, no. 4, p. 554, Apr. 2023, doi: 10.3390/ph16040554.

[49] S. Bhatia et al., "Fabrication, Characterization, and Antioxidant Potential of Sodium Alginate/Acacia Gum Hydrogel-Based Films Loaded with Cinnamon Essential Oil," *Gels*, vol. 9, no. 4, p. 337, Apr. 2023, doi: 10.3390/gels9040337.

[50] P. Chuysinuan et al., "Development of gelatin hydrogel pads incorporated

with Eupatorium adenophorum essential oil as antibacterial wound dressing," *Polym. Bull.*, vol. 76, no. 2, pp. 701–724, 2019, doi: 10.1007/s00289-018-2395-x.

[51] B. Singh and Rajneesh, "Gamma radiation synthesis and characterization of gentamicin loaded polysaccharide gum based hydrogel wound dressings," *J. Drug Deliv. Sci. Technol.*, vol. 47, pp. 200–208, Oct. 2018, doi: 10.1016/j.jddst.2018.07.014.

[52] B. Singh, J. Singh, and Rajneesh, "Application of tragacanth gum and alginate in hydrogel wound dressing's formation using gamma radiation," *Carbohydr. Polym. Technol. Appl.*, vol. 2, no. March, p. 100058, 2021, doi: 10.1016/j.carpta.2021.100058.

[53] G. Liu, Z. Bao, and J. Wu, "Injectable baicalin / F127 hydrogel with antioxidant activity for enhanced wound healing," *Chinese Chem. Lett.*, vol. 31, no. 7, pp. 1817–1821, 2020, doi: 10.1016/j.cclet.2020.03.005.

[54] J. Majidi Ghatar et al., "A novel hydrogel containing 4-methylcatechol for skin regeneration: in vitro and in vivo study," *Biomed. Eng. Lett.*, vol. 13, no. 3, pp. 429–439, 2023, doi: 10.1007/s13534-023-00273-z.

[55] M. Rezvanian, S. F. Ng, T. Alavi, and W. Ahmad, "In-vivo evaluation of Alginate-Pectin hydrogel film loaded with Simvastatin for diabetic wound healing in Streptozotocin-induced diabetic rats," *Int. J. Biol. Macromol.*, vol. 171, pp. 308–319, 2021, doi: 10.1016/j.ijbiomac.2020.12.221.

[56] S. A. Alsareii, J. Ahmad, A. Umar, M. Z. Ahmad, and I. A. Shaikh, "Enhanced In Vivo Wound Healing Efficacy of a Novel Piperine-Containing

Bioactive Hydrogel in Excision Wound Rat Model," *Molecules*, vol. 28, no. 2, p. 545, Jan. 2023, doi: 10.3390/molecules28020545.

[57] G. M. Estrada-Villegas, G. Morselli, M. J. A. Oliveira, G. González-Pérez, and A. B. Lugão, "PVGA/Alginate-AgNPs hydrogel as absorbent biomaterial and its soil biodegradation behavior," *Polym. Bull.*, vol. 77, no. 8, pp. 4147–4166, 2020, doi: 10.1007/s00289-019-02966-x.

[58] M. A. A. I. T. Abdel-raheem and P. V. A. Á. A. Á. Hydroxyproline, "Accelerated wound healing and anti-inflammatory effects of physically cross linked polyvinyl alcohol – chitosan hydrogel containing honey bee venom in diabetic rats," *Arch. Pharm. Res.*, vol. 37, pp. 1016–1031, 2014, doi: 10.1007/s12272-013-0308-y.

[59] Y. Mehmood et al., "Amikacin-Loaded Chitosan Hydrogel Film Cross-Linked with Folic Acid for Wound Healing Application," *Gels*, vol. 9, no. 7, p. 551, Jul. 2023, doi: 10.3390/gels9070551.

[60] T. Khan, E. H. Mirza, N. J. Kurd, M. Naushad, and M. Z. Ul Haque, "Fabrication and in vitro evaluation of polyvinyl alcohol/bio-glass composite for potential wound healing applications," *Dig. J. Nanomater. Biostructures*, vol. 18, no. 3, pp. 821–840, Jul. 2023, doi: 10.15251/DJNB.2023.183.821.

CHAPTER – 5
Overall Conclusion and Future Prospects

5.1 Overall Conclusion

The fundamental goal of this research is to discuss classification, synthesis and applications of the hydrogels synthesized by using derivatized natural gums. Among various natural gums, three carboxymethylated natural gums were used for the synthesis of the hydrogels and their applications have been explored in bio-medical field. Gum Tragacanth and Locust bean gum were successfully carboxymethylated with 0.2 degree of substitution and were used for the synthesis of the hydrogel by using free radical co-polymerization technique. The synthesized hydrogels from the above carboxymethylated gums were characterized by FT-IR, XRD, SEM, TGA and ^{13}C NMR. Rheological studies for the synthesized hydrogels were done to determine the flow properties of the hydrogel. Swelling studies were performed at three different temperature and network parameters were also calculated with a function of temperature. The results so obtained from swelling studies confirmed the formation of the smart hydrogels. Both the hydrogels were explored as controlled drug delivery carrier by using Aceclofenac sodium and Metformin hydrochloride respectively as the model drugs. Hemolysis test confirms the bio-compatibility of the hydrogels. Carboxymethylated *Cassia fistula* gum based hydrogel was synthesized by esterification method. Synthesized hydrogel film was explored for the wound healing application. Essential oils loaded hydrogel film was confirmed to be best fit for the wound healing application by analyzing the results of mechanical test, anti-oxidant test, permeability test and protein adsorption test. Highly biodegradable properties

were confirmed by performing the soil burial experiment and TGA. *In- vitro* and *in-vivo* test confirmed the bio-compatibility and effective wound healing properties of the hydrogel film. Overall, the synthesized CMGT, CMLB and CCFG based hydrogels can be the promising carriers for the drug delivery.

5.2 Future prospects and Scope

Natural gum-based hydrogels are three-dimensional network which has the ability to swell and retain water due to their hydrophilic functional group on their cross-linked polymeric matrix/scaffolds. The unique properties of hydrogels, cost effectiveness, biodegradability and sustainability have led to their application in drug delivery, implantable devices, tissue engineering and topical formulations. The porous structure of these hydrogels is very useful to drug loading and slow/ controlled release of drugs, agrochemicals and fertilizers, bio-pesticides/bio-control agents for agriculture. They are also very useful in water purification and environmental applications to remove toxic and hazardous compounds. Hydrogel films are useful in food packaging, sensors, wound healing and transdermal drug delivery because of their non- invasive nature.

The research work embodied in this thesis is on carboxymethylated Gum (Tragacanth, Locust bean and C*assia fistula*) based hydrogels, which were used to formulate Metformin Hydrochloride, Aceclofenac sodium and mixture of essential oils. In future, these hydrogel's-based gels/films can be further investigated for their utility in agriculture for slow release of pesticides, bio-pesticides and possibly for immobilizing/trapping enzymes. Also, modeling tool can be generated for understanding structural activity relationship of the drugs with hydrogel.

5.3 List of Publications

1. **M. Tanwar**, R. K. Gupta, and A. Rani, "Carboxymethylated gum tragacanth crosslinked poly(sodium acrylate) hydrogel: Fabrication, characterization, rheology and drug-delivery application," ***Indian J. Chem. Technol***., vol. 30, pp. 308–319, 2023, doi: 10.56042/ijct.v30i3.70100 **(IF-0.76)**

2. **M. Tanwar**, A. Rani, and R. K. Gupta, Synthesis and Characterization of Carboxymethylated Locust Bean Gum-*co*-poly(SA)-*cl*-poly(MBA) pH Responsive Hydrogel for Controlled Drug Delivery of Metformin Hydrochloride," ***ChemistrySelect***., 8, pp-e202302525, 2023, doi: 10.1002/slct.202302525 **(IF-2.307)**

3. **M. Tanwar**, R. K. Gupta, and A. Rani, "Natural gums and their derivatives based hydrogels: in biomedical, environment, agriculture, and food industry," ***Crit. Rev. Biotechnol***., 44, pp. 275-301, 2024, doi: 10.1080/07388551.2022.2157702 **(IF-9.062)**

4. **M. Tanwar[1]**, A. Rani[1], N. Gautam[2], S. Talegaonkar[2], and R. K. Gupta[1], "Essential oils loaded carboxymethylated *Cassia fistula* gum-based novel hydrogel films for wound healing"**,** , ***Int. J. Biol. Macromol.,*** 2024(**IF-8.2**) (under review)

5.4 List of Conferences proceedings

1. **Meenakshi Tanwar**, Rajinder K. Gupta and Archna Rani "Synthesis and Applications of Modified Natural Polysaccharides" at International Symposium "Chemical Wisdom by Her" Organized by Department of Chemistry, Deshbandhu College (DU) held on 31st January, 2022 through online mode.

2. **Meenakshi Tanwar**, Rajinder K. Gupta and Archna Rani "Fabrication of Carboxymethylated Xanthan Gum-Based Hydrogels" at 1st international conference on "recent trends in chemical sciences and sustainable energy" organized by held at National Institute of Technology Delhi during 24th - 25th March, 2023.

3. **Meenakshi Tanwar**, Rajinder K. Gupta and Archna Rani, "Fabrication of Carboxymethylated Xanthan Gum and Hydroxypropyl Guar Gum based Hydrogels" at International Chemistry Symposium 2023, organinzed by Thieme group and Department of Chemistry, University of Delhi on 25th October 2023